Supplemental Material

Supplemental Methods

Interpretation of flow cytometry data for fission yeast cell cycle analysis

Note that the fission yeast cell cycle differs from that of a number of model systems, as the G1 phase is short and S phase occurs prior to cytokinesis. As a result, cells have a 2C DNA content during most phases of their cycle. When analyzing DNA content in cultures synchronized in G2, a transient 4C peak is observed, as genome duplication takes place in binucleated cells, and this is resolved upon cytokinesis. This 4C peak is barely detectable in asynchronous cultures due to the low percentage of cells undergoing DNA replication in such populations at any given time. Conversely, the appearance of a 1C peak is the result of an elongation of G1 / delay of S phase, as cytokinesis takes place prior to S phase in these conditions.

Validation of copy number analysis by competitive hybridization using microarrays

To verify the ability of our microarrays to determine 2-fold differences in copy number, we have taken advantage of a strain in which we identified a duplication of a ~2.5 kb genomic region on chromosome III during the course of other studies (strain PN1400). For copy number analysis, we extracted genomic DNA from PN1400 and from a wild-type strain (PN1), followed by differential labeling of these samples and competitive hybridization, as described in the Methods section. As shown in Supplemental Fig. S7A-B, we accurately detect the presence of the duplicated region, with an average amplitude of 1.91; this is comparable with our qPCR analyses of the duplication using specific primers (Supplemental Fig. S7C). These experiments thus confirm the sensitivity of our microarray approach.

Origin identification and determination of efficiencies

While treatment with 6 mM HU results in a broader extension of replication than in previous studies (10 – 15 mM HU), origins were still clearly identifiable; importantly, CIOs appear as individual, distinct peaks. However, as designation of precise origin positions was more difficult in our assays, we used our published datasets for *cdc25-22* cells treated with 12 mM HU (Wu and Nurse 2014) as a guide (Supplemental Fig. S8); these previous experiments were performed using the same microarrays and

methods as the present study. The two experiments reported in our earlier work (Wu and Nurse 2014) were averaged, and the moving geometric means over five consecutive probes along the chromosomes were calculated. This procedure was repeated on the resulting dataset for a total of 10 rounds of smoothing. Sites were then selected as origins if the copy number ratio of HU-treated S phase DNA vs. unreplicated DNA was greater than 1.05, which represents a clear increase over the background after smoothing. The position of each origin was then assigned based on the local maximum followed by visual confirmation. In addition, when two origins were less than 5 kb apart, they were considered as a single origin and the position of the peak with the higher copy number was assigned to the origin. This is validated by the observation that the extent of replication surrounding an origin in 12 mM HU can reach 10-15 kb (Heichinger et al. 2006). Once the positions of the origins were determined, their precise efficiencies were obtained from the non-smoothed dataset, and a threshold of 1.04 for the copy number was applied. This gave rise to a set of 852 origins that was used as a reference to analyze our data for 6 mM HU.

To establish origin efficiencies in *cdc25-22* and *cdc25-22 rad3Δ* cells in 6 mM HU, we averaged the three experiments performed for each strain and assessed the moving geometric means over five consecutive probes along the chromosomes for the averaged datasets. The assigned positions of the 852 origins described above were used to derive the efficiency of each of these origins in these strains and conditions. In addition, in performing these analyses, we noted 24 additional sites in *cdc25-22 rad3Δ* cells that showed clear peaks greater than the threshold of 1.04. These additional origins were then added to the overall list, resulting in a final set of 876 origins (Supplemental Table S1).

For *nda3-km311* and *nda3-km311 rad3Δ* cells treated with 6 mM HU, two experiments were performed and processed as above, assigning origin efficiencies based on the set of 876 origins. For *cdc25-22 rif1Δ* and *cdc25-22 rif1Δ rad3Δ*, three experiments were performed. In this background, we noted minor variations in the positions of local maxima associated with origins. Thus, to obtain accurate data for efficiencies, we assigned the highest value within a distance of 5 probes (~1.25 kb) for each of the 876 origins (Supplemental Table S4). For the analyses in Fig. 6 and Supplemental Fig. S6, the probe positions associated with these values were used as the origin coordinates.

Identification of deregulated origins

To identify origins deregulated in replication stress conditions, we began by demonstrating that individual experiments performed for the *cdc25-22* and *cdc25-22 rad3Δ* backgrounds were highly reproducible (Supplemental Fig. S9A): the Pearson correlation coefficient (r) for each pairwise comparison of experiments showed strong positive correlations (p-value<0.001). Next, we set the threshold for assessing deregulated origins. For this, we estimated the experimental noise in our mapping assay. This was achieved by measuring the dispersion between the three experiments for *cdc25-22* cells, establishing the standard deviation of the efficiency of each origin (Supplemental Fig. S9B). The average and standard deviation of this set of values for all origins was found to be 3.3 and 2.1, respectively. We then calculated 1.5 standard deviations above the mean variability ((1.5*2.1)+3.3=6.5). We note that this corresponds to 1.5 times the interquartile range (IQR) above the third quartile (Q3 + 1.5(IQR)) for the complete set of standard deviations; this means that within the *cdc25-22* datasets, all standard deviations other than outliers are below 8% efficiency. Based on this analysis, we established a stringent threshold of 8% efficiency difference for deregulated origins in *rad3Δ* compared to wild-type cells.

To determine CIOs in HU-treated *rad3Δ* cells, we started with a list of 191 origins that showed ≥ 8% absolute efficiency differences between the averaged *cdc25-22* and *cdc25-22 rad3Δ* origin datasets (Supplemental Table S1). We then visually confirmed the selection of these origins and ensured that the identification of a site as a CIO was not simply due to one aberrantly high value in the datasets. To this end, origins were considered as deregulated only when we observed ≥ 8% efficiency differences in at least two out of the three pairs of *cdc25-22* and *cdc25-22 rad3Δ* experiments (pairs correspond to experiments performed in parallel). This resulted in a final set of 176 origins that showed ≥ 8% absolute efficiency increases in *cdc25-22 rad3Δ* (Supplemental Table S2). 6 sites displayed ≥ 8% absolute efficiency decreases (Supplemental Table S3); these represented a minority of the sites and were not analyzed in more detail. The same methodology was applied for identifying *rif1*-CIOs in *cdc25-22 rif1Δ* vs. *cdc25-22 rif1Δ rad3Δ*. For comparing *nda3-km311* and *nda3-km311 rad3Δ*, origins were considered deregulated when we observed ≥ 8% absolute efficiency difference in the average of the two experiments.

To validate further the statistical significance of our CIO threshold, we performed two complementary analyses. First, we established the standard deviation (std. dev.) of the efficiency for each origin and compared results obtained using the following datasets (Supplemental Fig. S9C): a) all origins in the three *cdc25-22* experiments; b) all origins in the three *cdc25-22 rad3Δ* experiments; c) unaffected origins when pooling all *cdc25-22* and *cdc25-22 rad3Δ* experiments; d) CIOs when pooling all *cdc25-22* and *cdc25-22 rad3Δ* experiments. If CIOs show high levels of deregulation, we would expect the combined pool of *cdc25-22* and *cdc25-22 rad3Δ* experiments to have significantly higher std. devs. for CIOs (d) than 1) the std. devs. between unaffected origins (c) and 2) the std. devs. between all origins in the three *cdc25-22* (a) or the three *cdc25-22 rad3Δ* (b) experiments. This was confirmed by T-tests comparing these datasets (p-value<0.001 for each comparison). Second, we established the differences in the efficiencies of unaffected origins or CIOs between individual experiments for either the *cdc25-22* or *cdc25-22 rad3Δ* backgrounds as well as between the averaged *cdc25-22* and *cdc25-22 rad3Δ* datasets (*rad3Δ* – WT). If significant deregulation is observed at CIOs, we expect that the differences in efficiency between *cdc25-22 rad3Δ* and *cdc25-22* for CIOs to be greater than 1) the differences at unaffected origins or CIOs between individual *cdc25-22* experiments; 2) the differences at unaffected origins or CIOs between individual *cdc25-22 rad3Δ* experiments; and 3) the differences in efficiency in the cohort of unaffected origins between *cdc25-22* and *cdc25-22 rad3Δ*. As anticipated, T-tests confirm that there is a statistically significant difference between the *rad3Δ* – WT CIO data and each of the indicated datasets in Supplemental Fig. S9D (p-value<0.001 for each comparison).

Collectively, these data confirm the reproducibility and robustness of our origin efficiency measurements as well as our analyses of origin deregulation.

Supplemental Figure S1

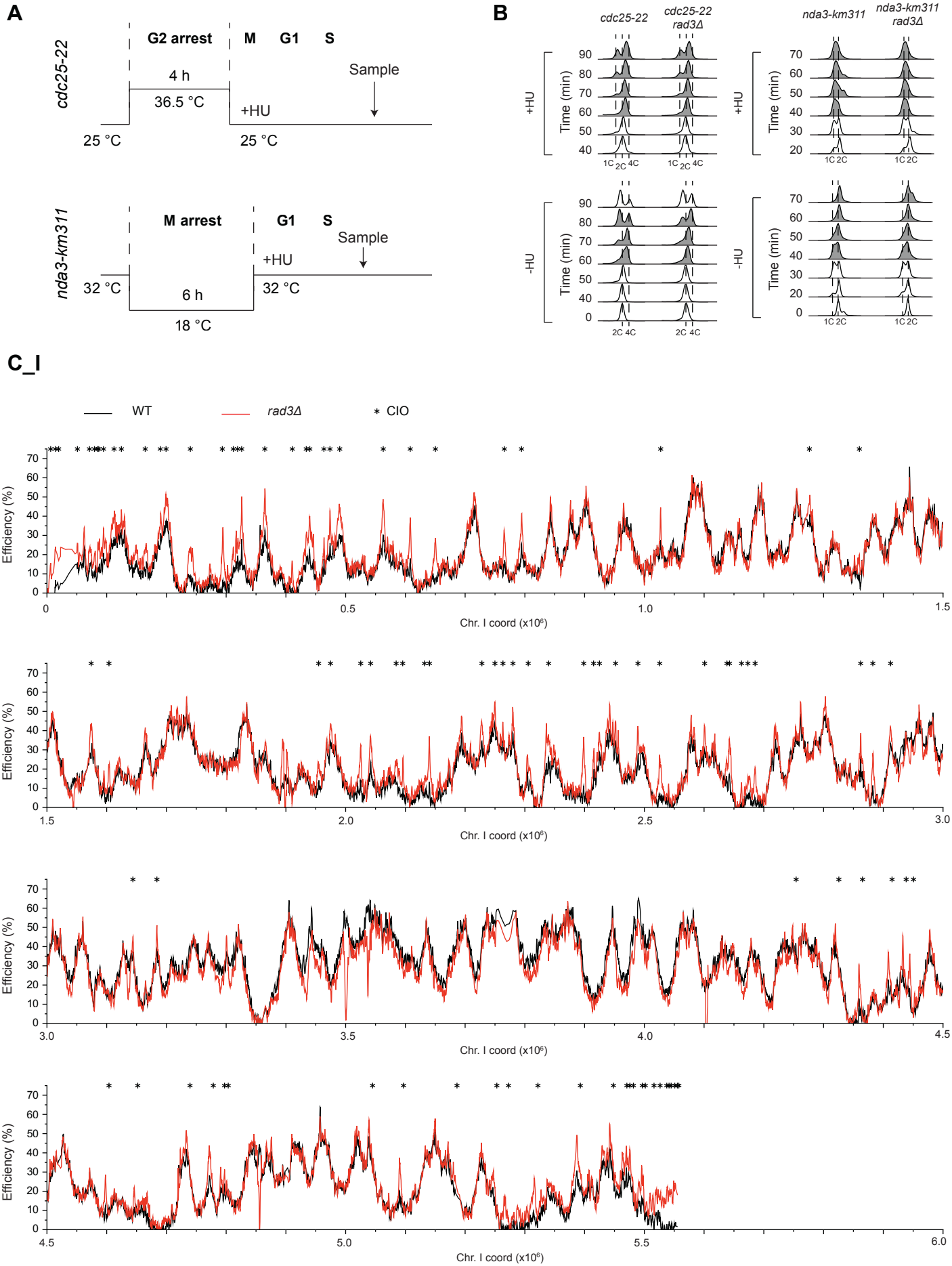

Supplemental Figure S1

C_II

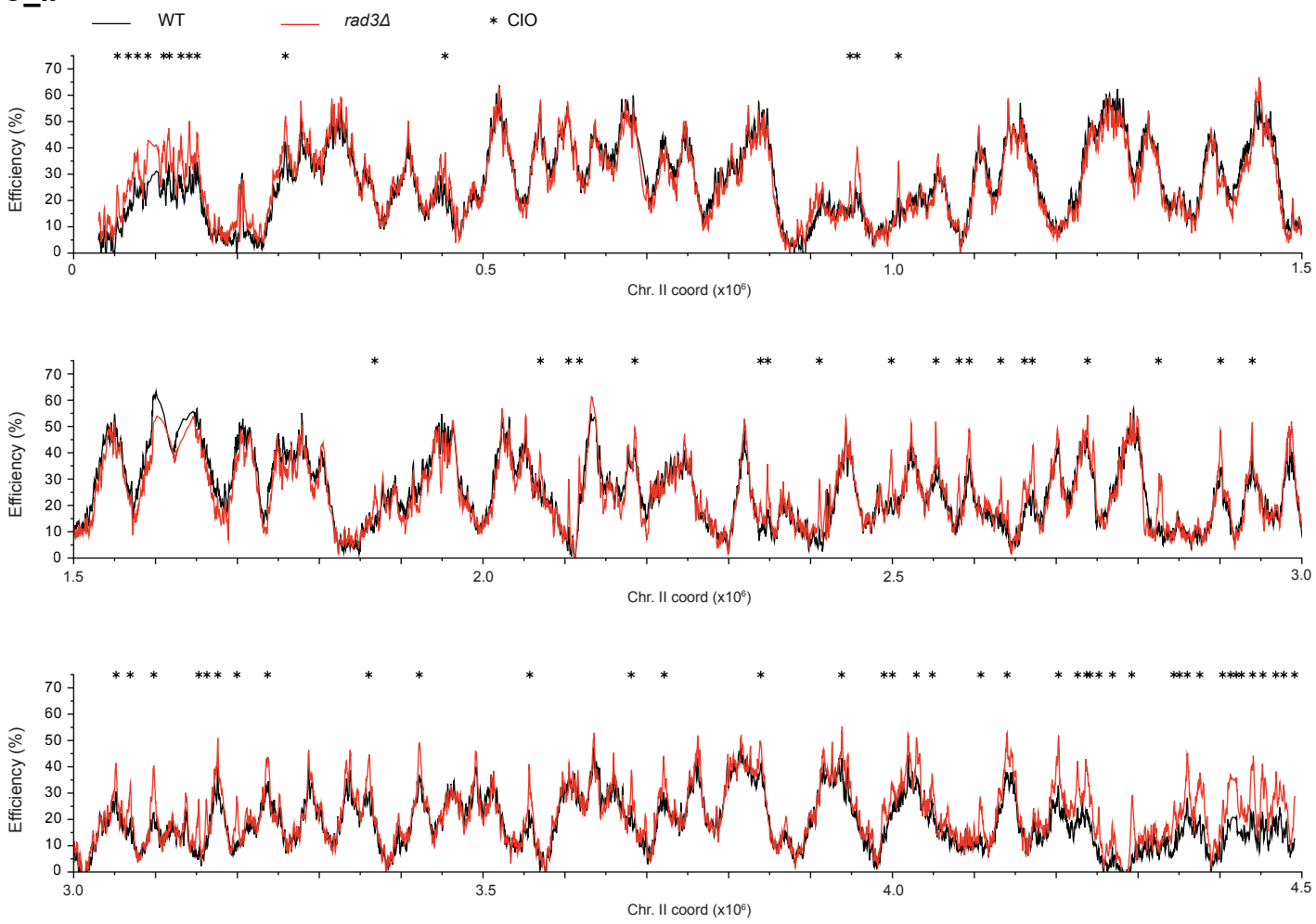

C_III

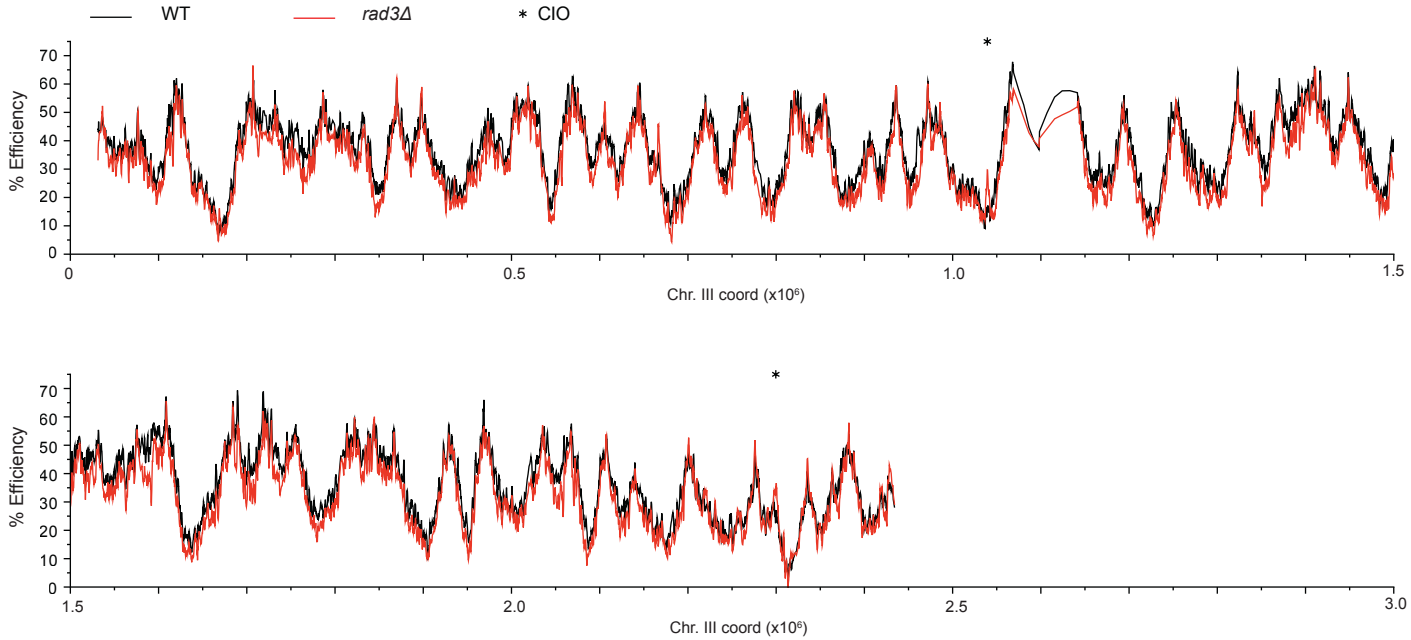

Supplemental Figure S1

D

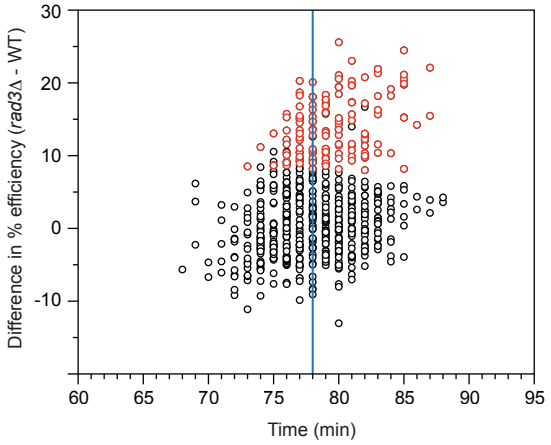

E

	This study	Heichinger *et al.*	Mickle *et al.*	Hayashi *et al.*	Feng *et al.*
Total number of ori.	876	904	657	460	321
Checkpoint-inhibited ori.	176	10	21	96	90
% deregulated ori.	20	1.1	3.2	20.8	28

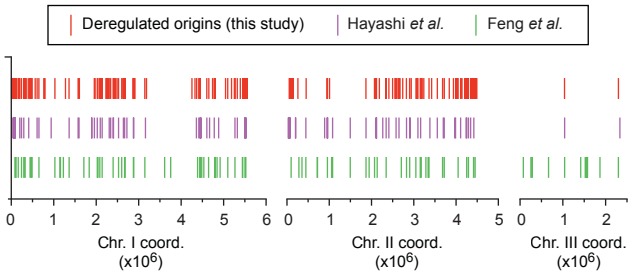

F

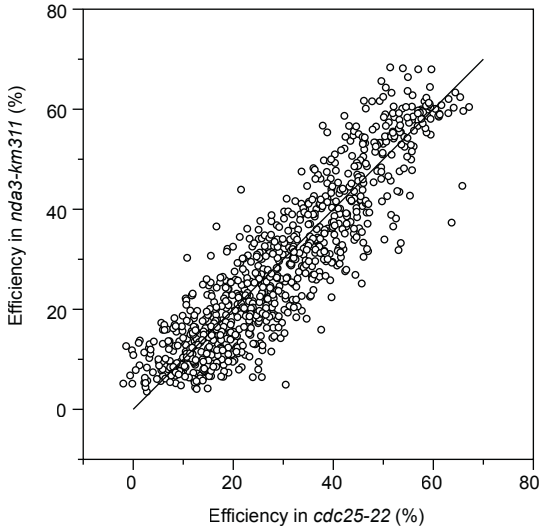

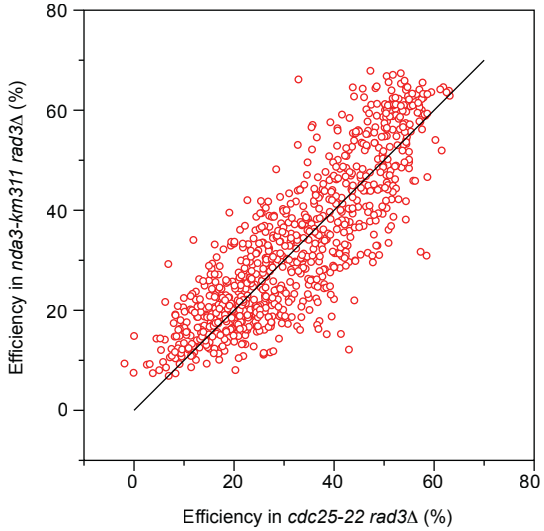

G

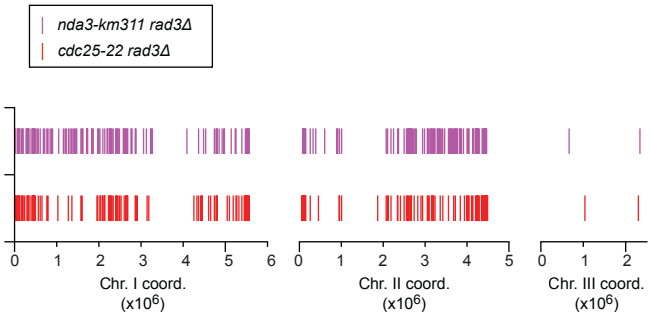

Supplemental Figure S1: Checkpoint regulation of origin firing in replication stress conditions.

A) Experimental design for determining the replication profiles in *cdc25-22* and *nda3-km311* cells. Top: schematic for *cdc25-22* cells. Bottom: schematic for *nda3-km311* cells. **B)** DNA content analysis of *cdc25-22* and *cdc25-22 rad3Δ* (left) as well as *nda3-km311* and *nda3-km311 rad3Δ* (right) cells undergoing a synchronous S phase in the presence or absence of 6 mM HU. Experimental procedures were as in A. These assays allowed the determination of the timing of sampling in the presence of HU. In 6 mM HU, S phase progression is slowed but not completely arrested in both wild-type and *rad3Δ* cells, in contrast to earlier studies using higher concentrations (Heichinger et al. 2006; Wu and Nurse 2014). Samples in which cells are undergoing DNA replication are shown in gray. Left panel/-HU: Cells are initially arrested in G2 (Time 0) with a 2C DNA content. They enter S phase around 50-60 min following the release from G2. This leads to the appearance of a 4C peak, which is resolved upon cytokinesis shortly after the genome is duplicated. Left panel/+HU: Cells enter S phase at the same time as in –HU and then undergo cytokinesis, resulting in the appearance of a peak with a DNA content between 1C and 2C. Right panel/-HU: Cells are initially arrested in M phase (Time 0) with a 2C DNA content. They then begin cytokinesis, resulting in the appearance of a 1C peak, followed by DNA synthesis. Right panel/+HU: Cells begin to divide and then enter S phase at the same time as in –HU. Due to incomplete genome duplication, cells accumulate with a DNA content between 1C and 2C. For interpretation of flow cytometry profiles in fission yeast, see the Supplemental Methods. **C)** Profiles of origin usage in *cdc25-22* (black, WT) and *cdc25-22 rad3Δ* (red, *rad3Δ*) cells treated with 6 mM HU. Asterisks indicate CIOs. x-axis: chromosome coordinates, y-axis: origin efficiency. **D)** Timing of origin firing during S phase. Each origin identified in our experiments was considered to match one from the dataset from Heichinger et al. 2006 if the two sites were less than 5 kb apart. Timing information was thus available for 680 out of 876 origins (140 out of 170 CIOs). x-axis: timing of origin firing (data are from Heichinger et al. 2006 and represent the time of 50% replication of the origin), y-axis: difference in origin efficiency between *rad3Δ* and wild-type cells in the presence of HU (data from Supplemental Table S1). Red circles: CIOs, black circles: unaffected origins. The vertical blue line indicates the median firing time of the origins in the genome (78 min). Consistent with these data, 30% of RSOs fire with efficiencies greater than the median efficiency of all 876 origins identified in 6 mM HU (27.6%; data from Fig. 1B). **E)** Comparisons of CIOs with previous datasets of checkpoint-inhibited origins. Top: Number of deregulated origins identified in each study. For Feng *et al*., the total number of origins corresponds to those mapped in *cds1Δ*

(321), of which 241 were also identified in wild-type cells; the number of checkpoint-inhibited origins in this study as estimated by (Hayashi et al. 2007) is shown. Bottom: distributions of deregulated origins in the indicated experiments. Red: CIOs identified in our study; purple: deregulated origins from (Hayashi et al. 2007); green: deregulated origins from (Feng et al. 2006). **F)** To assess whether the distribution of CIOs was specific to our experimental conditions, we used an alternative method to synchronize cells using a cold-sensitive mutation of the *nda3* gene (*nda3-km311*). We first compared origin efficiencies in *cdc25-22* and *nda3-km311* cells treated with 6 mM HU and found that they are highly similar between cells synchronized in either G2 (*cdc25-22*) or M phase (*nda3-km311*) (left panel). In addition, analysis of *cdc25-22 rad3Δ* and *nda3-km311 rad3Δ* cells treated with 6 mM HU showed that replication initiation is highly comparable in these two genetic backgrounds (right panel). x-axis: origin efficiencies in *cdc25-22* (left) or *cdc25-22 rad3Δ* (right). y-axis: origin efficiencies in *nda3-km311* (left) or *nda3-km311 rad3Δ* (right). The lines indicate efficiencies if they were identical in the compared backgrounds. **G)** Deregulated origins in *nda3-km311 rad3Δ* (purple) and *cdc25-22 rad3Δ* (red) cells are clustered in the same late-firing and inefficient genomic regions. Bars indicate the positions of deregulated origins along the chromosomes. x-axis: chromosome coordinates.

Supplemental Figure S2

A

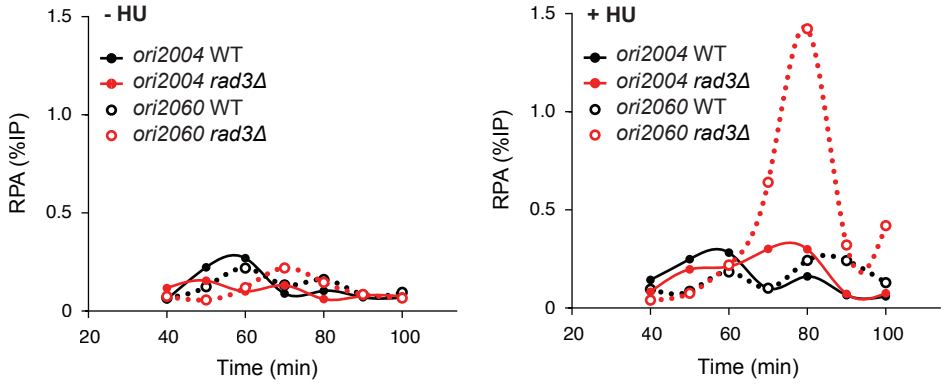

B_I

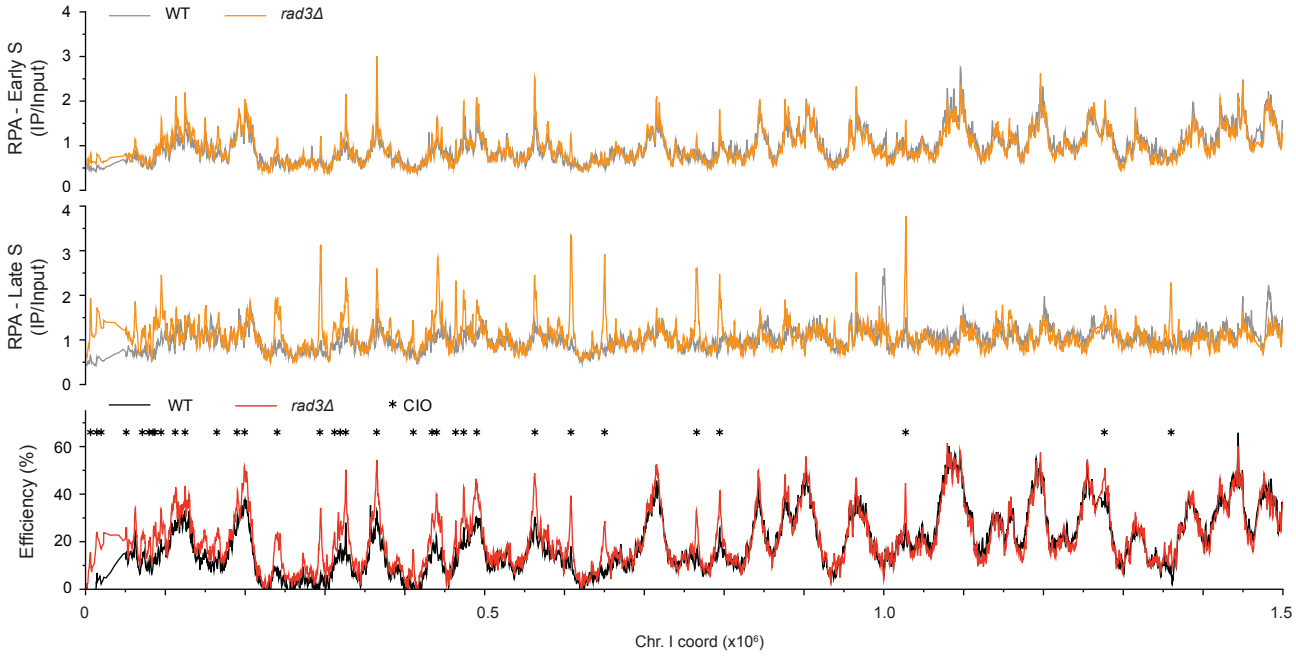

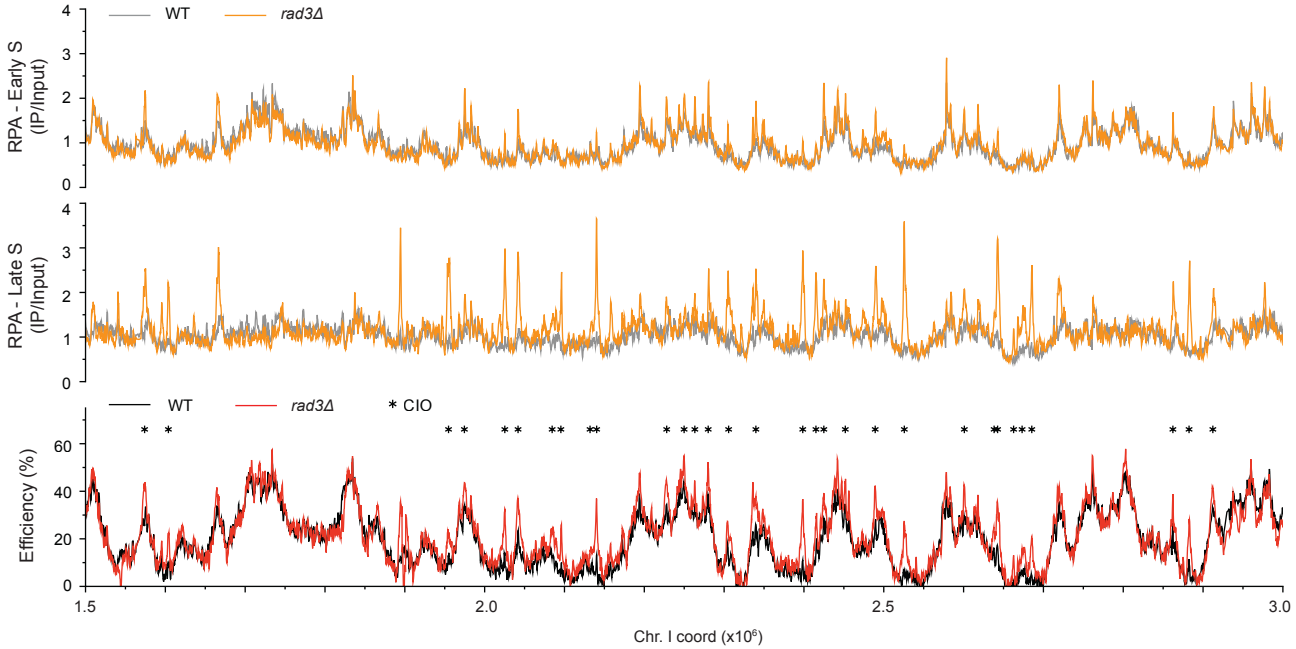

Supplemental Figure S2

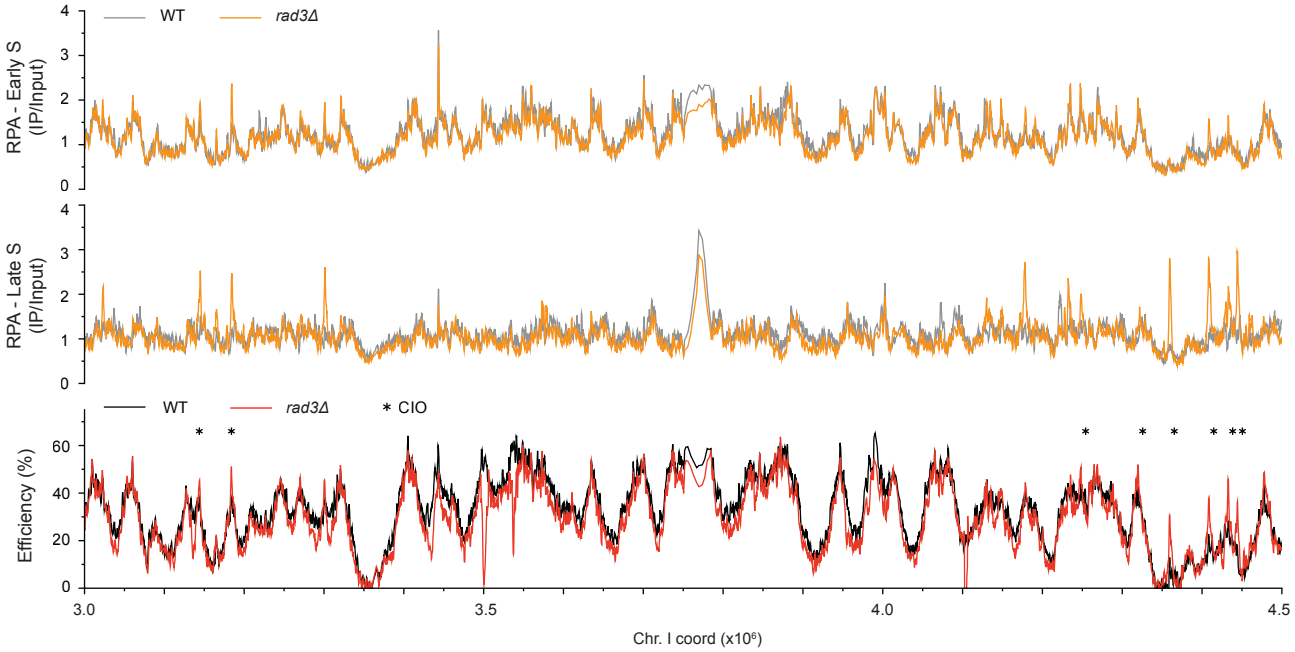

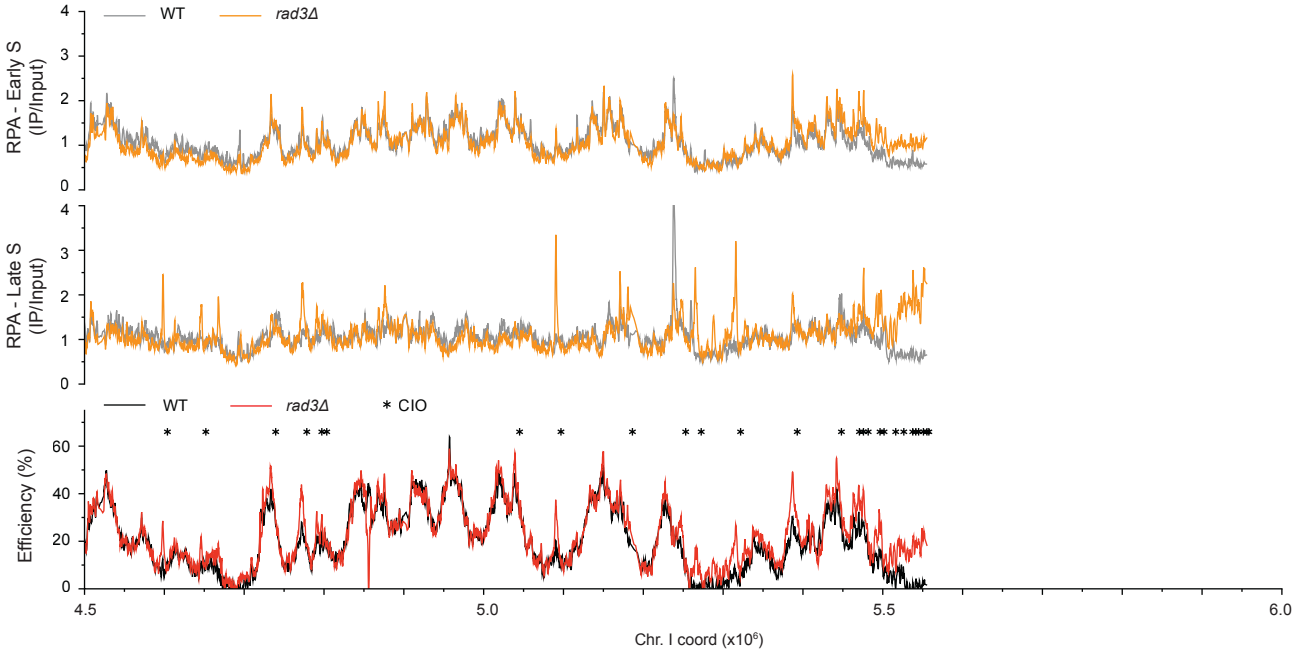

B_II

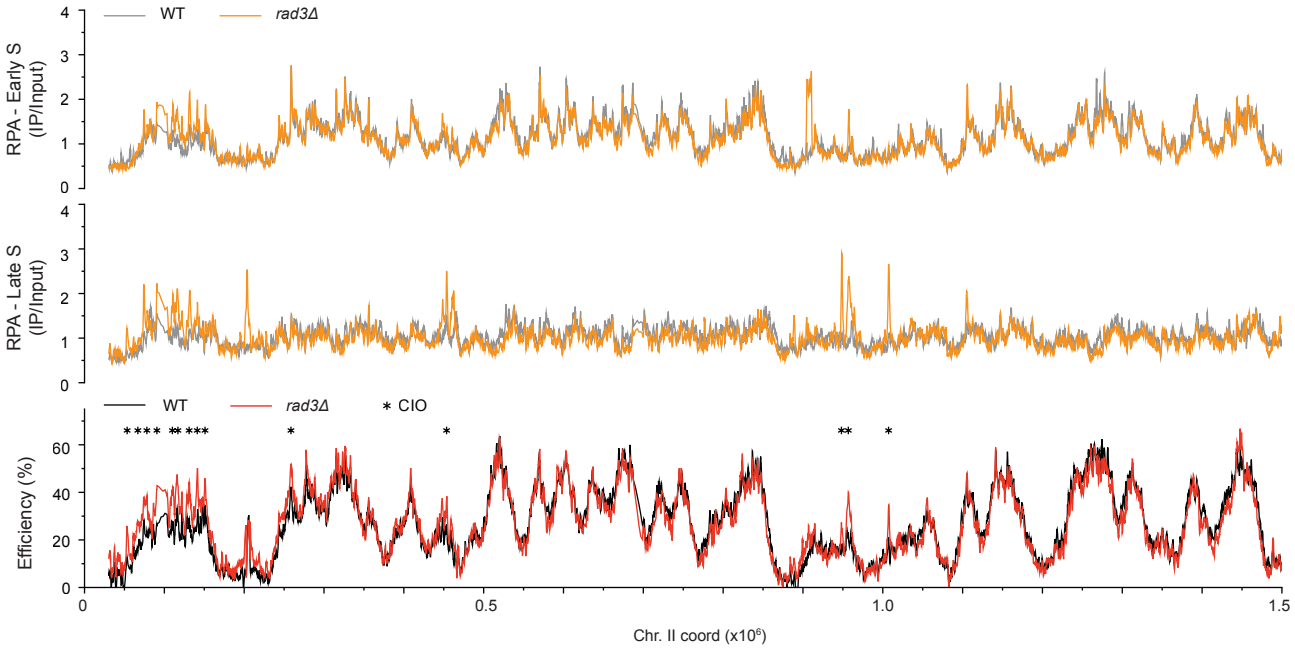

Supplemental Figure S2

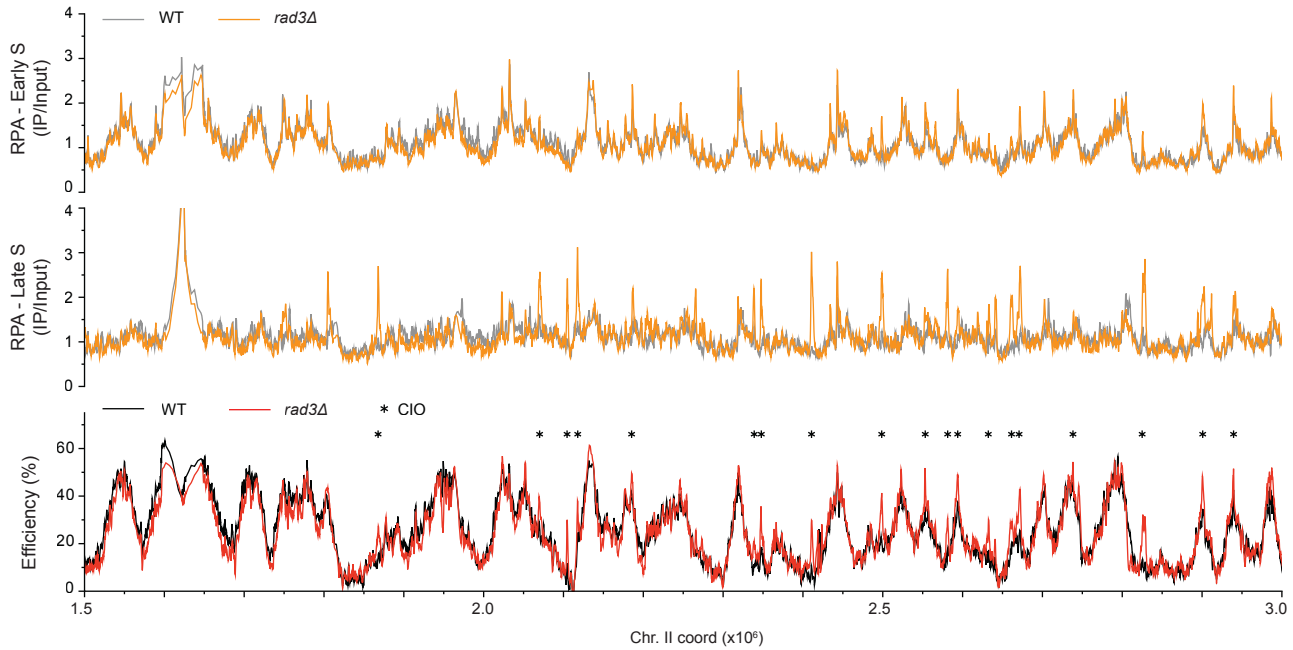

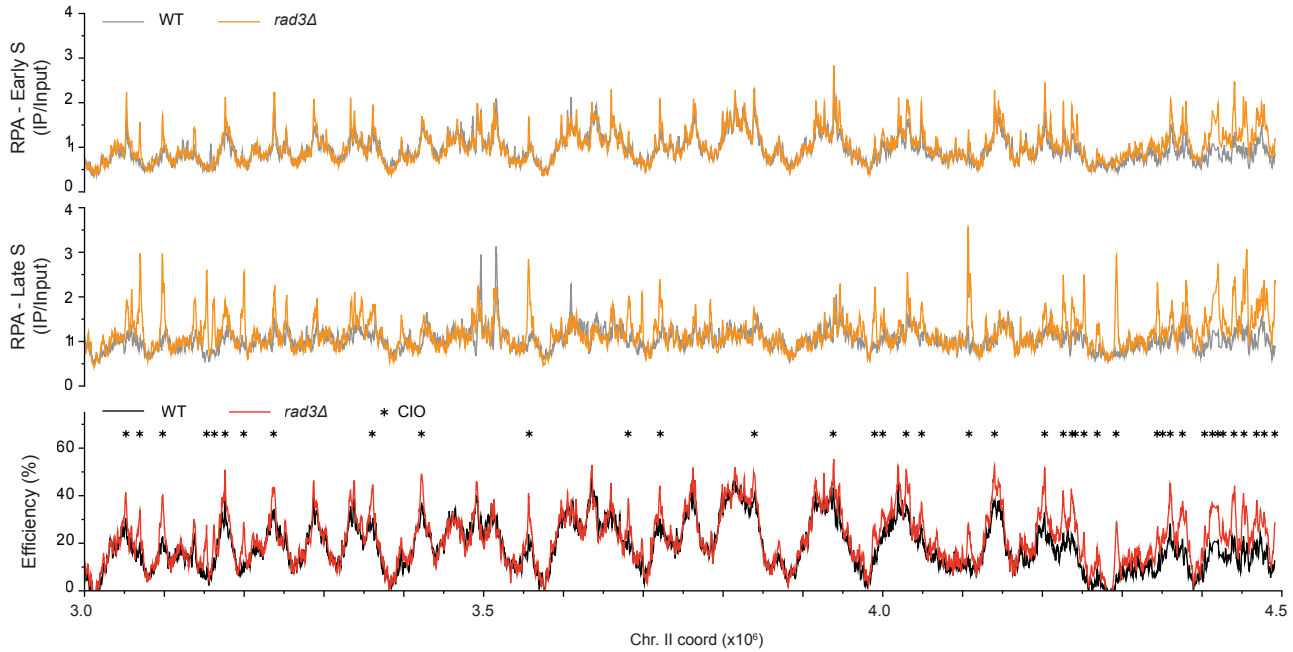

B_III

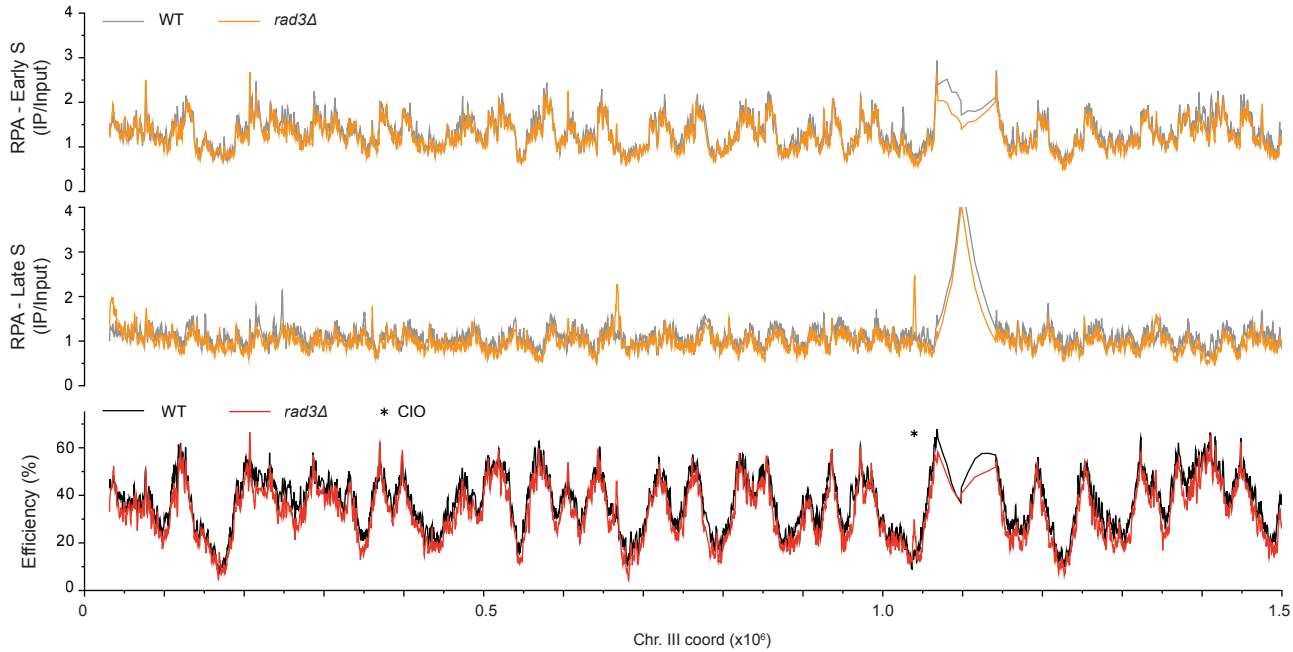

Supplemental Figure S2

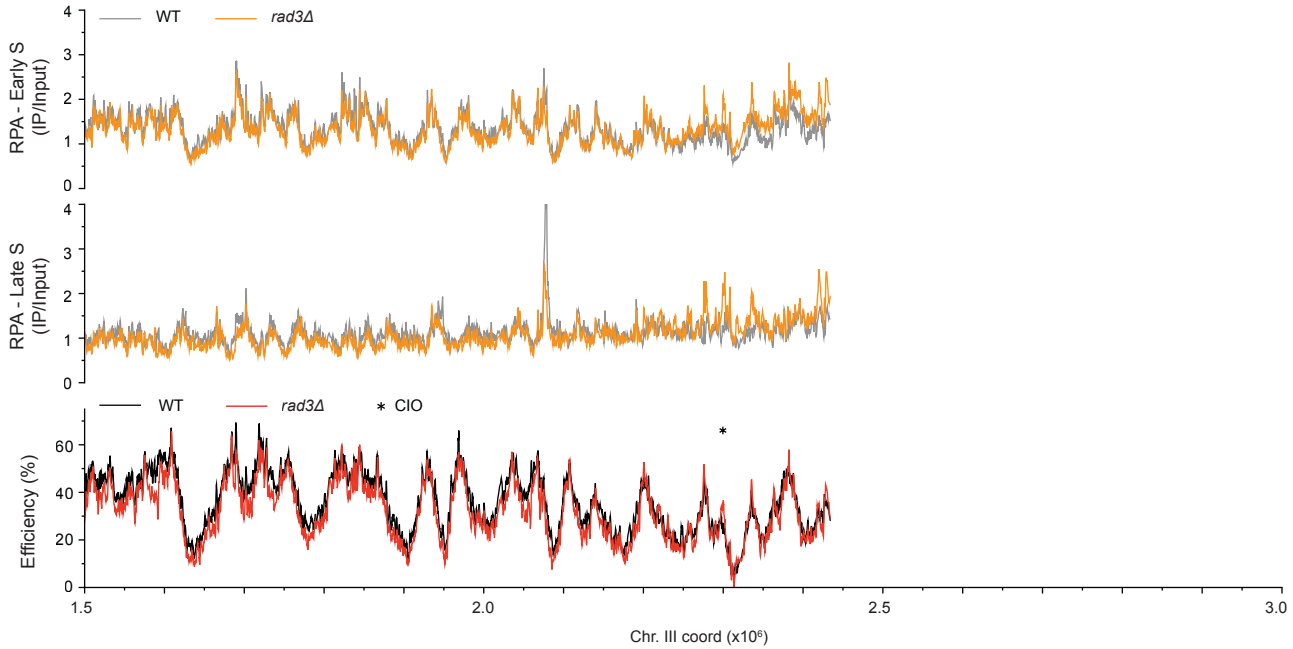

C

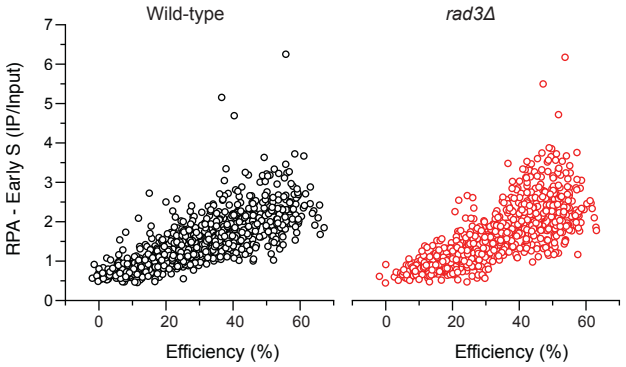

D

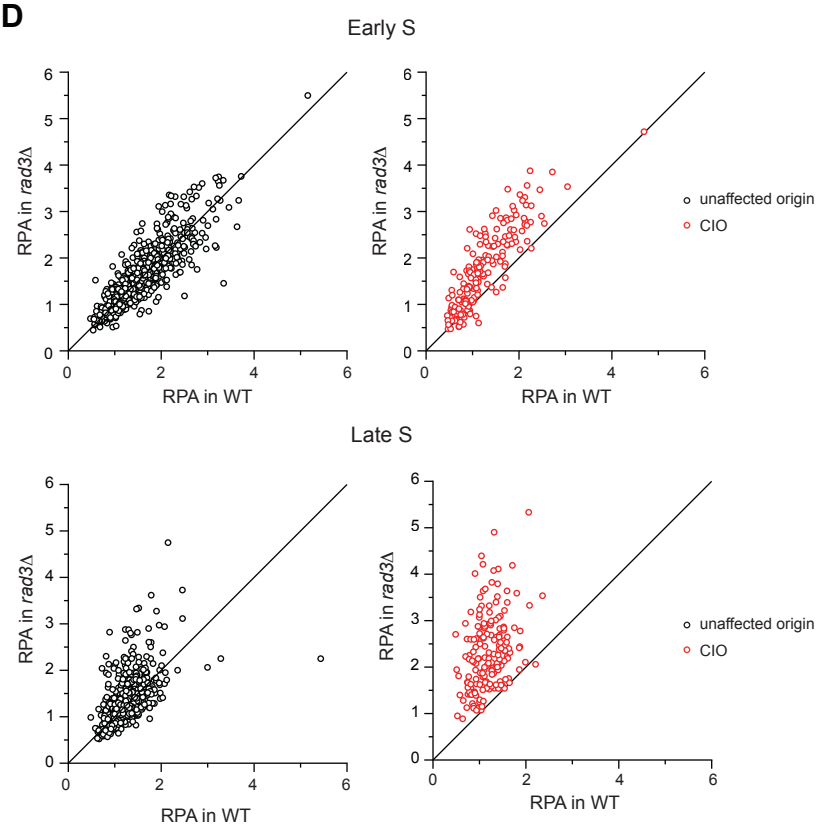

Supplemental Figure S2

E

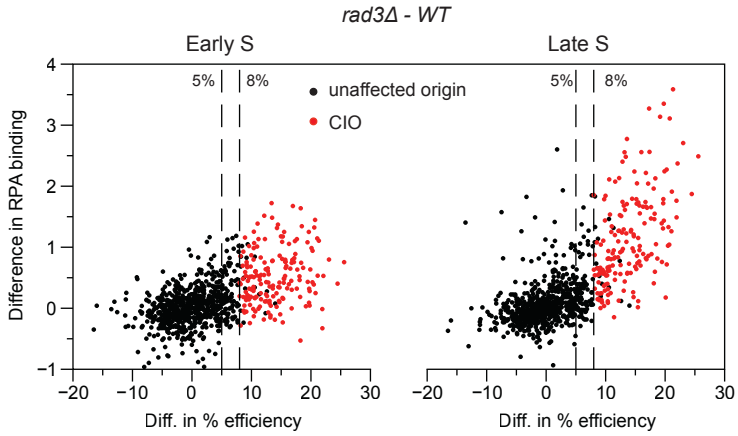

F

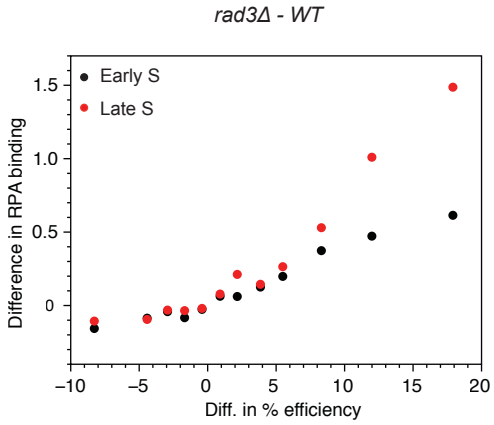

G

Total RPA peaks	153
RPA peaks associated with CIOs	102 (67%)
RPA peaks associated with unaffected origins	31 (20%)
CIOs associated with RPA peaks	97 (55%)
Unaffected origins associated with RPA peaks	31 (4%)
RPA peaks associated with origins	133 (87%)

Supplemental Figure S2: Analysis of ssDNA accumulation in HU-treated checkpoint-defective cells. **A)** Time course of Ssb1/RPA binding in *cdc25-22* (WT, black) and *cdc25-22 rad3Δ* (*rad3Δ*, red) cells at an unaffected origin (*ori2004*, closed circles) and a CIO (*ori2060*, open circles). Cells were released from G2 arrest in the absence or presence of HU and sampled at the indicated time points. Left: -HU, right: 6 mM HU. x-axis: time after release, y-axis: RPA occupancy (%IP). **B)** Genome-wide profiles of RPA binding in *cdc25-22* (gray, WT) and *cdc25-22 rad3Δ* (orange, *rad3Δ*) cells exposed to 6 mM HU. Top: RPA in early S phase (60 min), Middle: RPA in late S phase (80 min). Note that a number of origins have initiated replication at 60 min, as indicated by RPA binding (see also Fig. 2B-C) and by the flow cytometry profiles (Supplemental Fig. S1B); for simplicity and by comparison with the 80 min time point, we refer to this time point as "early S." y-axis: RPA binding (IP/input). Bottom: Origin efficiencies in wild-type (black, WT) and *rad3Δ* (red, *rad3Δ*) as in Supplemental Fig. S1C are shown for comparison. y-axis: origin efficiency. Asterisks indicate CIOs. For all panels, x-axis indicates chromosome coordinates. **C)** Analysis of RPA recruitment to origins in early S phase (60 min) in HU-treated wild-type (left panel) and *rad3Δ* (right panel) cells. RPA levels are highly correlated with origin efficiencies in both backgrounds. Each circle represents an origin. x-axis: origin efficiency; y-axis: RPA binding (IP/Input). **D)** Comparison of RPA levels (IP/input) between HU-treated wild-type (x-axis) vs. *rad3 Δ* (y-axis) cells. Top panels: Early S phase, Bottom panels: Late S phase. Black circles: unaffected origins, red circles: CIOs. Left: Correspondence between the levels of RPA recruited to unaffected origins. Right: Higher RPA levels are recruited to CIOs in *rad3Δ* cells in both early and late S phase. In all graphs, the diagonal line indicates RPA levels if they were identical in wild-type and *rad3Δ*. **E)** Correlation of the differences in RPA binding and the differences in origin usage between *rad3Δ* and wild-type (WT) in early (left plot) and late (right plot) S phase. Black: unaffected origins; red: CIOs. Dotted lines mark 5% and 8% differences in absolute efficiency between *rad3Δ* and WT. x-axes: difference in origin efficiency (*rad3Δ* - WT), y-axis: difference in RPA binding (*rad3Δ* - WT). **F)** Correlation between the differences in RPA binding and in origin usage between *rad3Δ* and wild-type (WT) as in Fig. 2E, except with data from both early (black dots) and late (red dots) S phase. Non-averaged data are as in *E*. Origins were divided into 12 equal subsets (73 origins/group) based on the changes in their efficiencies (*rad3Δ* – WT). The average differences in efficiency (x-axis) and in RPA occupancy (y-axis) for each group are shown. **G)** Comparison of sites of significant RPA binding (cutoff = 2.0) with CIOs.

Supplemental Figure S3

A

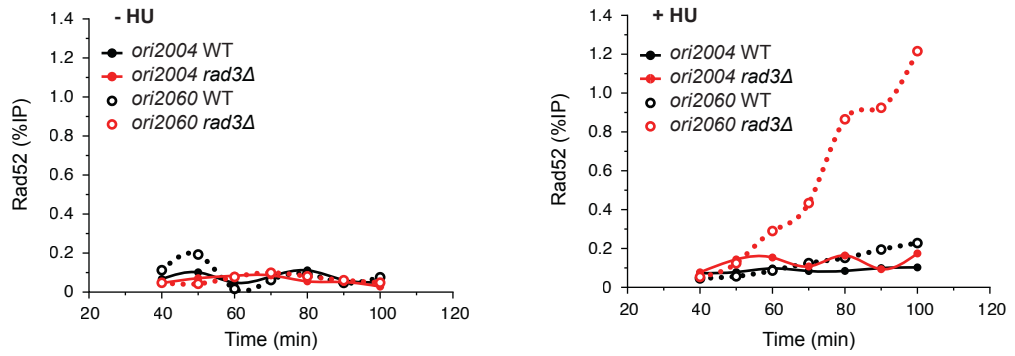

B_I

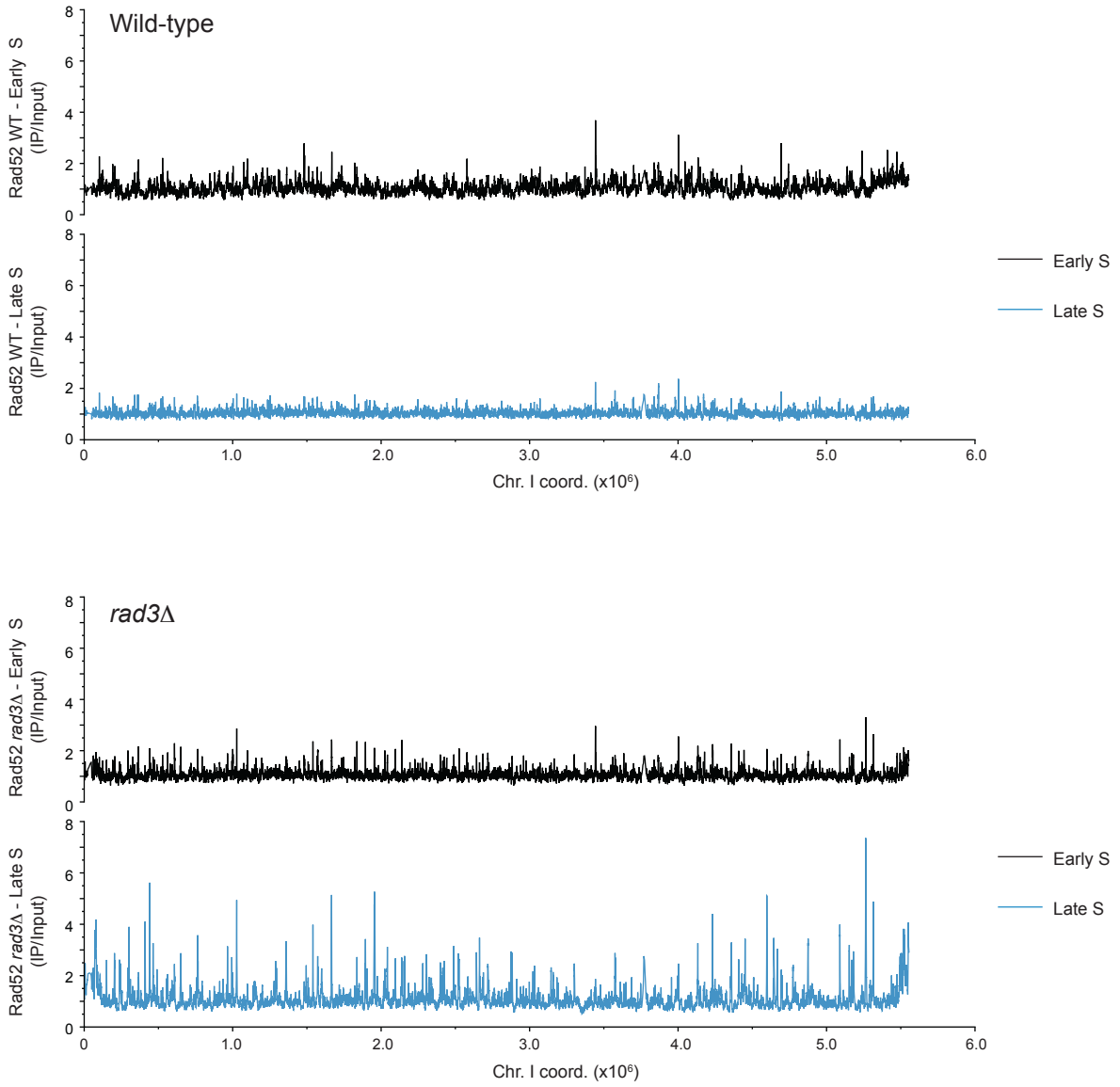

Supplemental Figure S3

B_II

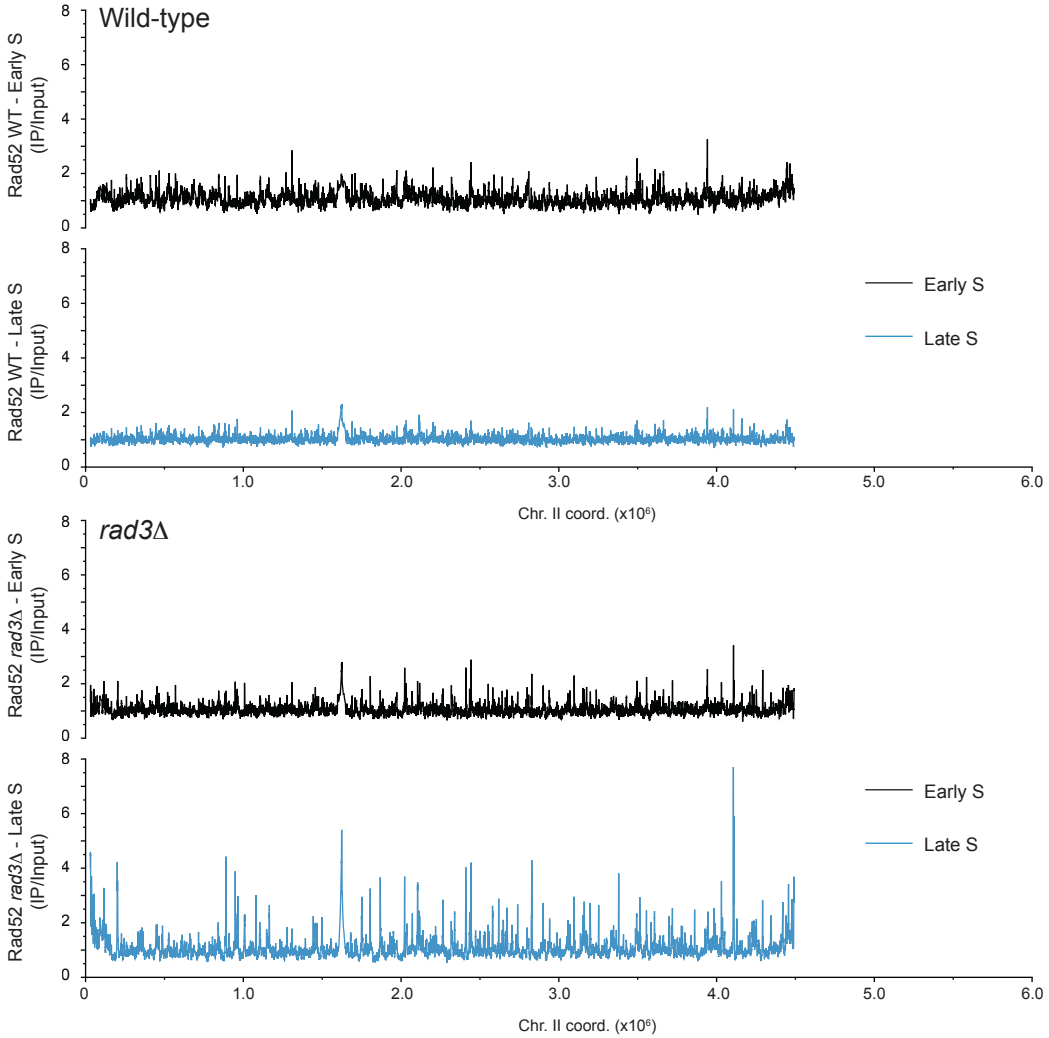

B_III

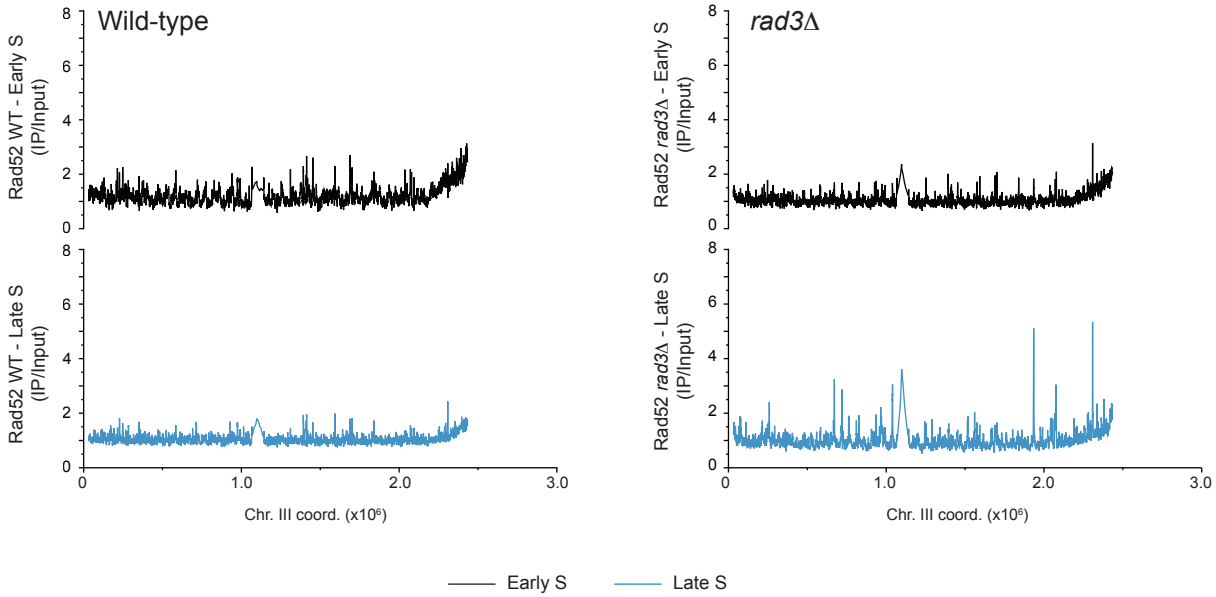

Supplemental Figure S3

C

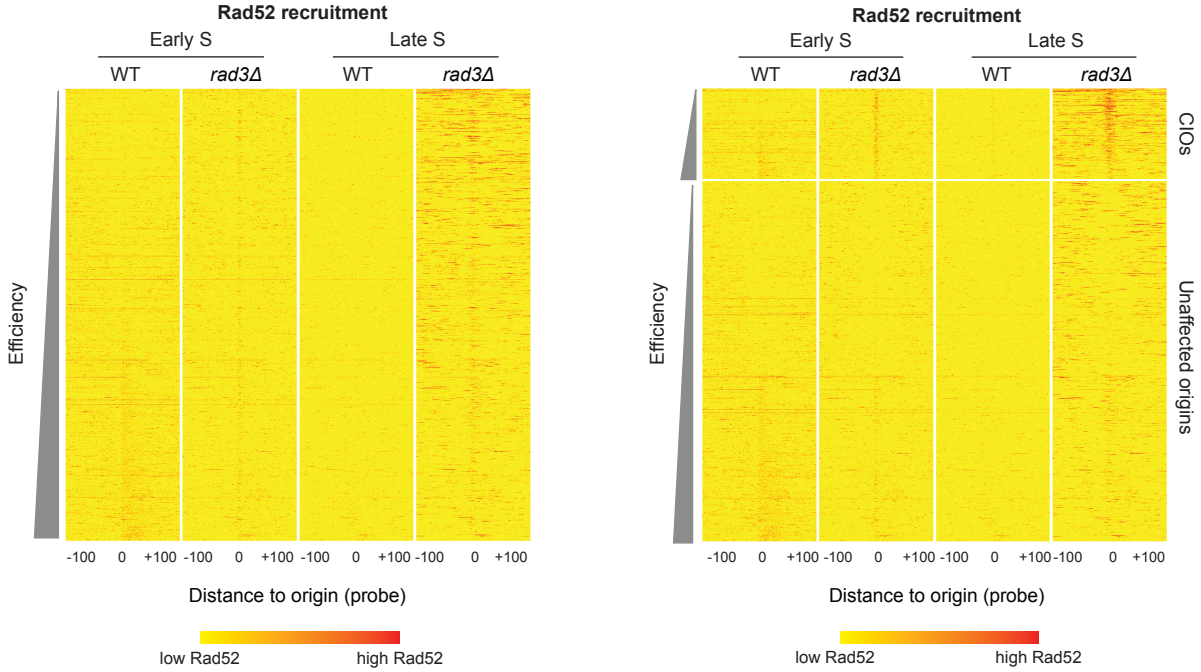

D

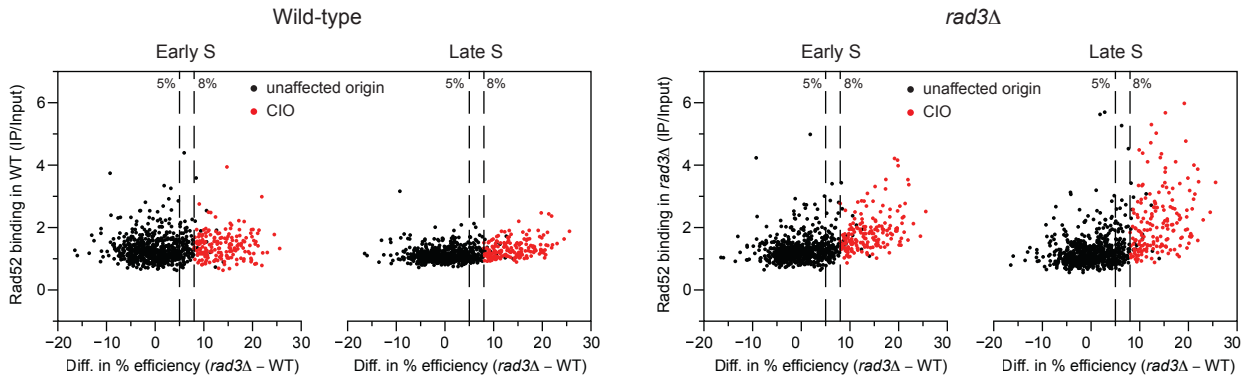

E

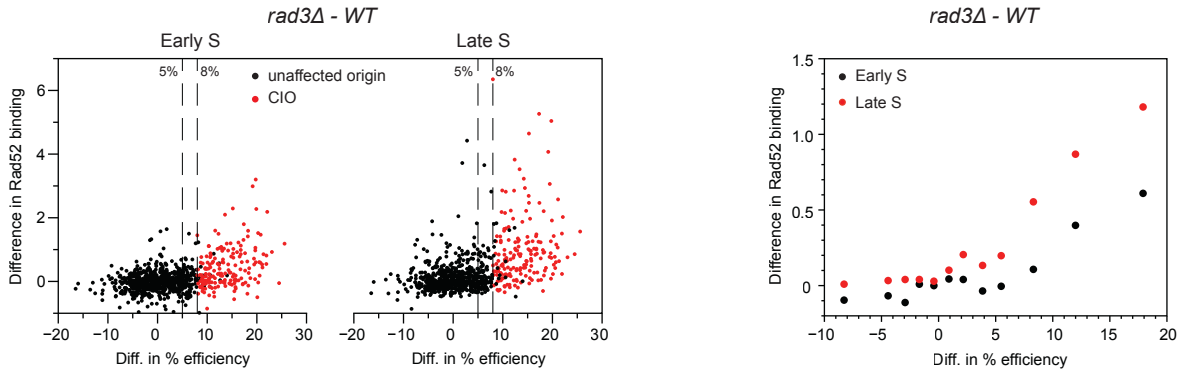

F

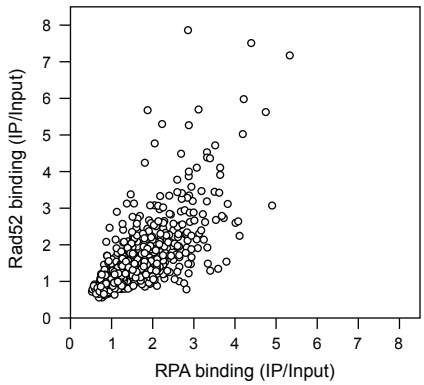

Supplemental Figure S3

G_I

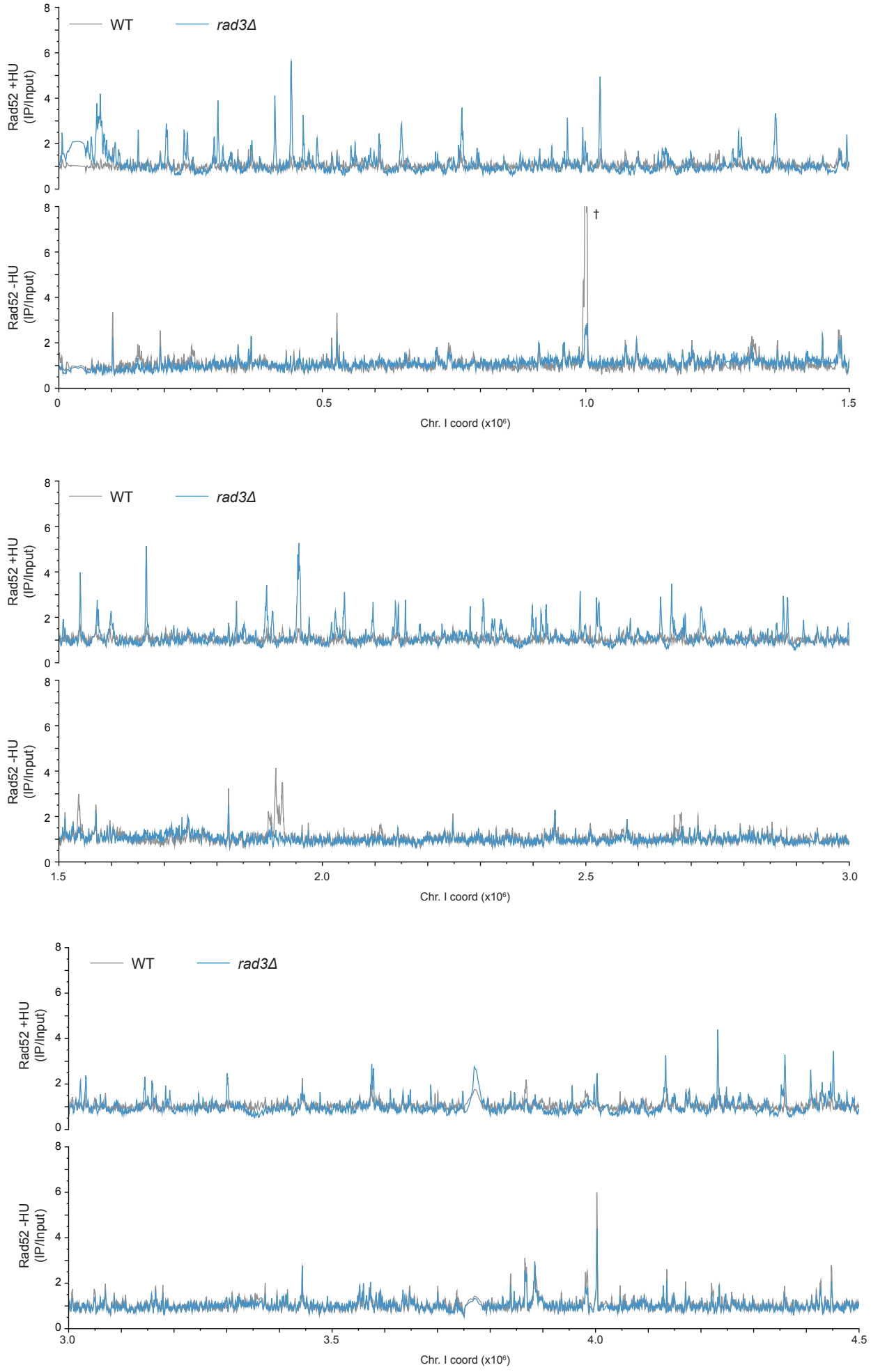

Supplemental Figure S3

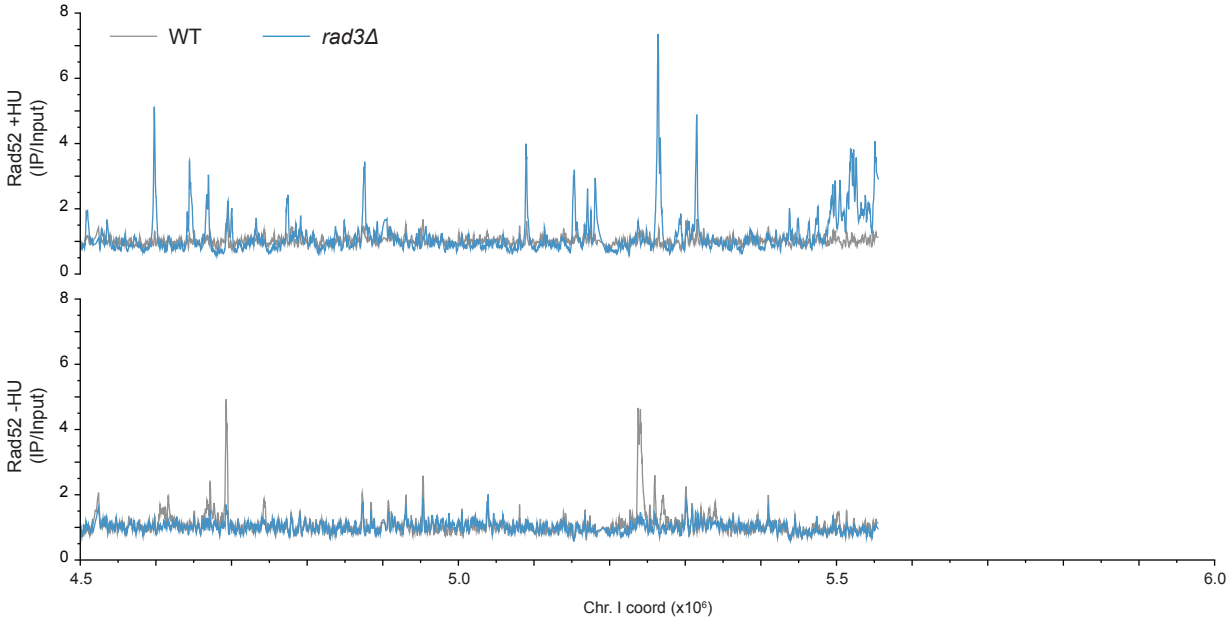

G_II

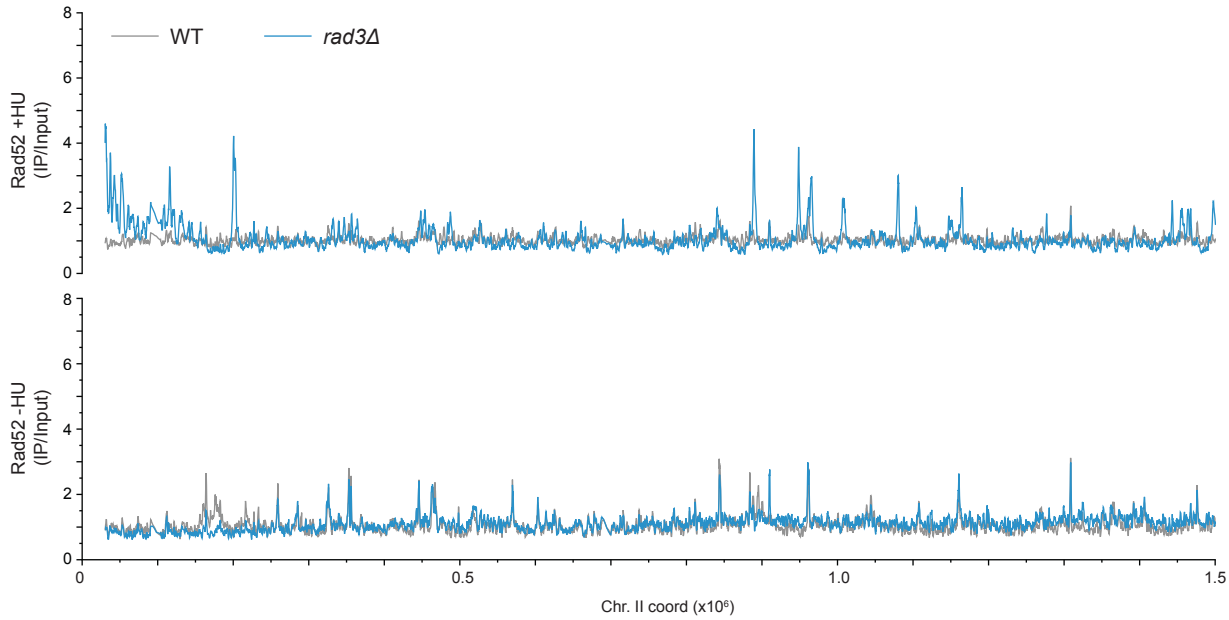

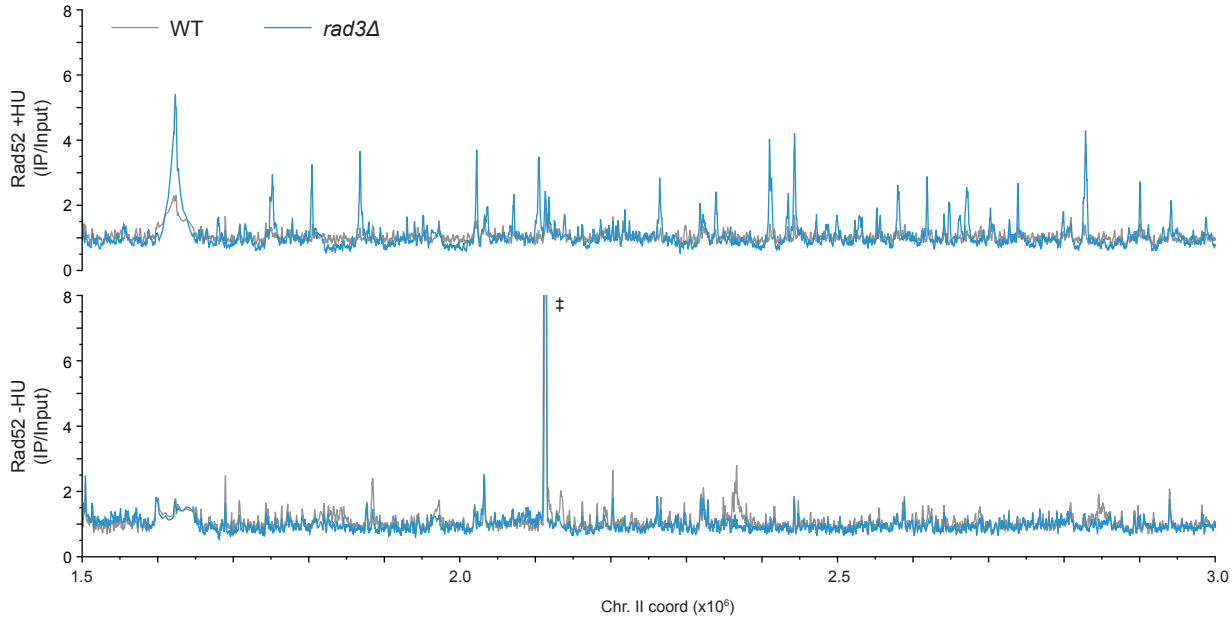

Supplemental Figure S3

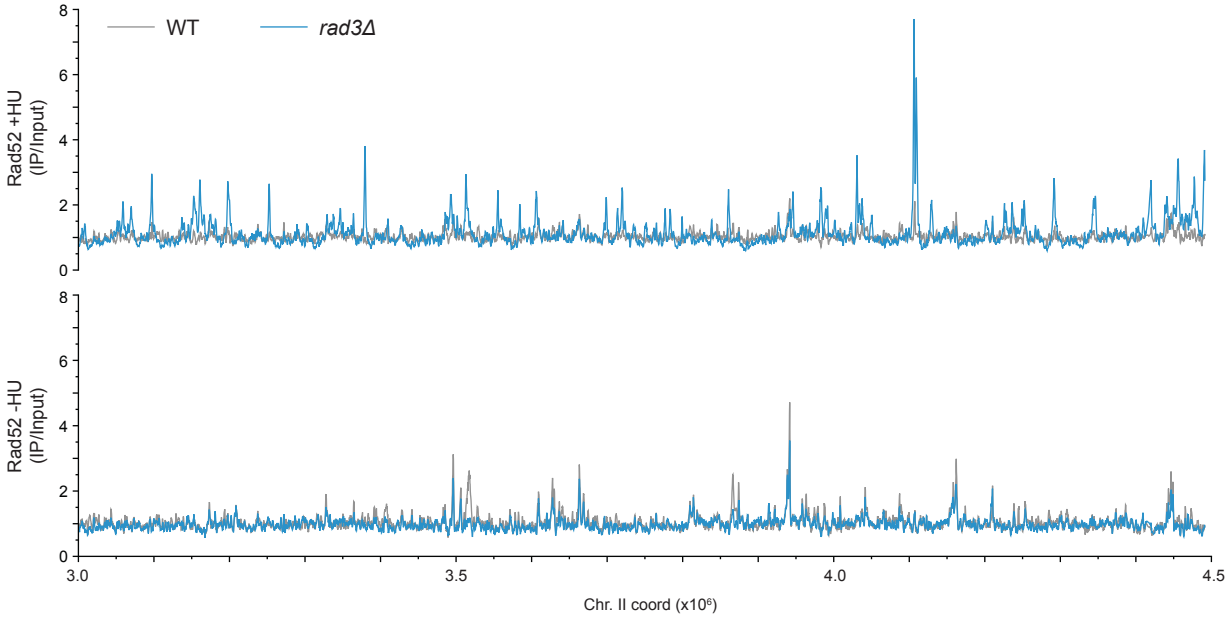

G_III

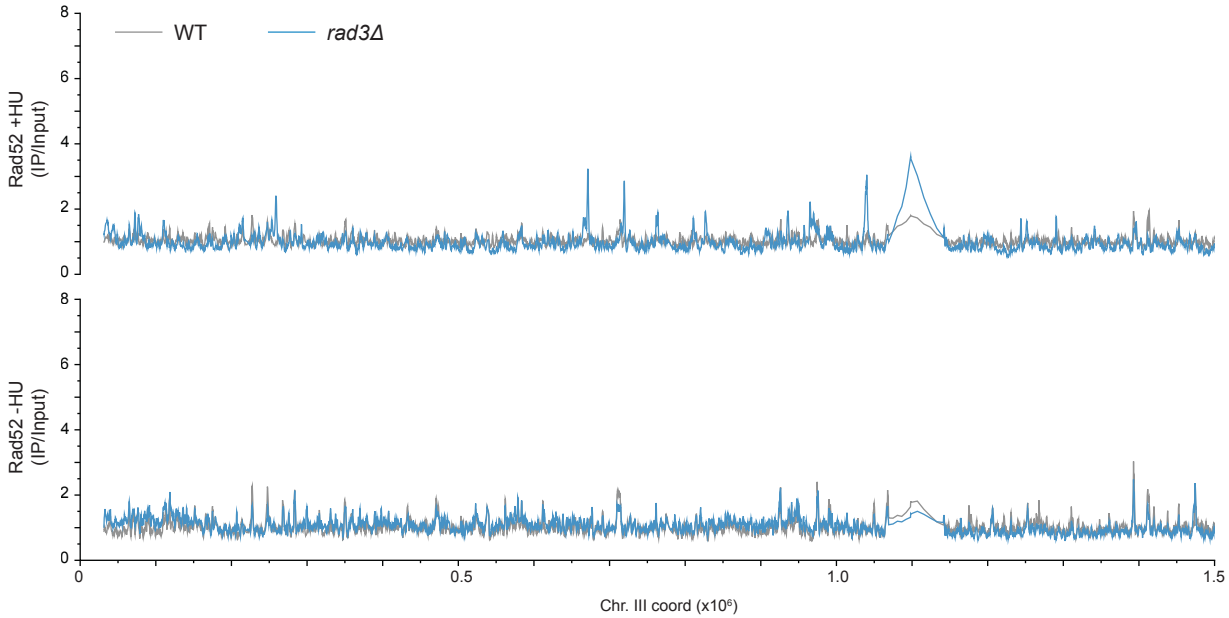

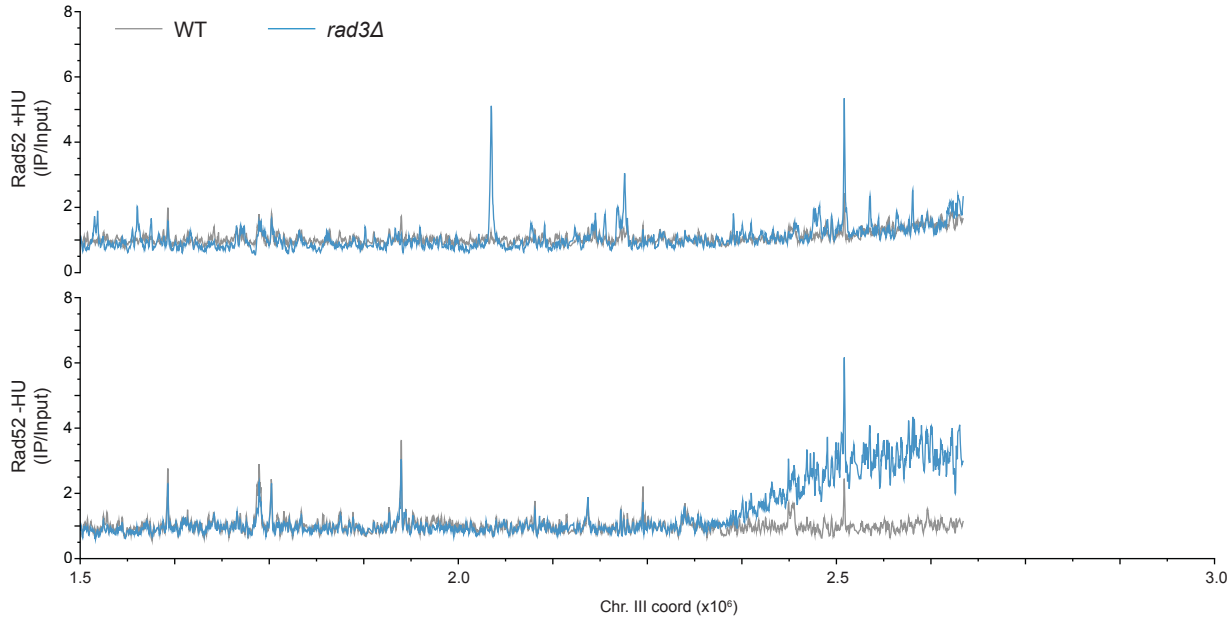

Supplemental Figure S3

H

		+ HU	- HU
wild-type	Total Rad52 peaks	64	216
	Rad52 peaks associated with CIOs	7 (11%)	11 (5%)
	Rad52 peaks associated with unaffected origins	13 (20%)	63 (29%)
	Rad52 peaks associated with origins	20 (31%)	73 (34%)
	CIOs associated with Rad52 peaks	8 (5%)	11 (6%)
	Unaffected origins associated with Rad52 peaks	14 (2%)	62 (9%)
	Origins associated with Rad52 peaks	22 (2.5%)	73 (8.3%)
rad3Δ	Total Rad52 peaks	435	215
	Rad52 peaks associated with CIOs	136 (31%)	9 (4%)
	Rad52 peaks associated with unaffected origins	135 (31%)	74 (34%)
	Rad52 peaks associated with origins	271 (62%)	84 (39%)
	CIOs associated with Rad52 peaks	124 (70%)	9 (5%)
	Unaffected origins associated with Rad52 peaks	130 (18%)	65 (9%)
	Origins associated with Rad52 peaks	254 (30%)	74 (8.4%)

Co-localization of origins with Rad52 sites

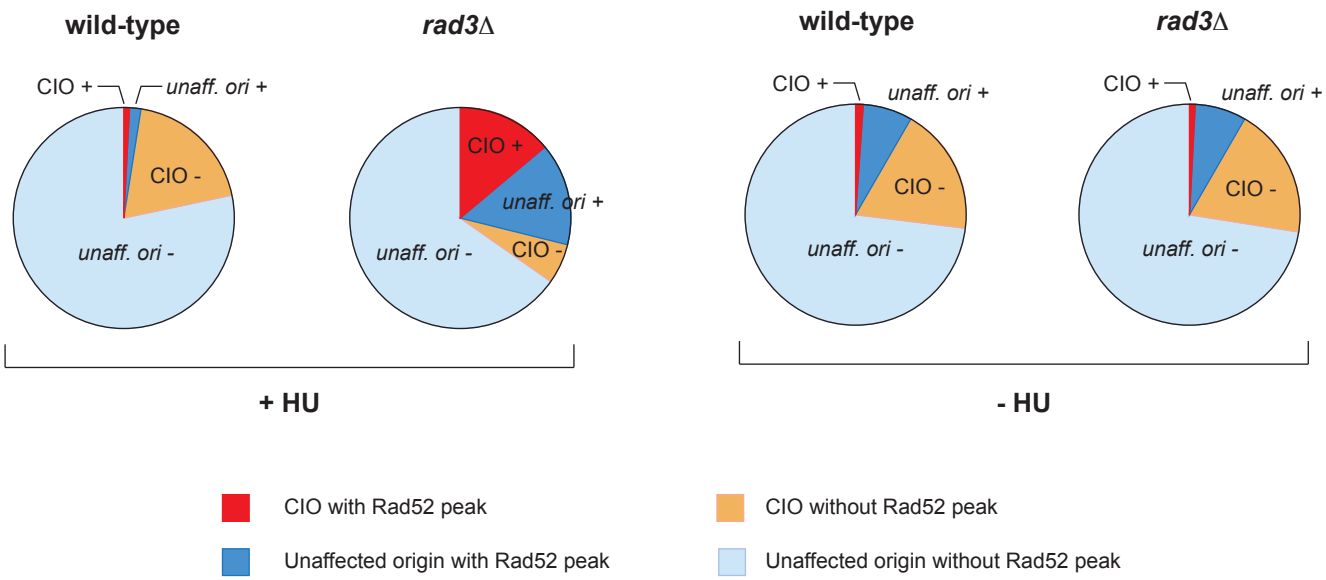

Supplemental Figure S3: Analysis of Rad52 accumulation in HU-treated checkpoint-defective cells. **A)** Time course of Rad52 binding in *cdc25-22* (WT, black) and *cdc25-22 rad3Δ* (*rad3Δ*, red) cells at an unaffected origin (*ori2004,* closed circles) and a CIO (*ori2060*, open circles). Experiment was performed as for Supplemental Fig. S2A. Left: -HU, right: 6 mM HU. x-axis: time after release from G2 arrest, y-axis: Rad52 occupancy (%IP). **B)** Genome-wide profiles of Rad52 binding in *cdc25-22* (WT) and *cdc25-22 rad3Δ* (*rad3Δ*) cells exposed to 6 mM HU. Black: early S (60 min), blue: late S (90 min). x-axis: chromosomal coordinates, y-axis: Rad52 binding (IP/input). Our data show low levels of Rad52 binding across the genome in early S in HU-treated wild-type and *rad3Δ* cells. In late S, Rad52 is clearly recruited at high levels to a number of loci only in *rad3Δ* cells. **C)** Heat maps of Rad52 recruitment at origins in HU-treated wild-type (WT) and *rad3Δ* cells in early and late S phase. Data are from ChIP-chip experiments in Fig. 3A and Supplemental Fig. S3B. Left: All origins are shown in order of increasing efficiency; the most efficient origins are at the bottom of the plot. Right: Origins are divided into two categories: unaffected origins and CIOs (data are the same as in the left panel). Origins in each category are displayed in order of increasing efficiency. Position 0: central probe for each origin; values in a window of 100 probes on either side of each origin are displayed. A more intense red represents a higher level of Rad52. In *rad3Δ* cells, Rad52 binding at CIOs is detectable at low levels in early S phase and increases through late S. In contrast, we do not detect high levels of Rad52 accumulation at unaffected origins in either early or late S phase. Similarly, Rad52 is not significantly enriched at either unaffected origins or CIOs in wild-type cells. **D)** Levels of Rad52 binding at origins in the indicated backgrounds in the presence of HU (left panel, WT; right panel, *rad3Δ*) vs. differences in origin usage between HU-treated *rad3Δ* and WT cells. For each panel, left plot: early S, right plot: late S. Black: unaffected origins; red: CIOs. Dotted lines mark 5% and 8% differences in absolute efficiency between *rad3Δ* and WT. x-axis: difference in origin efficiency (*rad3Δ* - WT), y-axis: Rad52 binding (IP/input). In contrast to wild-type, a low level of Rad52 enrichment is observed at a subset of CIOs in *rad3Δ* cells in early S phase, and Rad52 recruitment is significantly increased at CIOs in late S. **E)** Correlation between the differences in Rad52 binding at origins and the differences in origin usage between HU-treated *rad3Δ* and WT cells. Left panel, left plot: early S, right plot: late S. Black: unaffected origins; red: CIOs. Dotted lines mark 5% and 8% differences in absolute efficiency between *rad3Δ* and WT. x-axis: difference in origin efficiency (*rad3Δ* - WT), y-axis: difference in Rad52 binding (*rad3Δ* - WT). Right panel: data from the left panel are grouped into 12 equal subsets of origins (73 per group) based on the changes in

their efficiencies (*rad3Δ* – WT). The average differences in efficiency (x-axis) and in Rad52 occupancy (y-axis) for each group are shown. **F)** Direct correspondence between the levels of Rad52 and RPA binding at origins in late S phase. x-axis: level of RPA (IP/Input), y-axis: level of Rad52 (IP/input). Each circle represents an origin. **G)** Genome-wide profiles of Rad52 binding in *cdc25-22* (gray, WT) and *cdc25-22 rad3Δ* (blue, *rad3Δ*) cells. Cells were released from G2 arrest and allowed to undergo S phase in 6 mM HU (Top, data as in *B*) or in the absence of HU (Bottom). Samples were collected in late S phase (90 min after the release). x-axis: chromosomal coordinates, y-axis: Rad52 binding (IP/input). For ease of visualization, the full amplitudes of the following peaks are not shown in the graph: † (chr I: 998594; WT – 12.00); ‡ (chr II: 2113263; WT – 21.41, *rad3Δ* - 25.41). **H)** Comparison of sites of significant Rad52 binding (cutoff = 1.5) in the different conditions. Pie charts indicate the proportions of CIOs and unaffected origins that are associated with Rad52 peaks. Red: CIOs that colocalize with a Rad52 site (CIO +), blue: unaffected origins that colocalize with a Rad52 site (unaff. ori +), orange: CIOs not associated with a Rad52 site (CIO -), light blue: unaffected origins not associated with a Rad52 site (unaff. ori. -).

Supplemental Figure S4

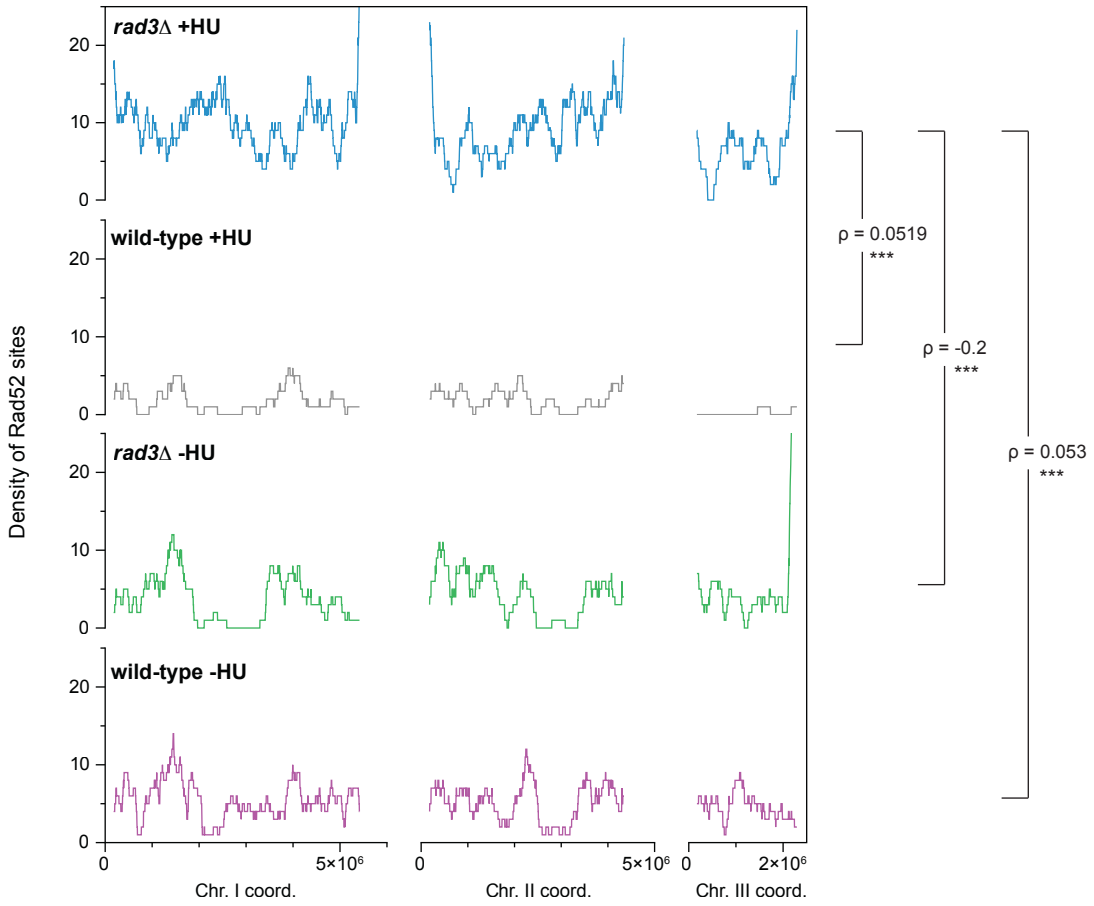

Supplemental Figure S4: Checkpoint-defective cells exposed to replication stress display a unique distribution of Rad52 hotspots. Regional comparisons of Rad52 binding sites in *rad3Δ* (blue) and wild-type (gray) cells in 6 mM HU or *rad3Δ* (green) and wild-type (purple) cells in the absence of HU. Data are from analyses of the ChIP-chip experiments in Supplemental Figs. S2B and S3B. The densities of Rad52 sites were calculated over continuous 1000-probe windows, as in Fig. 4. x-axis: chromosome coordinates; y-axis: density of Rad52 sites. The Spearman's correlation coefficients for the different comparisons are indicated and show no correspondence between *rad3Δ* +HU and the other conditions. ***: p-value<0.001.

Supplemental Figure S5

A

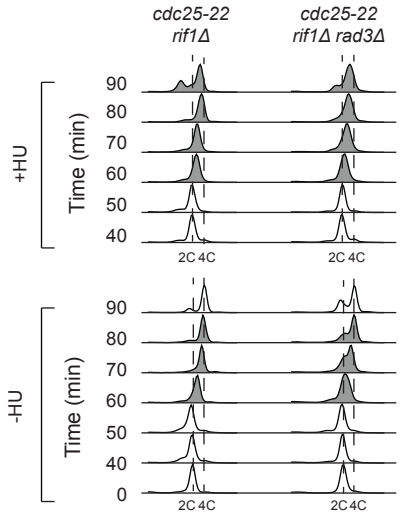

B

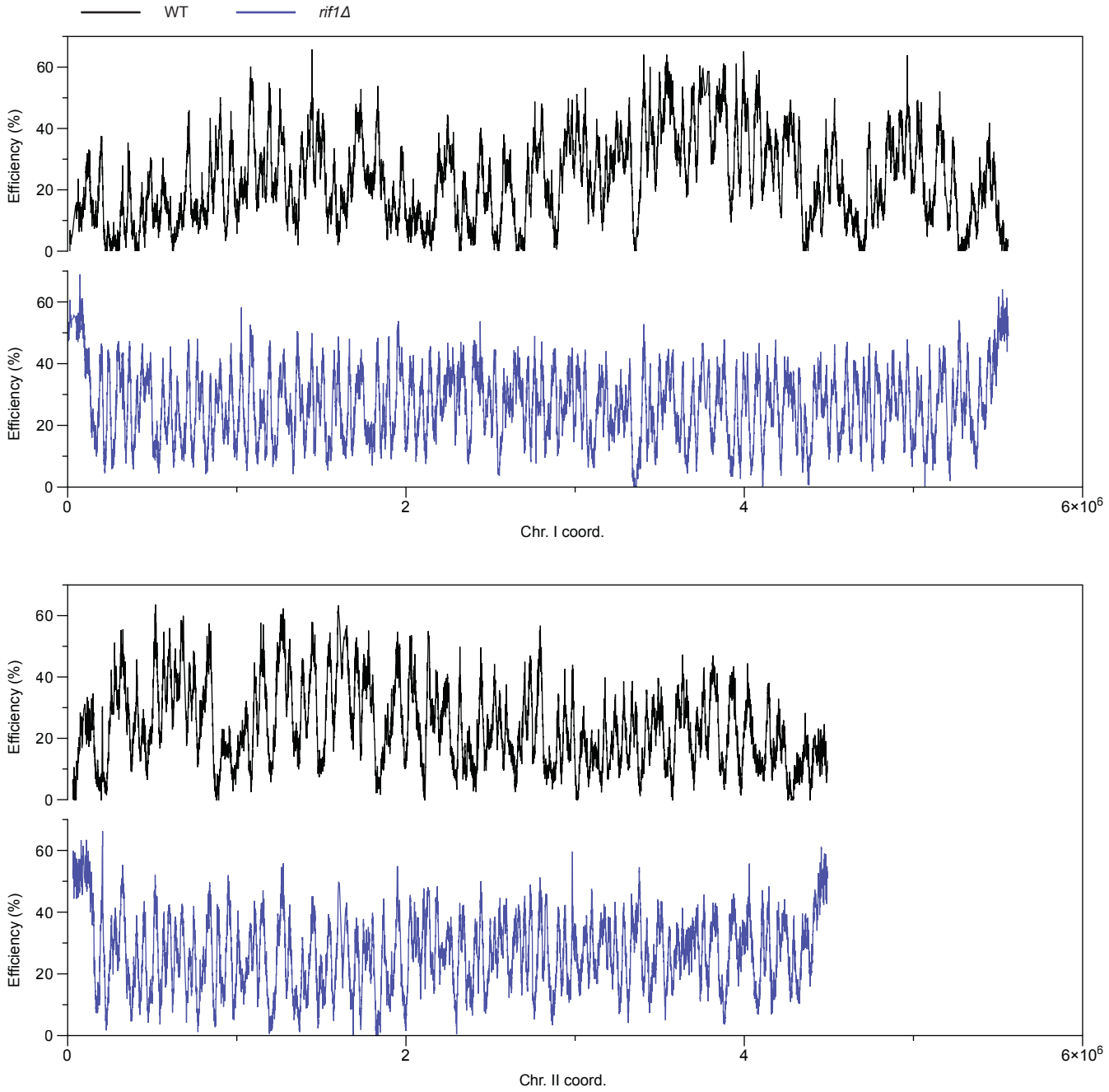

Supplemental Figure S5

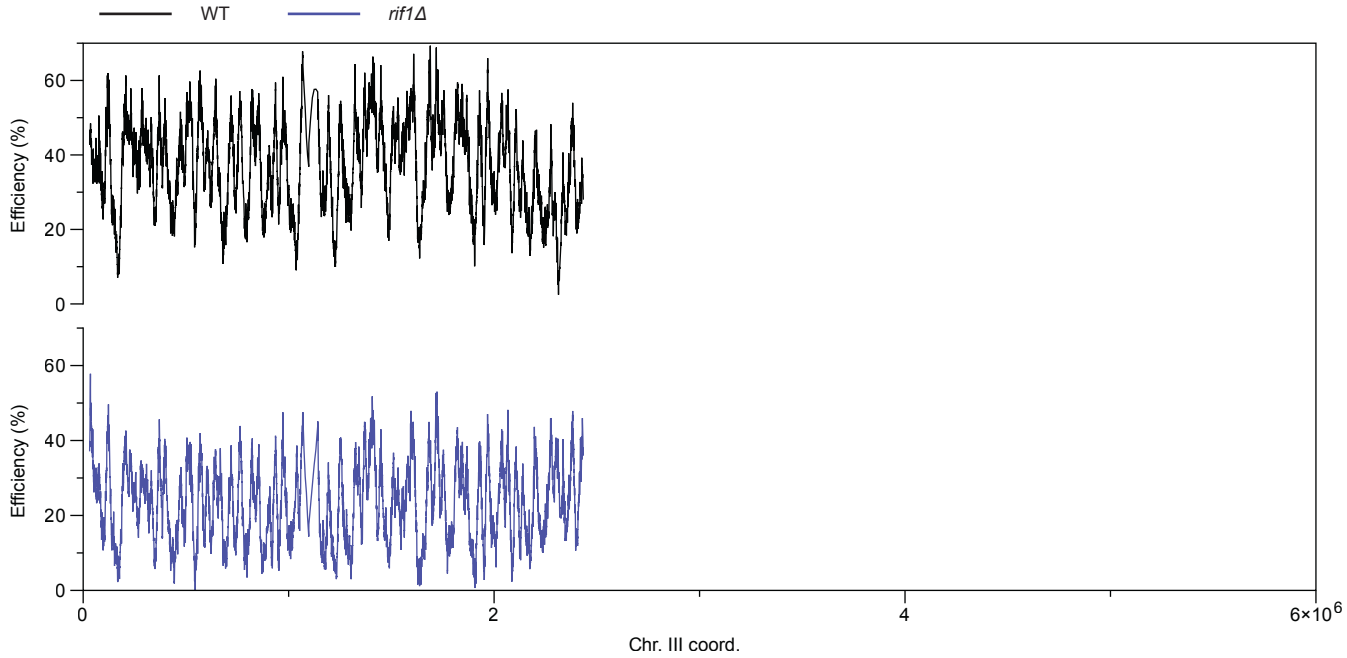

C_I

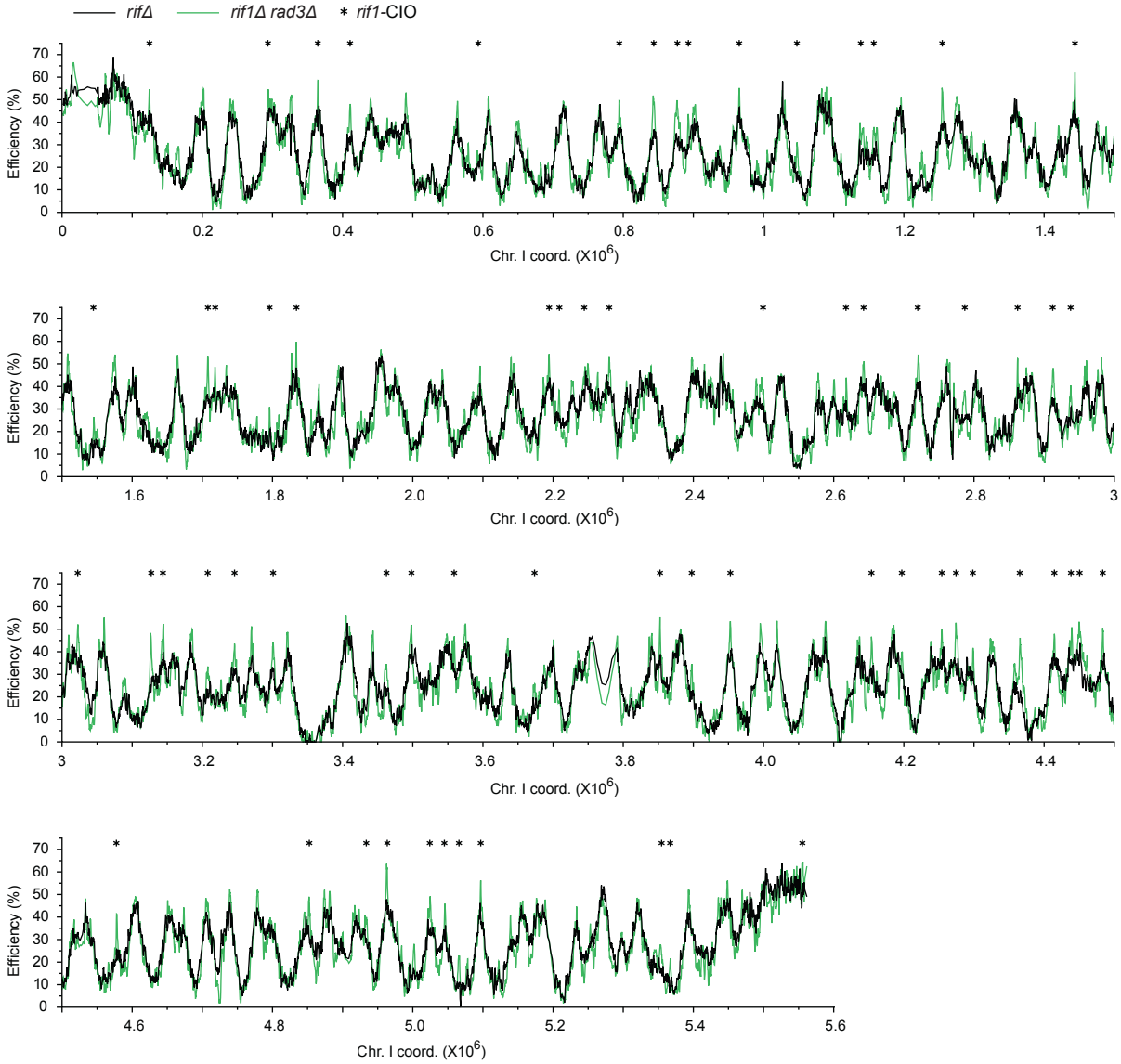

Supplemental Figure S5

C_II

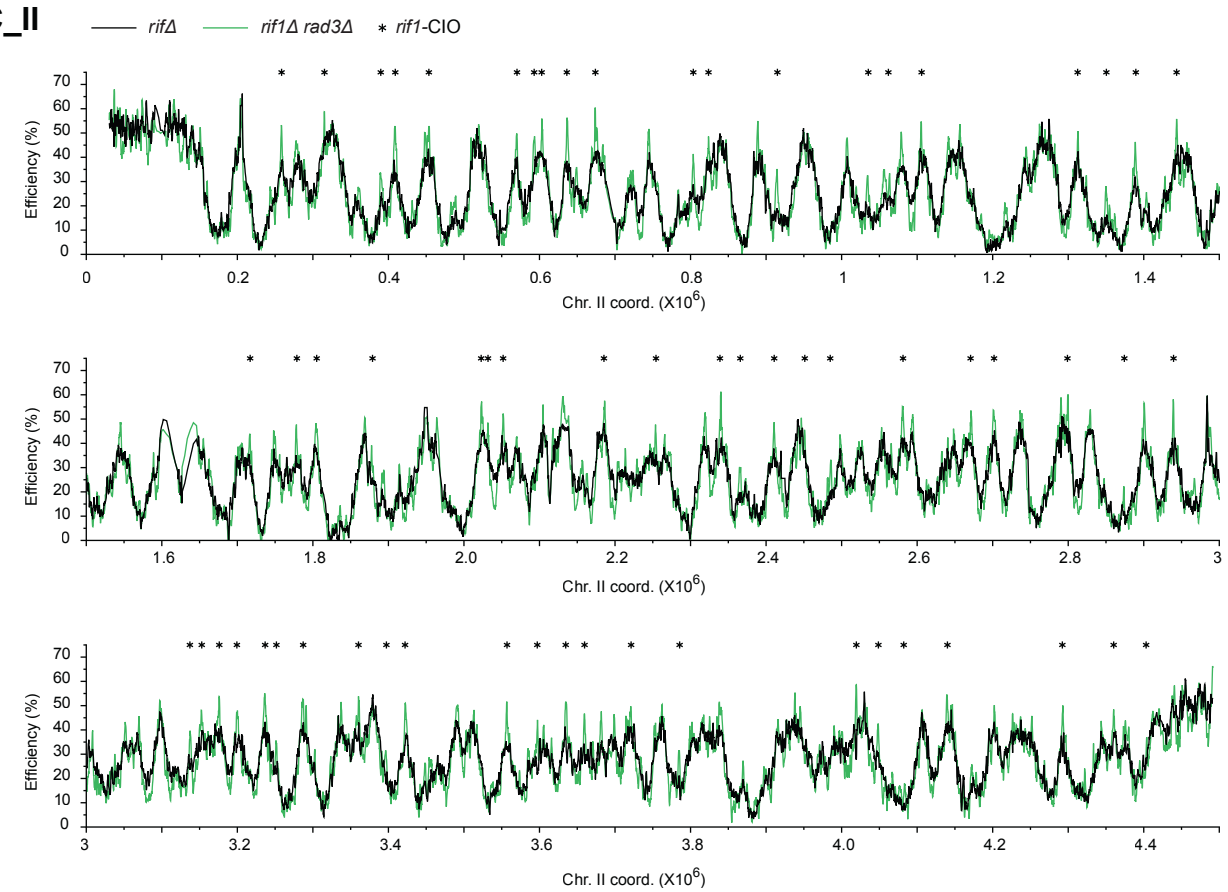

C_III

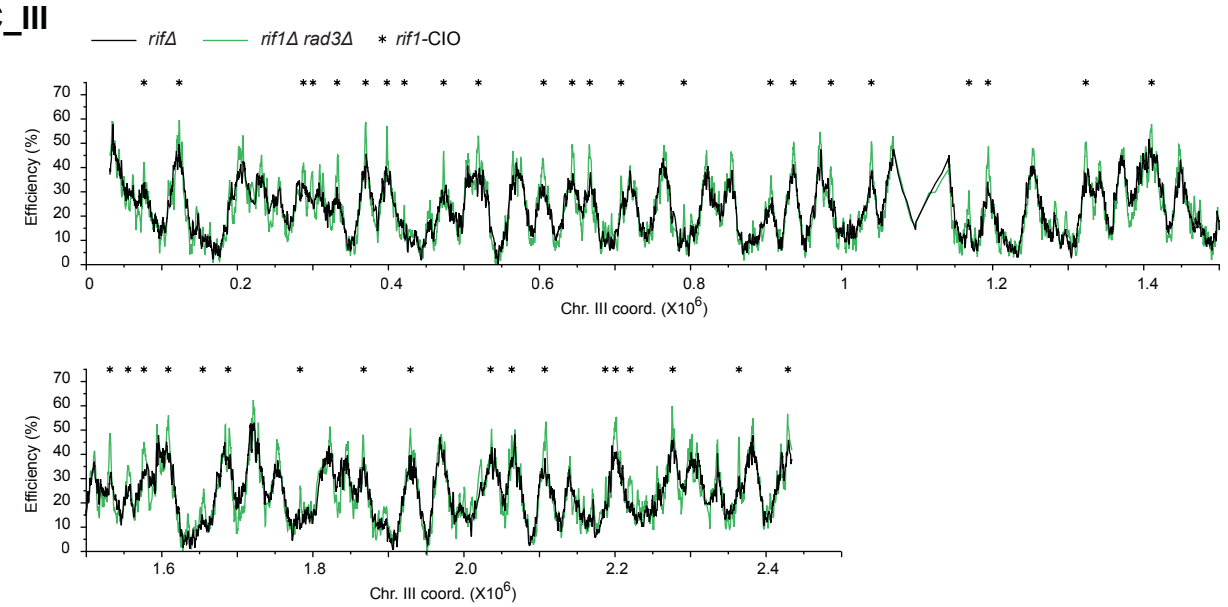

D

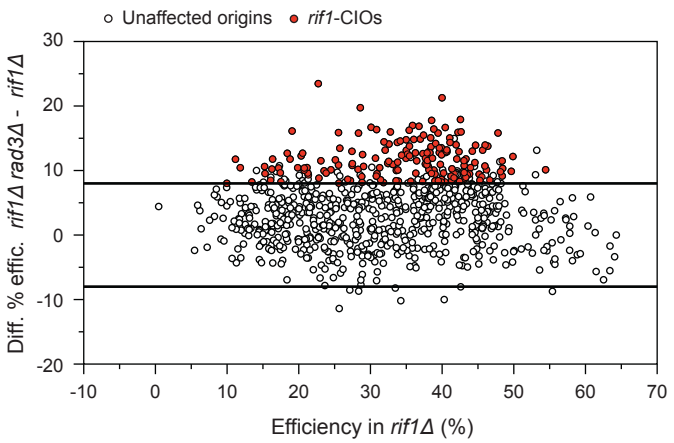

Supplemental Figure S5: Alteration of the replication program in *rif1Δ* cells results in a redistribution of checkpoint-regulated origins. A) DNA content analysis of *cdc25-22 rif1Δ* and *cdc25-22 rif1Δ rad3Δ* cells undergoing a synchronous S phase. The experimental procedures were as described for *cdc25-22* (Supplemental Fig. S1A). Samples in which cells are undergoing DNA replication are shown in gray. Cells were initially arrested in G2 (Time 0) with a 2C DNA content; they entered S phase ~60 min following the release from G2. **B)** Profiles of origin usage in *cdc25-22* (black, WT) and *cdc25-22 rif1Δ* (blue, *rif1Δ*) cells treated with 6 mM HU. x-axis: chromosome coordinates, y-axis: origin efficiencies. **C)** Profiles of origin usage in *cdc25-22 rif1Δ* (black, *rif1Δ*, as in B) and *cdc25-22 rif1Δ rad3Δ* (green, *rif1Δ rad3Δ*) cells treated with 6 mM HU. x-axis: chromosome coordinates, y-axis: origin efficiencies. Asterisks mark *rif1*-CIOs. **D)** Differences in origin efficiencies in *rif1Δ rad3Δ* vs. *rif1Δ* as a function of the efficiencies in *rif1Δ*. x-axis: origin efficiency in *rif1Δ*, y-axis: difference in origin efficiency (*rif1Δ rad3Δ* - *rif1Δ*). Open circles: unaffected origins; red circles: *rif1*-CIOs. Lines mark 8% differences in absolute origin efficiency.

Supplemental Figure S6

A

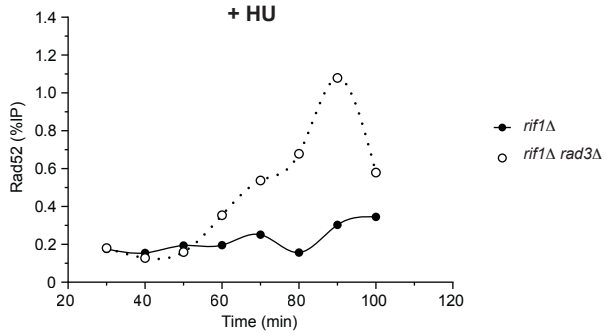

B_I

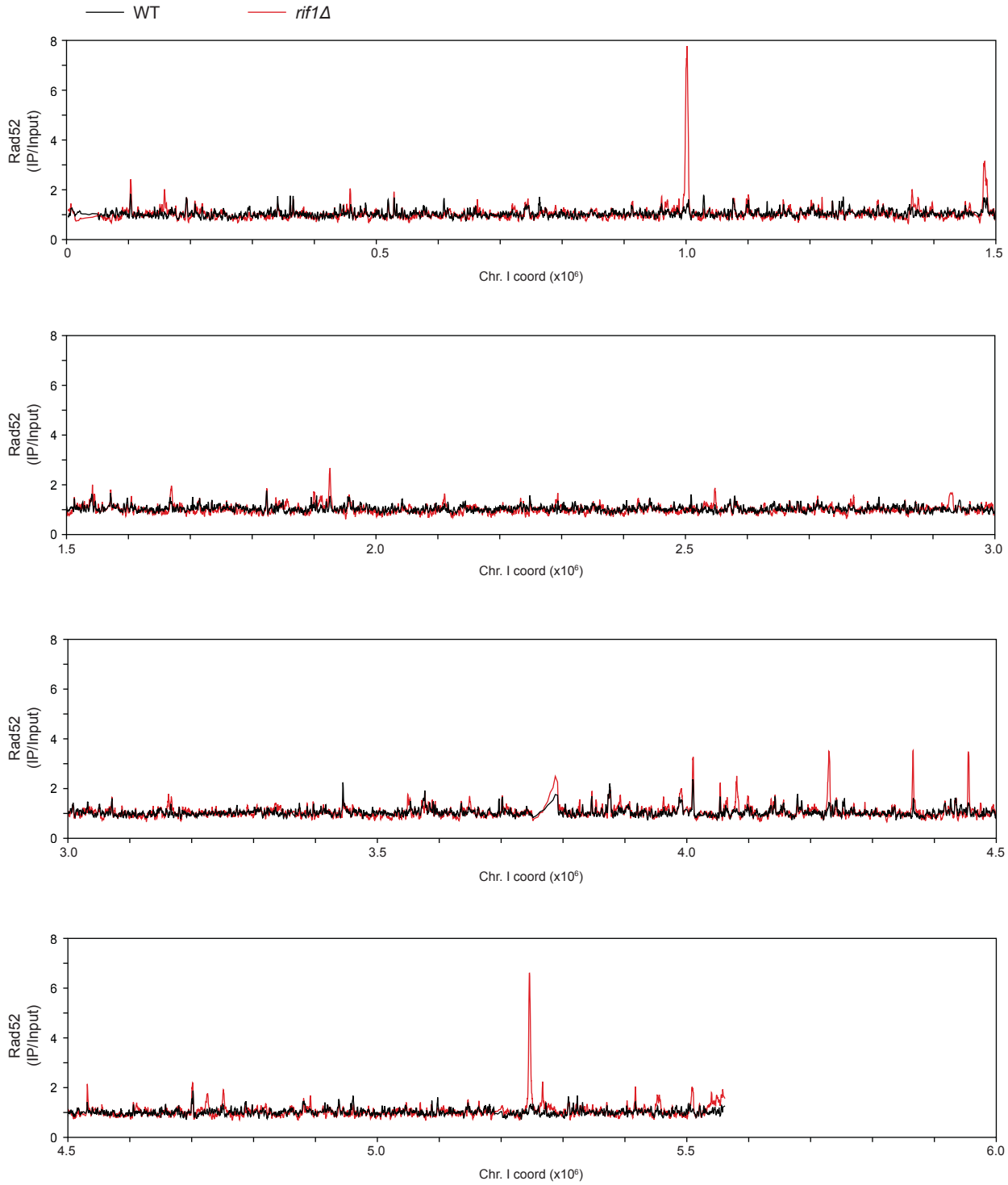

Supplemental Figure S6

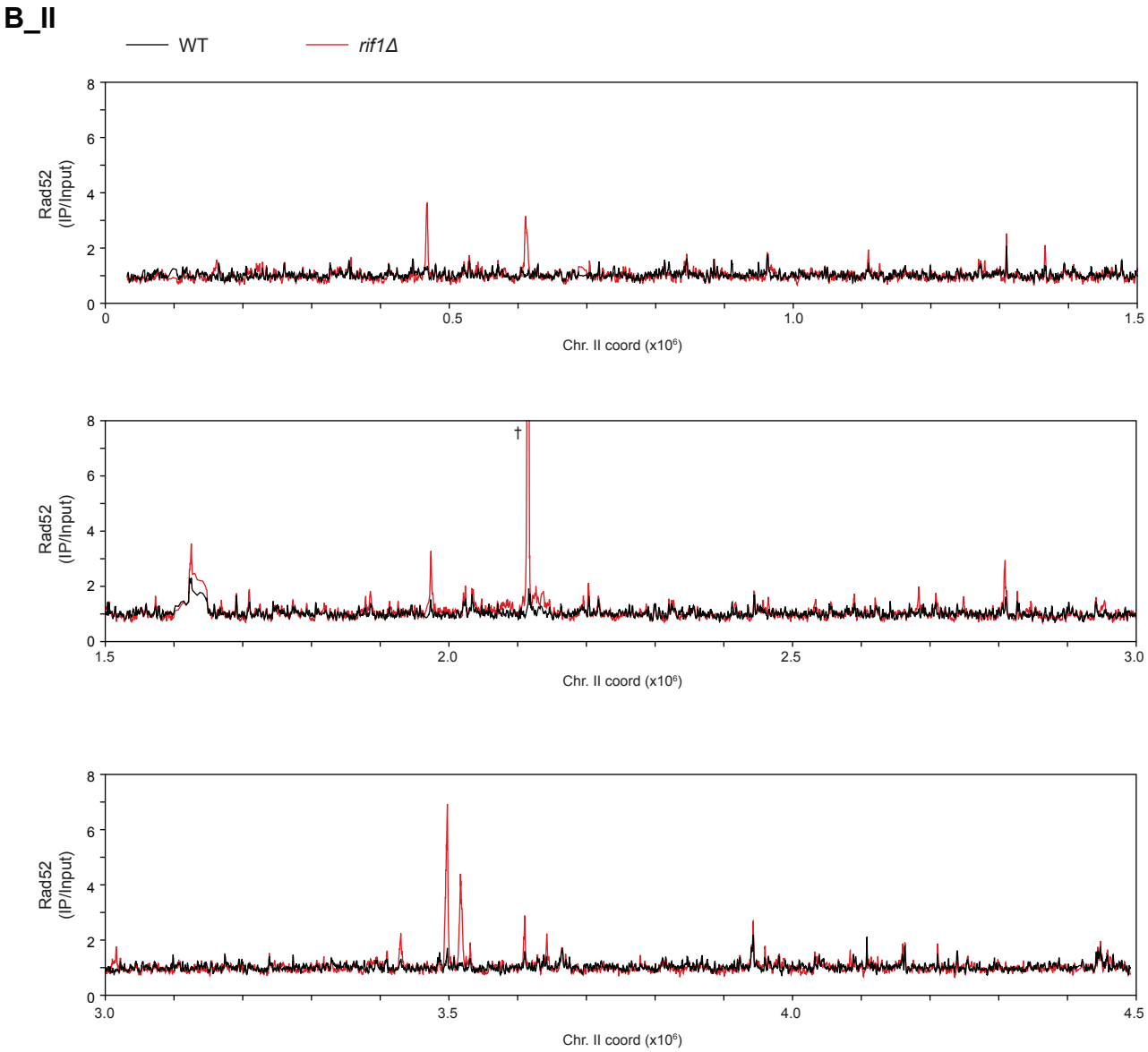

Supplemental Figure S6

B_III

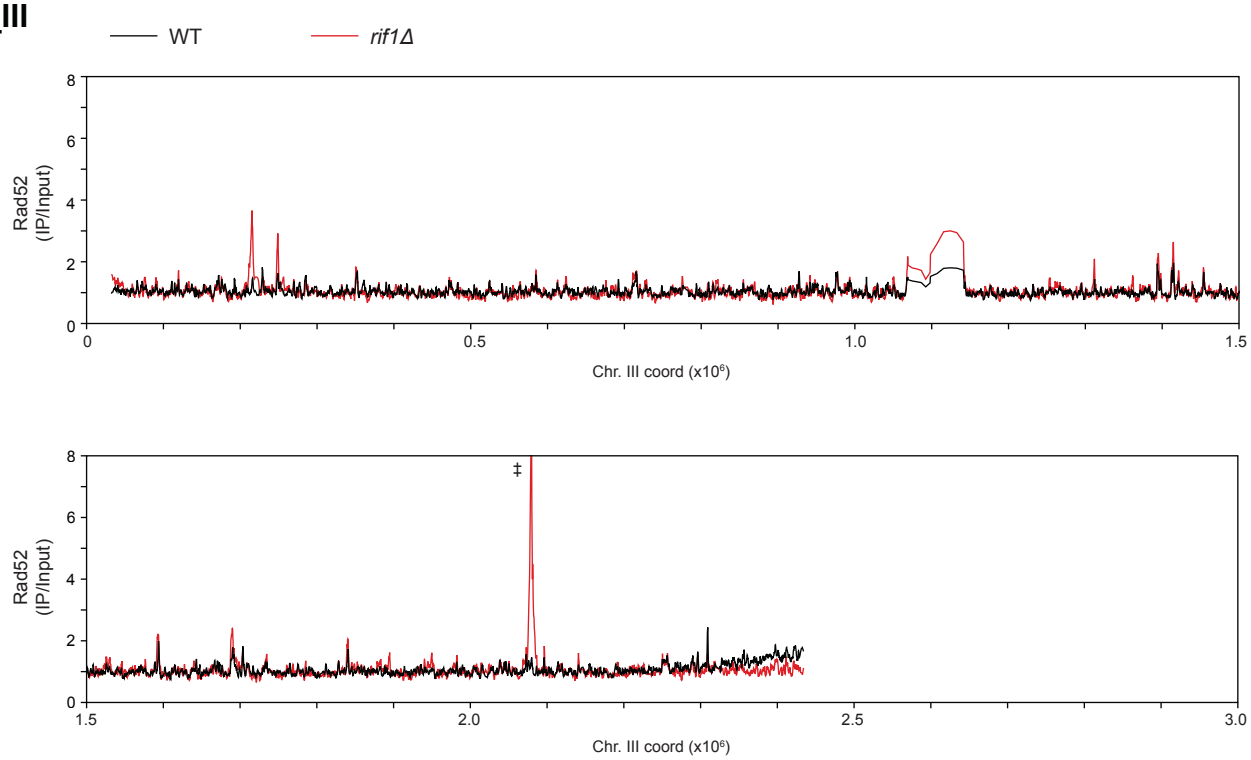

C

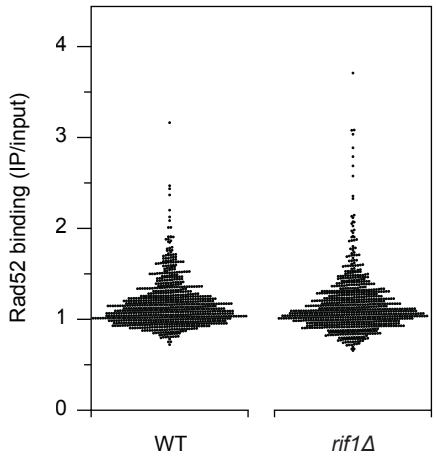

Supplemental Figure S6

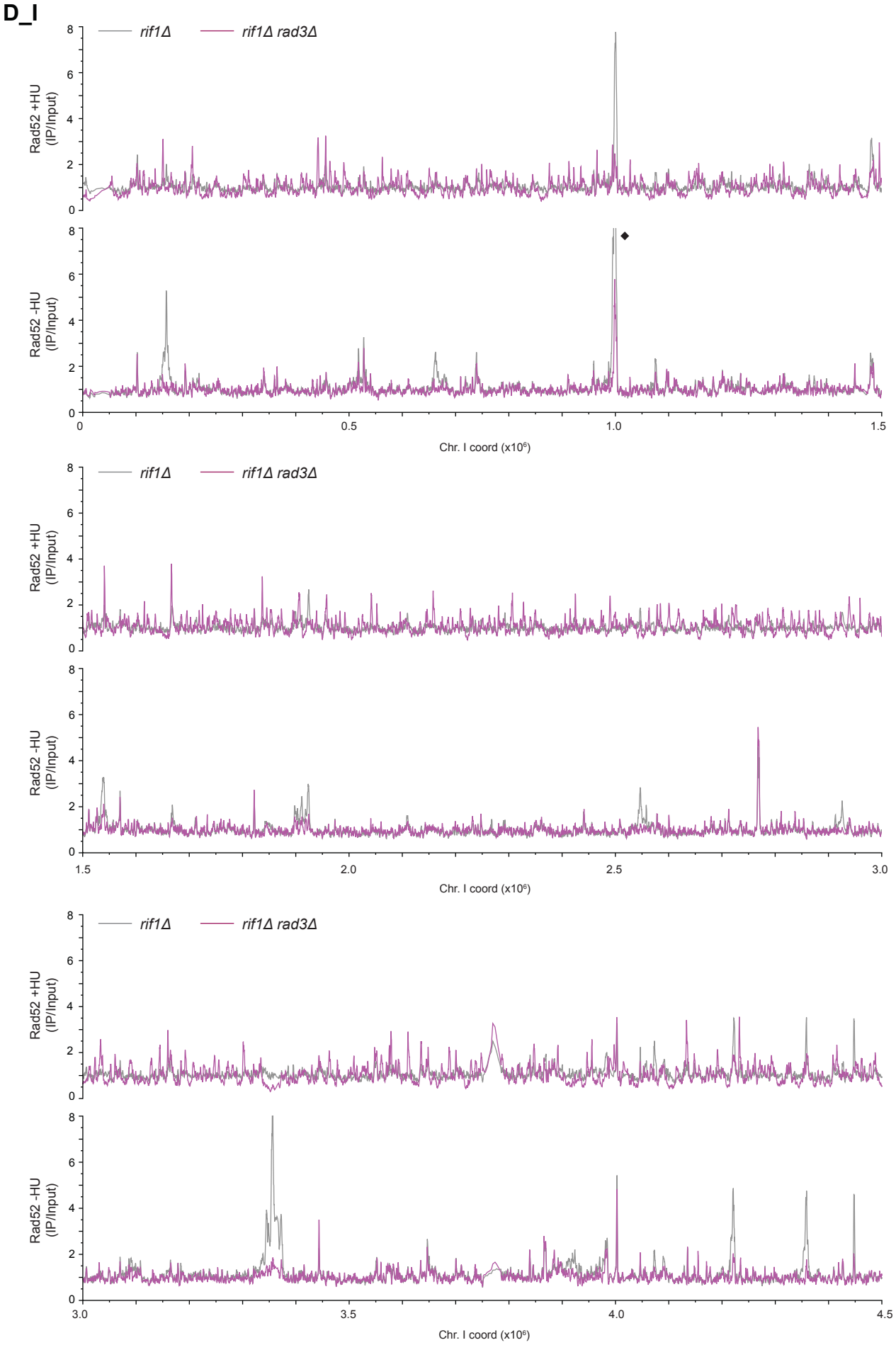

Supplemental Figure S6

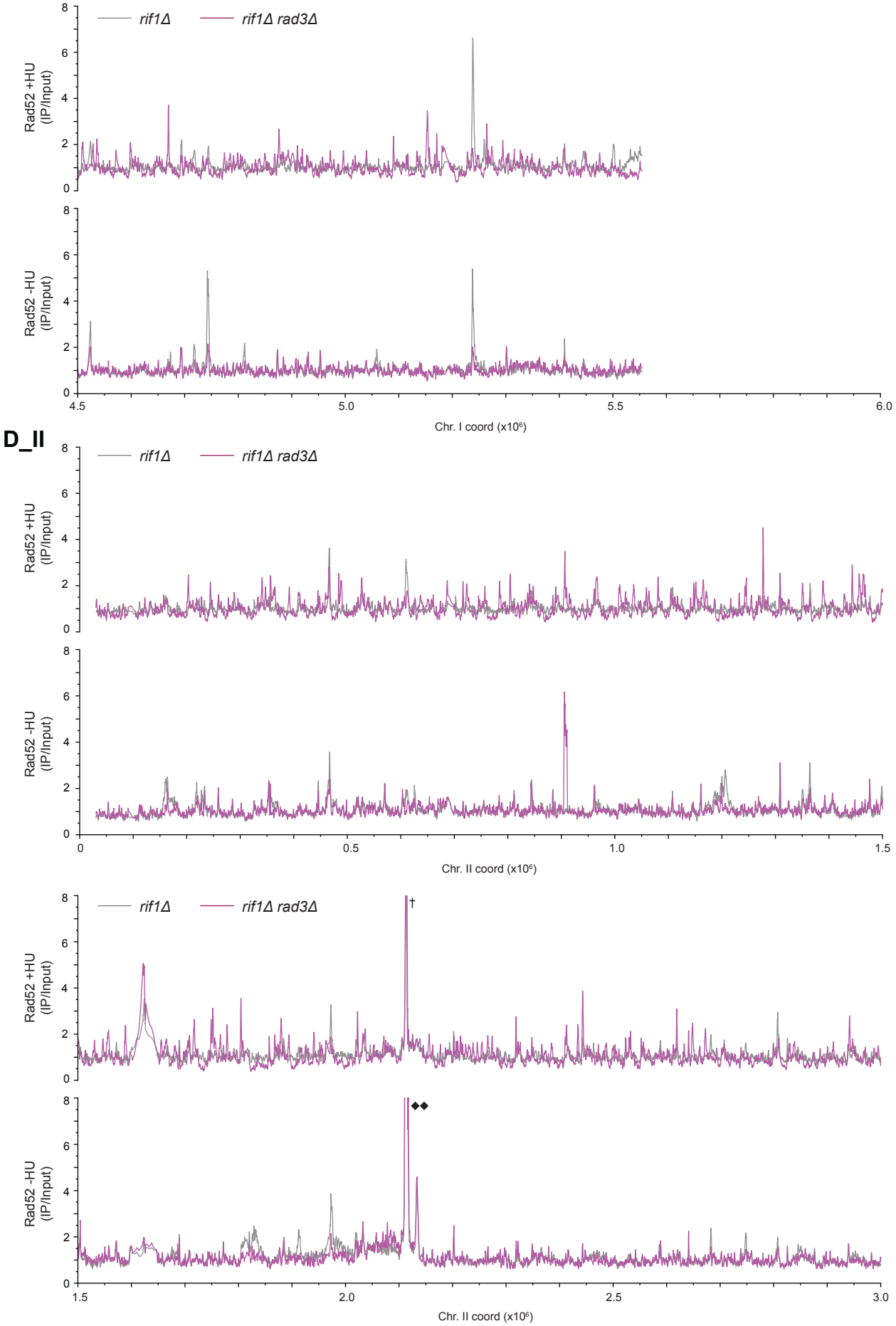

Supplemental Figure S6

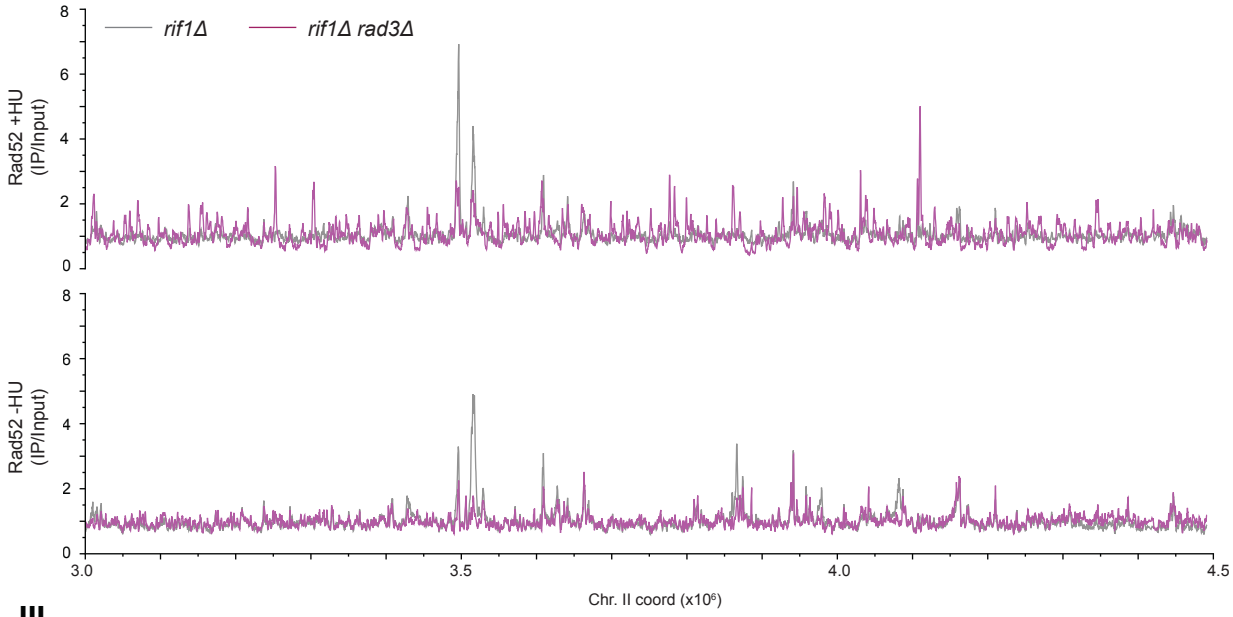

D_III

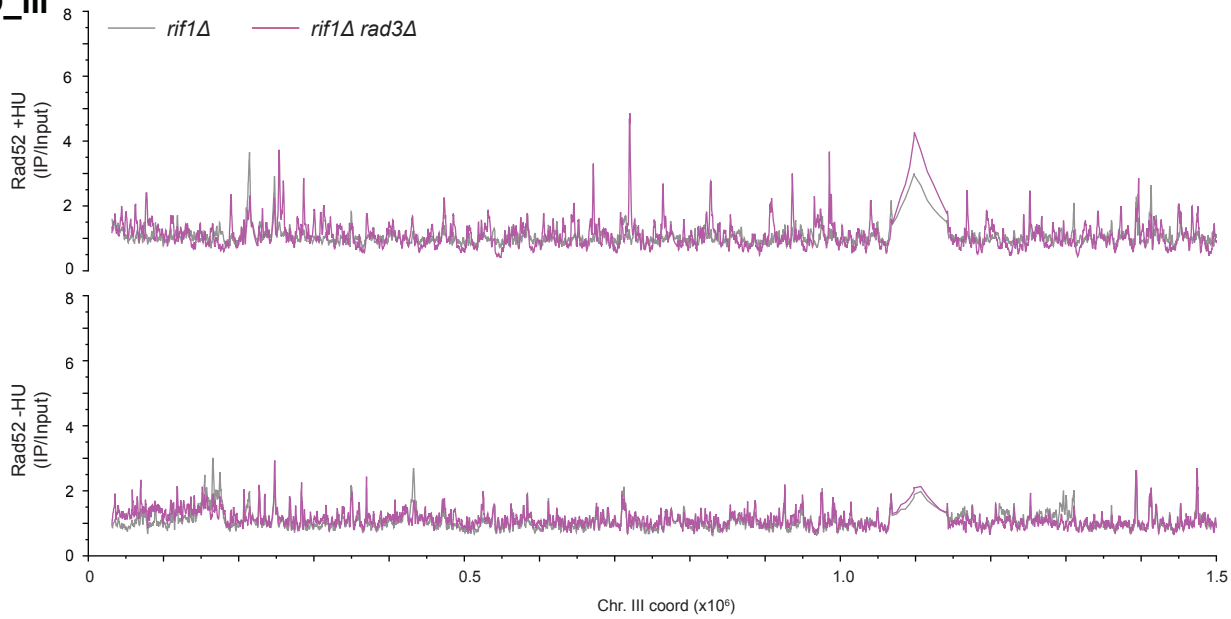

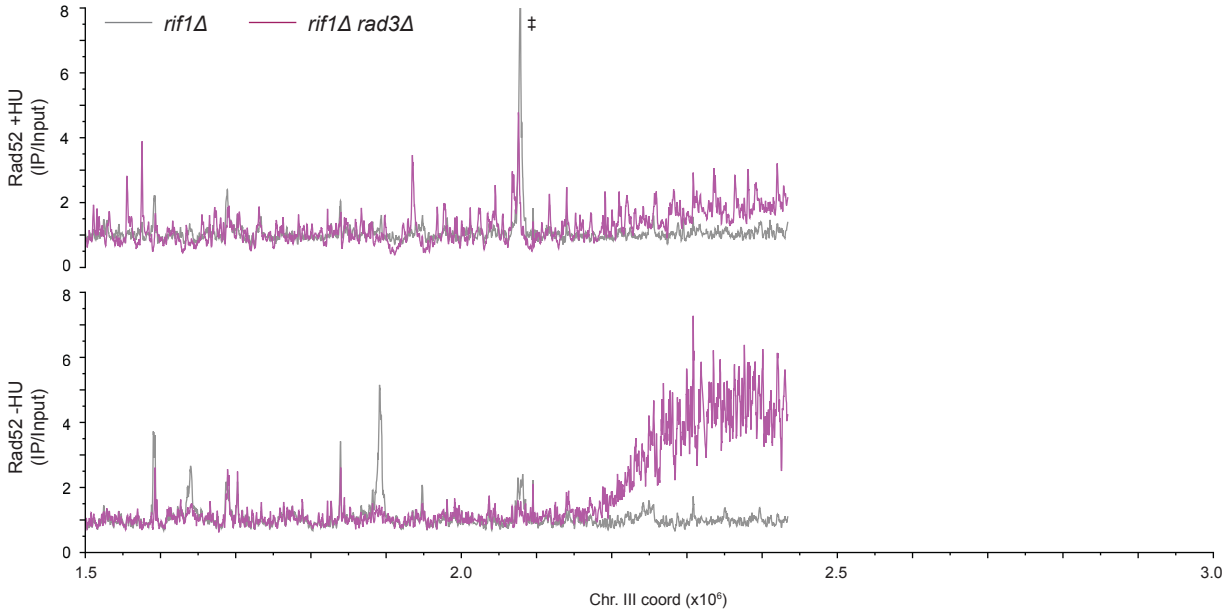

Supplemental Figure S6

E

		+ HU	- HU
***rif1*Δ**	Total Rad52 peaks	94	260
	Rad52 peaks associated with *rif1*-RSOs	8 (8.5 %)	18 (7 %)
	Rad52 peaks associated with unaffected origins	22 (23%)	86 (33 %)
	Rad52 peaks associated with origins	29 (30 %)	103 (40 %)
	rif1-RSOs associated with Rad52 peaks	8 (4.7%)	17 (10 %)
	Unaffected origins associated with Rad52 peaks	22 (3.1%)	79 (11%)
	Origins associated with Rad52 peaks	30 (3.4%)	96 (11%)
***rif1*Δ *rad3*Δ**	Total Rad52 peaks	618	241
	Rad52 peaks associated with *rif1*-RSOs	108 (18 %)	20 (8.3 %)
	Rad52 peaks associated with unaffected origins	305 (49 %)	70 (29 %)
	Rad52 peaks associated with origins	413 (67 %)	89 (37 %)
	rif1-RSOs associated with Rad52 peaks	105 (62 %)	17 (10 %)
	Unaffected origins associated with Rad52 peaks	292 (41%)	65 (9.2%)
	Origins associated with Rad52 peaks	397 (45%)	82 (9.4%)

Co-localization of origins with Rad52 sites

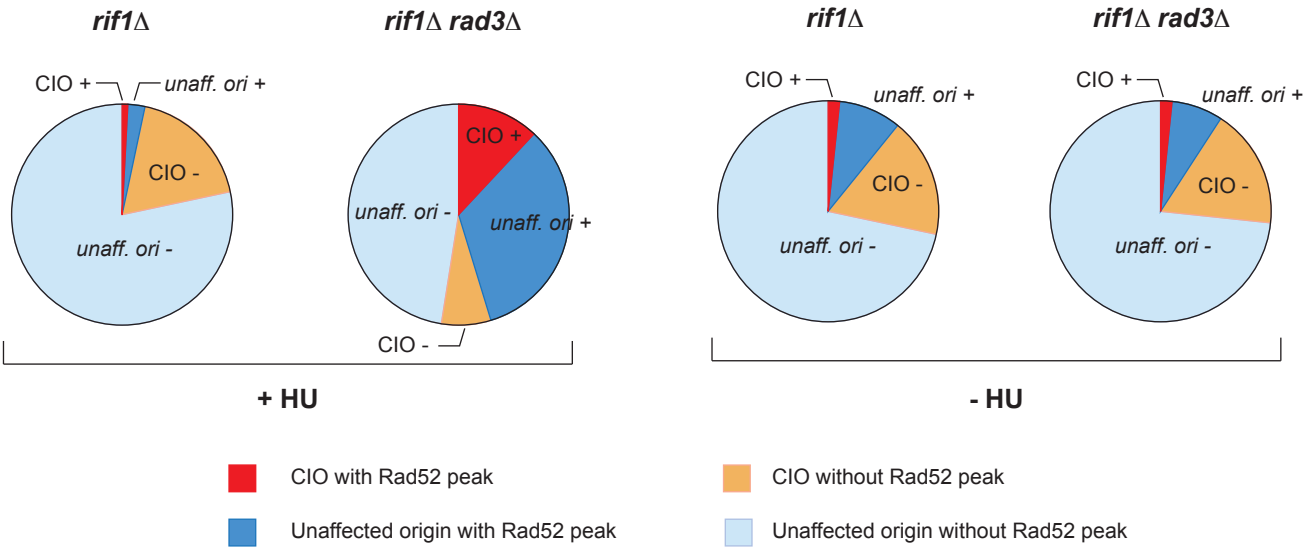

Supplemental Figure S6: Changes to the profile of Rad52 recruitment as a result of origin deregulation in *rif1Δ rad3Δ* cells. A) Time course of Rad52 binding in *cdc25-22 rif1Δ* (*rif1Δ*, closed circle) and *cdc25-22 rif1Δ rad3Δ* (*rif1Δ rad3Δ*, open circle) cells at the *rif1*-CIO *oriBGE3101*. Cells were released from G2 arrest in 6 mM HU and sampled at the indicated time points. x-axis: time after release, y-axis: Rad52 occupancy (%IP). **B)** Genome-wide profiles of Rad52 binding in *cdc25-22* (black, WT) and *cdc25-22 rif1Δ* (red, *rif1Δ*) cells exposed to 6 mM HU. x-axis: chromosomal coordinates, y-axis: Rad52 binding (IP/input). For ease of visualization, the full amplitudes of the following peaks in *rif1Δ* are not shown in the graph: † (chr II: 2113565) – 18.44; ‡ (chr III: 2078653) – 9.74. **C)** Rad52 levels at origins in *cdc25-22* (left, WT) and *cdc25-22 rif1Δ* (right, *rif1Δ*) cells. Each dot represents an origin plotted according to the level of Rad52 recruited at the site. Changes in origin usage in *rif1Δ* do not lead to major alterations in Rad52 binding. **D)** Genome-wide profiles of Rad52 binding in *cdc25-22 rif1Δ* (gray, *rif1Δ*) and *cdc25-22 rif1Δ rad3Δ* (purple, *rif1Δ rad3Δ*) cells exposed to 6 mM HU (Top) or in the absence of HU (Bottom). The profile for Rad52 in HU-treated *cdc25-22 rif1Δ* is as in A. x-axis: chromosomal coordinates, y-axis: Rad52 binding (IP/input). For ease of visualization, the full amplitudes of the following peaks are not shown in the graph: † and ‡ are as in A; ◆ (chr I: 998594) - 16.08; ◆◆ (chr II: 2113263; *rif1Δ* - 37.80, *rif1Δ rad3Δ* - 34.42). **E)** Comparison of sites of significant Rad52 binding (cutoff = 1.5) in the different conditions. Pie charts indicate the proportions of CIOs and unaffected origins that are associated with Rad52 peaks. Red: CIOs that colocalize with a Rad52 site (CIO +), blue: unaffected origins that colocalize with a Rad52 site (unaff. ori +), orange: CIOs not associated with a Rad52 site (CIO -), light blue: unaffected origins not associated with a Rad52 site (unaff. ori. -).

Supplemental Figure S7

A

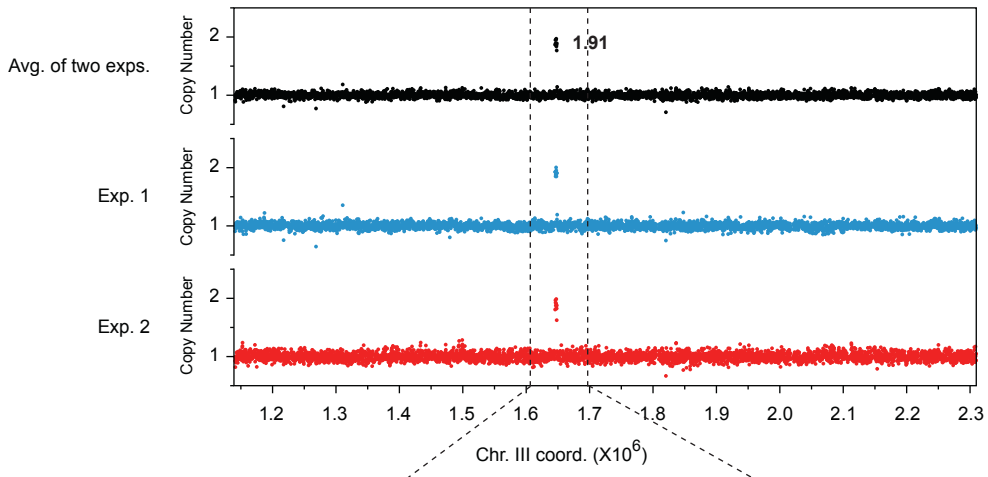

B

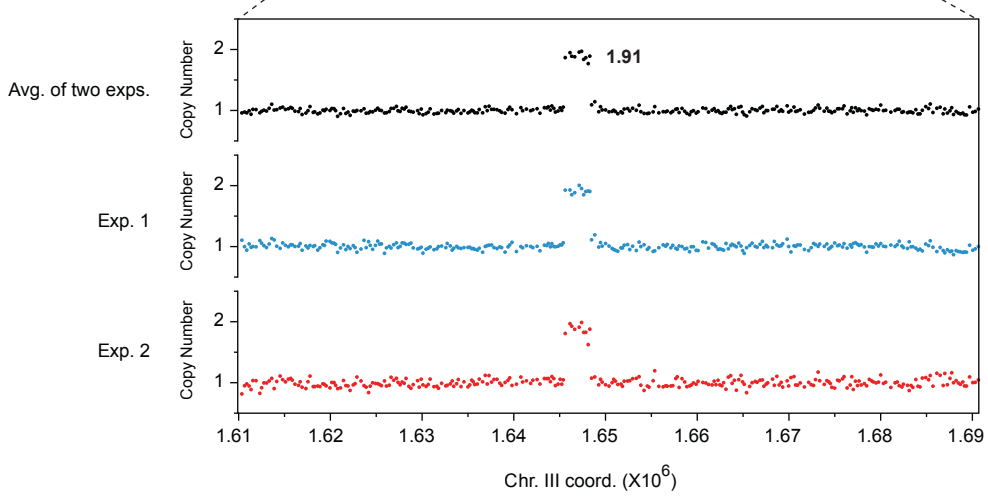

C

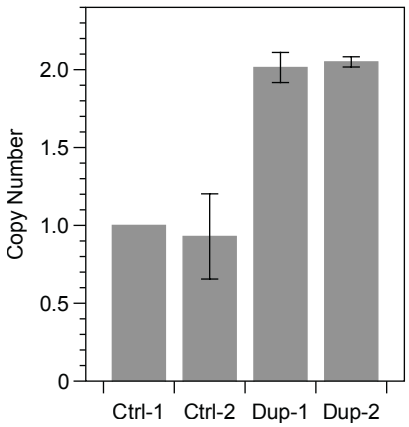

Supplemental Figure S7: Copy number detection using competitive hybridization on microarrays. A-B) Microarray analysis of a duplicated region of chromosome III. Genomic DNA from asynchronous cultures of strains PN1400 (containing the duplication, see Supplemental Methods for details) and PN1 (wild-type) was harvested and subjected to reciprocal labeling for competitive hybridization. Black: average of two experiments; blue and red: individual experiments. Each point represents a probe on the microarray. The average copy number for the probes in the duplicated region is indicated for the average of the two experiments. x-axis: chromosome coordinates, y-axis: copy number. B shows a detailed view of the region displayed in A. **C)** Quantitative PCR analysis of the duplicated region. Two primers sets outside of the duplicated region (Ctrl-1 and Ctrl-2) and two primer sets within the duplicated region (Dup-1 and Dup-2) were used. y-axis: copy number. n=2, error bars indicate standard deviations.

Supplemental Figure S8

A_I

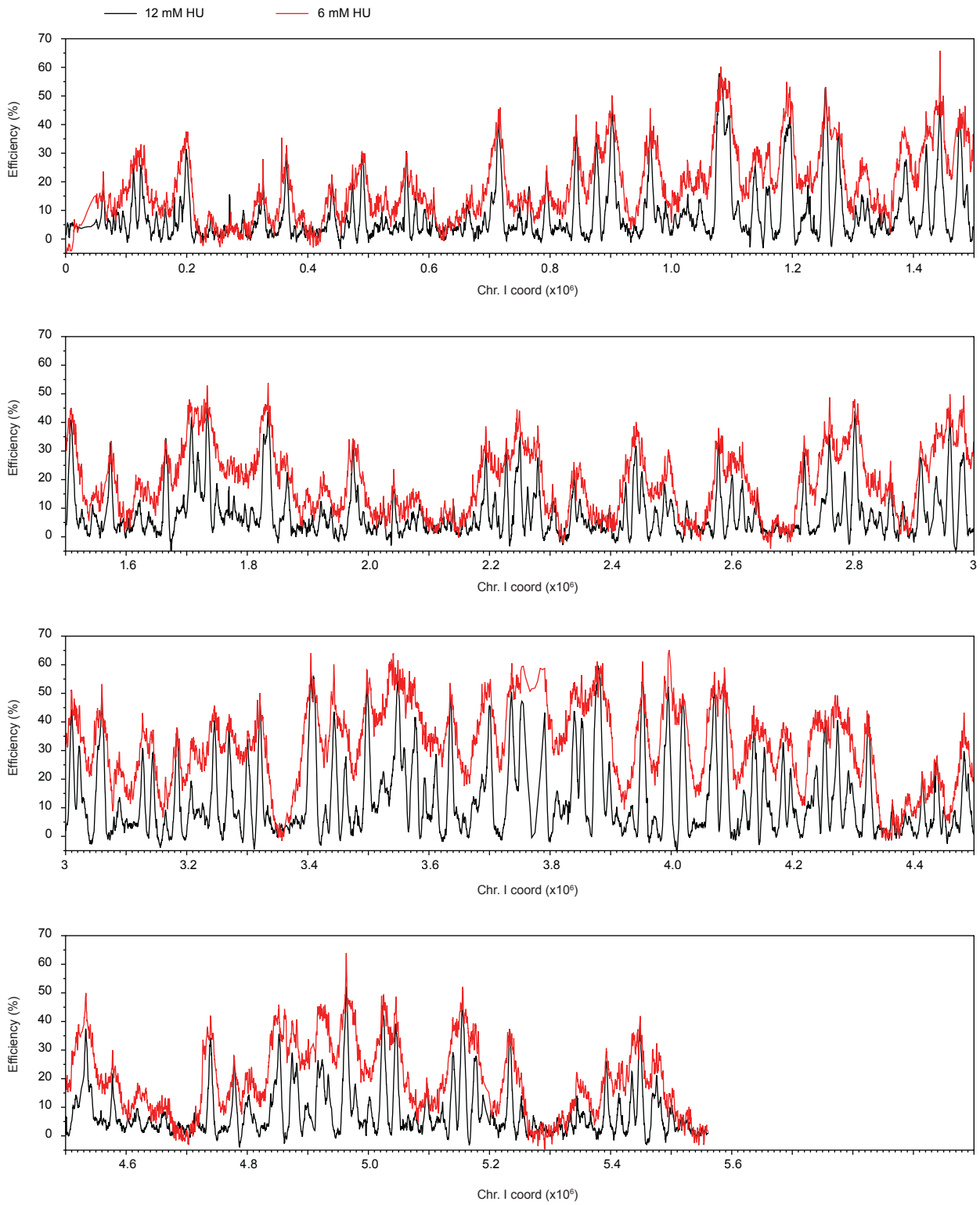

Supplemental Figure S8

A_II

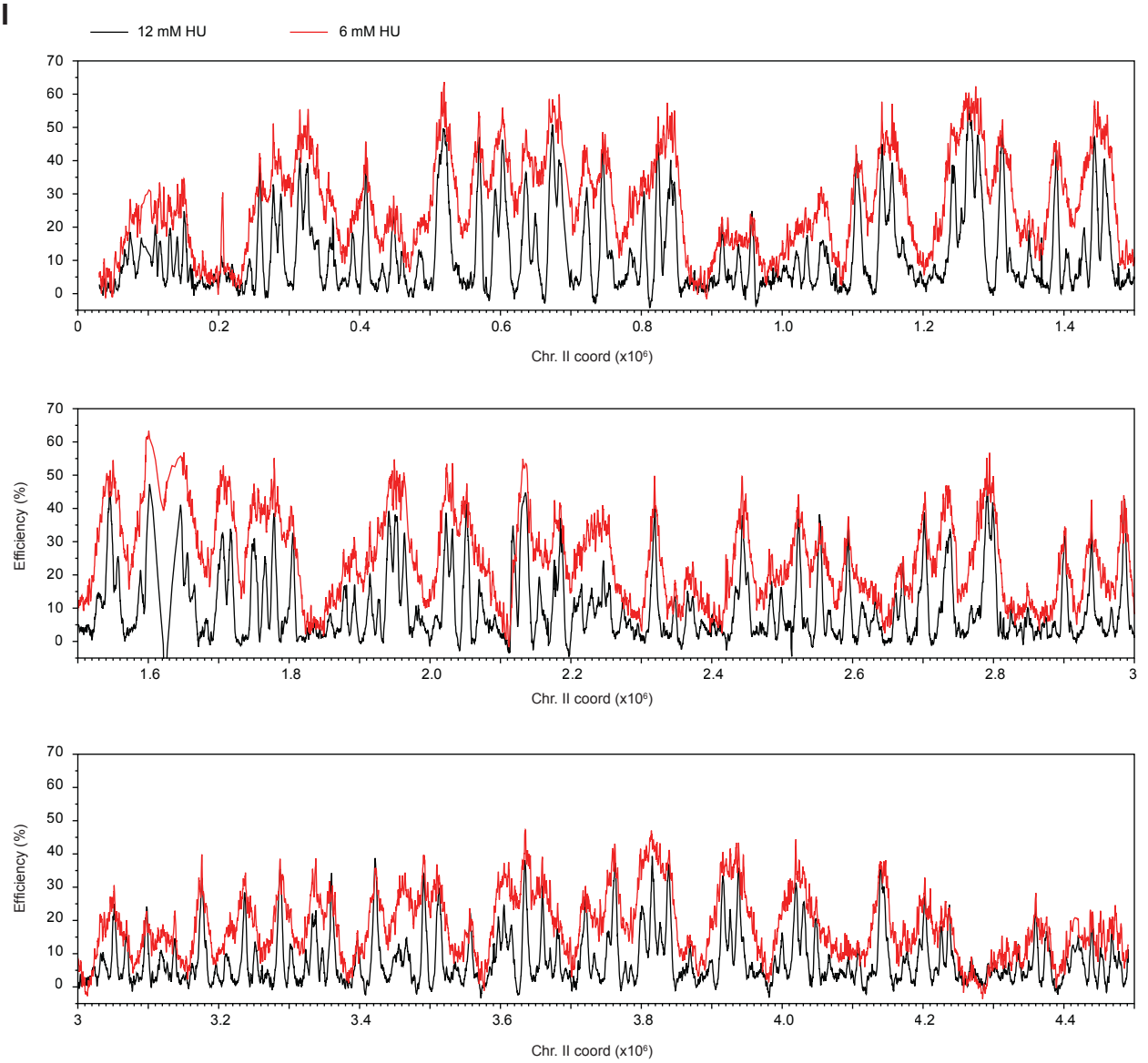

A_III

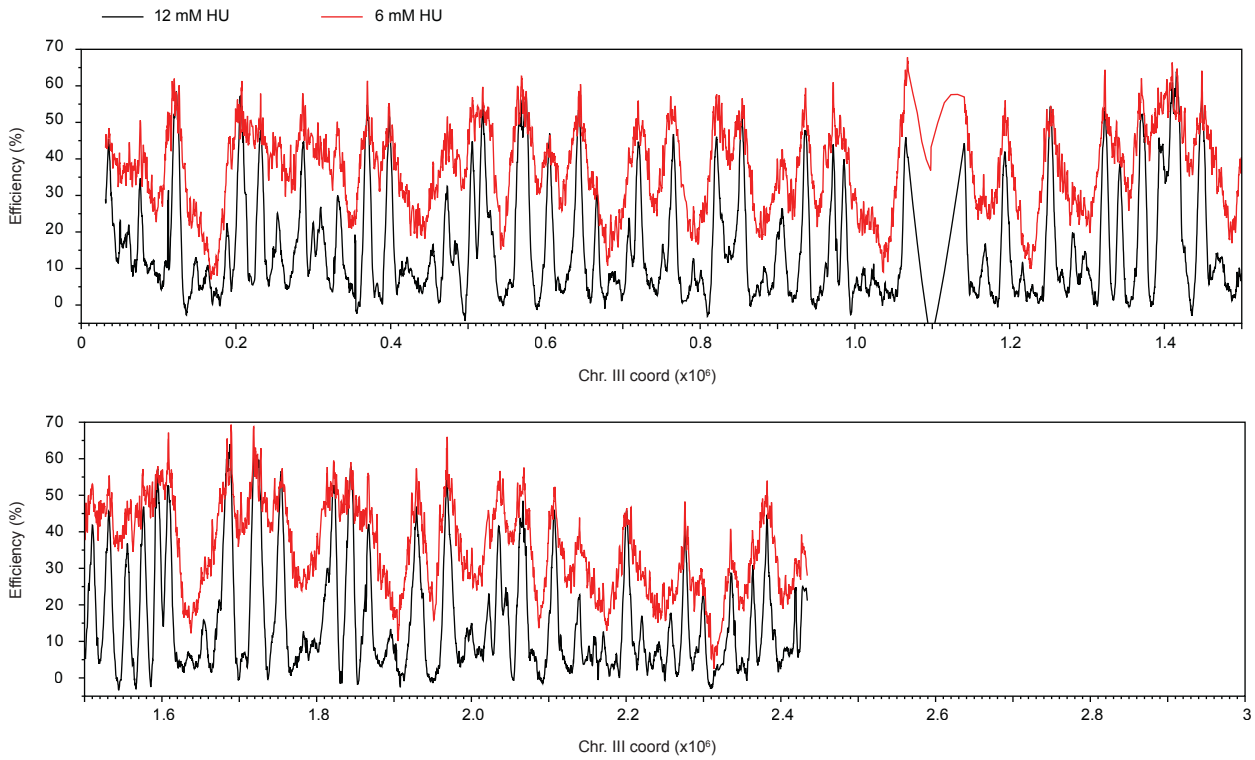

Supplemental Figure S8: Origin profiles in wild-type cells treated with 6 mM vs. 12 mM HU. Cells were arrested in G2 using *cdc25-22* and released to undergo a synchronous S phase in either 12 mM (black) or 6 mM (red) HU. Cultures were harvested 90 min after release from G2 arrest. The data for 6 mM HU are as in Supplemental Fig. S1C. The data for 12 mM HU are from (Wu and Nurse 2014).

Supplemental Figure S9

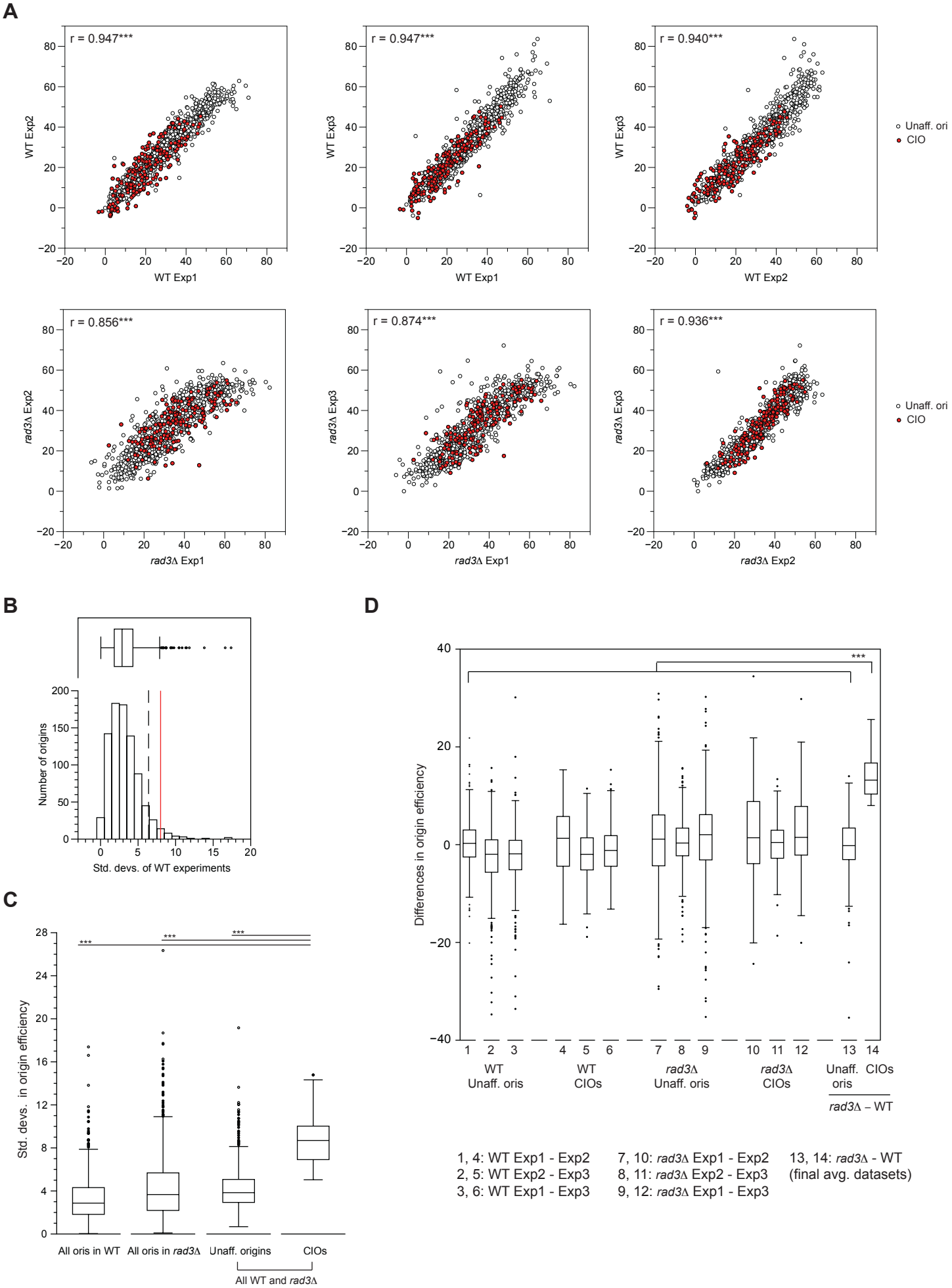

Supplemental Figure S9: Statistical analyses of origin efficiencies and CIO selection. A) Pairwise comparisons of origin mapping experiments performed using HU-treated *cdc25-22* (WT) and *cdc25-22 rad3Δ* (*rad3Δ*) cells. The Pearson correlation coefficient (r) for each comparison is displayed. ***: p-value<0.001. These results show the high level of reproducibility of our datasets. x- and y-axes: origin efficiencies in the indicated experiments. Black circles: unaffected origins; red circles: CIOs. **B)** Establishment of the threshold for identifying deregulated origins. The standard deviations (std. devs.) of the efficiency of each origin from three independent experiments for *cdc25-22* cells (WT) were determined and shown in a box and whiskers plot (Top panel) and a histogram (Bottom panel). Top: right whisker indicates 1.5 times the interquartile range (IQR) above the third quartile (Q3 + 1.5(IQR)=8); black circles represent outliers. Bottom: black dashed line indicates 1.5 standard deviations above the mean variability (a value of 6.5; see Supplemental Methods for details). Red line: 8% variability in efficiency. Based on this analysis, a stringent threshold of 8% efficiency difference between WT and *rad3Δ* was used for CIO selection. **C)** Standard deviations of efficiencies at individual origins for the indicated datasets. All oris in WT: all origins in the three *cdc25-22* experiments, data as in *B*, Top panel. All oris in *rad3Δ*: all origins in the three *cdc25-22 rad3Δ* experiments. All WT and *rad3Δ*, unaff. origins: unaffected origins when pooling all *cdc25-22* and *cdc25-22 rad3Δ* experiments. All WT and *rad3Δ*, CIOs: CIOs when pooling all *cdc25-22* and *cdc25-22 rad3Δ* experiments. y-axis: standard deviations of origin efficiency. Whiskers and circles are as in *B*, Top panel. Independent samples T-tests show that the standard deviations for the CIO dataset are significant greater than for each of the other datasets. ***: p-value<0.001. **D)** Differences in origin usage between the indicated pairs of experiments (1-12 on the x-axis) and between the averaged *cdc25-22 rad3Δ* and *cdc25-22* data (*rad3Δ* – WT) for unaffected origins or CIOs (13 and 14 on the x-axis, respectively). T-tests show that the changes in origin usage at CIOs (*rad3Δ* – WT) for the averaged data are significantly higher compared to 1) differences at unaffected origins (WT unaff. oris) or at CIOs (WT CIOs) between pairs of *cdc25-22* experiments, 2) differences at unaffected origins (*rad3Δ* unaff. oris) or at CIOs (*rad3Δ* CIOs) between pairs of *cdc25-22 rad3Δ* experiments and 3) differences at unaffected origins between the averaged *cdc25-22* and *cdc25-22 rad3Δ* datasets (*rad3Δ* – WT, unaff. oris). ***: p-value<0.001 for all comparisons. Whiskers and circles are as in *B*.

References

Feng W, Collingwood D, Boeck ME, Fox LA, Alvino GM, Fangman WL, Raghuraman MK, Brewer BJ. 2006. Genomic mapping of single-stranded DNA in hydroxyurea-challenged yeasts identifies origins of replication. *Nat Cell Biol* **8**: 148–155.

Hayashi M, Katou Y, Itoh T, Tazumi A, Tazumi M, Yamada Y, Takahashi T, Nakagawa T, Shirahige K, Masukata H. 2007. Genome-wide localization of pre-RC sites and identification of replication origins in fission yeast. *EMBO J* **26**: 1327–1339.

Heichinger C, Penkett CJ, Bähler J, Nurse P. 2006. Genome-wide characterization of fission yeast DNA replication origins. *EMBO J* **25**: 5171–5179.

Wu P-YJ, Nurse P. 2014. Replication origin selection regulates the distribution of meiotic recombination. *Mol Cell* **53**: 655–662.

Supplemental Table S1: Replication origins mapped in this study. Asterisks mark origins that were added after analysis of the *rad3*Δ dataset. Values indicate origin efficiencies.

Origin name	Chromosome I coordinates	WT	*rad3*Δ	CIO
oriBGE1001*	6212	-2.0	15.6	+
oriBGE1002	14096	2.8	23.3	+
oriBGE1003*	19570	2.2	16.9	+
oriBGE1004	51004	12.8	21.9	+
oriBGE1005	61479	19.0	30.4	
oriBGE1006	71137	12.8	22.3	+
oriBGE1007	79544	10.0	20.3	+
oriBGE1008	84480	9.6	18.4	+
oriBGE1009	86730	12.4	22.6	+
oriBGE1010	94607	20.9	33.8	+
oriBGE1011	108926	26.1	33.7	
oriBGE1012	112286	29.2	39.6	+
oriBGE1013	124602	33.1	43.5	+
oriBGE1014	129236	30.5	38.0	
oriBGE1015	135930	17.9	23.0	
oriBGE1016	149874	15.0	21.9	
oriBGE1017	164454	11.7	22.0	+
oriBGE1018	179994	19.3	22.8	
oriBGE1019	182947	19.1	23.5	
oriBGE1020	189672	26.3	36.0	+
oriBGE1021	199362	36.9	50.5	+
oriBGE1022	217312	3.2	5.8	
oriBGE1023	240008	5.9	21.6	+
oriBGE1024	262399	1.3	2.6	
oriBGE1025	272762	9.5	15.3	
oriBGE1026	282257	3.9	7.5	
oriBGE1027	293566	2.3	24.2	+
oriBGE1028	311940	13.5	23.8	+
oriBGE1029	319141	18.6	26.7	+
oriBGE1030	325923	28.0	48.7	+
oriBGE1031	364660	31.1	52.2	+
oriBGE1032	377863	11.4	14.2	
oriBGE1033	391595	9.2	13.3	
oriBGE1034*	410626	2.7	16.7	+
oriBGE1035	434067	17.3	30.9	+
oriBGE1036	439953	20.5	40.0	+
oriBGE1037	463593	17.8	27.7	+
oriBGE1038	473721	24.5	43.0	+
oriBGE1039	490088	28.1	43.0	+
oriBGE1040	511808	10.8	13.3	
oriBGE1041	521997	9.9	12.4	
oriBGE1042	529837	15.5	16.1	

oriBGE1043	545580	8.0	9.0	
oriBGE1044	552529	12.4	14.4	
oriBGE1045	557636	18.6	21.5	
oriBGE1046	562906	28.4	47.1	+
oriBGE1047	578212	15.9	21.8	
oriBGE1048	593361	15.1	20.7	
oriBGE1049	608104	18.0	39.3	+
oriBGE1050	633702	7.3	10.7	
oriBGE1051	650229	7.3	27.5	+
oriBGE1052	664249	13.4	15.0	
oriBGE1053	679422	12.0	12.6	
oriBGE1054	682491	13.4	17.4	
oriBGE1055	692396	16.0	19.6	
oriBGE1056	703344	31.9	35.6	
oriBGE1057	715157	45.2	50.7	
oriBGE1058	732054	15.8	16.5	
oriBGE1059	739340	12.1	11.7	
oriBGE1060	750097	12.3	14.0	
oriBGE1061	765612	14.2	31.5	+
oriBGE1062	794338	25.5	39.8	+
oriBGE1063	808637	11.9	12.8	
oriBGE1064	815833	8.4	12.0	
oriBGE1065	821657	12.0	8.3	
oriBGE1066	827583	18.1	15.1	
oriBGE1067	843514	38.1	42.4	
oriBGE1068	877149	35.7	40.4	
oriBGE1069	892911	39.6	37.0	
oriBGE1070	902339	50.2	55.8	
oriBGE1071	912127	31.6	34.9	
oriBGE1072	920404	22.4	22.2	
oriBGE1073	926532	14.0	14.5	
oriBGE1074	939514	5.4	6.4	
oriBGE1075	956909	33.7	35.8	
oriBGE1076	965347	45.7	46.7	
oriBGE1077	978611	29.5	24.3	
oriBGE1078	988261	19.0	17.5	
oriBGE1079	990658	17.0	18.4	
oriBGE1080	1006046	16.0	15.7	
oriBGE1081	1015417	19.3	20.5	
oriBGE1082	1020873	21.2	21.6	
oriBGE1083	1027338	26.7	44.0	+
oriBGE1084	1047551	26.7	24.1	
oriBGE1085	1079582	55.7	61.5	
oriBGE1086	1082706	53.2	50.4	
oriBGE1087	1094633	51.5	53.5	
oriBGE1088	1110449	31.2	28.8	
oriBGE1089	1123466	20.8	15.1	
oriBGE1090	1138662	27.8	25.9	

oriBGE1091	1147053	25.0	26.2	
oriBGE1092	1157145	30.2	34.1	
oriBGE1093	1161340	29.7	29.9	
oriBGE1094	1190256	51.6	49.3	
oriBGE1095	1196036	49.7	55.0	
oriBGE1096	1214950	19.6	16.0	
oriBGE1097	1225944	22.4	25.9	
oriBGE1098	1254773	53.0	54.3	
oriBGE1099	1276292	36.0	46.4	+
oriBGE1100	1280410	32.6	37.1	
oriBGE1101	1304791	15.6	17.4	
oriBGE1102	1315078	28.4	32.2	
oriBGE1103	1324363	20.7	21.8	
oriBGE1104	1342185	12.0	12.4	
oriBGE1105	1351531	14.8	19.0	
oriBGE1106*	1359944	8.4	20.0	+
oriBGE1107	1371515	22.8	23.6	
oriBGE1108	1377924	30.4	29.6	
oriBGE1109	1387499	35.7	41.2	
oriBGE1110	1399420	21.7	22.7	
oriBGE1111	1421370	42.6	45.5	
oriBGE1112	1436643	46.0	45.3	
oriBGE1113	1443998	65.8	60.3	
oriBGE1114	1476258	45.5	48.8	
oriBGE1115	1487922	37.3	32.4	
oriBGE1116	1508761	44.2	47.1	
oriBGE1117	1527151	23.2	24.4	
oriBGE1118	1544677	12.6	0.0	
oriBGE1119	1550346	17.7	14.7	
oriBGE1120	1559381	18.2	17.0	
oriBGE1121	1574006	25.4	41.2	+
oriBGE1122	1588042	8.5	8.3	
oriBGE1123	1590986	5.5	6.9	
oriBGE1124	1595138	12.4	18.1	
oriBGE1125	1603801	9.5	22.4	+
oriBGE1126	1616020	21.7	21.8	
oriBGE1127	1622617	19.7	24.0	
oriBGE1128	1637255	16.9	19.4	
oriBGE1129	1643552	12.4	13.5	
oriBGE1130	1665288	31.3	37.5	
oriBGE1131	1684582	25.1	25.3	
oriBGE1132	1694548	32.0	29.5	
oriBGE1133	1707991	45.5	53.1	
oriBGE1134	1718422	44.8	50.7	
oriBGE1135	1734302	51.0	49.8	
oriBGE1136	1749891	32.6	34.8	
oriBGE1137	1767565	26.6	26.2	
oriBGE1138	1777782	26.3	25.6	

oriBGE1139	1786355	23.3	17.0	
oriBGE1140	1790048	25.1	25.7	
oriBGE1141	1795812	22.2	26.3	
oriBGE1142	1805933	23.2	20.8	
oriBGE1143	1808730	25.5	21.0	
oriBGE1144	1815828	27.5	23.8	
oriBGE1145	1827393	44.2	46.5	
oriBGE1146	1834190	52.5	51.3	
oriBGE1147	1859028	26.6	19.8	
oriBGE1148	1866419	27.7	33.4	
oriBGE1149	1889028	5.1	3.1	
oriBGE1150	1892981	10.6	22.9	
oriBGE1151	1901978	15.0	29.0	
oriBGE1152	1907403	10.5	13.6	
oriBGE1153	1922052	17.7	22.5	
oriBGE1154	1928345	15.7	18.1	
oriBGE1155	1937932	12.2	15.1	
oriBGE1156	1954759	12.3	20.3	+
oriBGE1157	1974622	34.0	43.6	+
oriBGE1158	1982462	31.6	37.5	
oriBGE1159	1991421	21.5	26.4	
oriBGE1160	2000501	13.8	13.4	
oriBGE1161	2018737	5.9	11.7	
oriBGE1162	2025258	14.3	32.6	+
oriBGE1163	2041847	23.2	36.6	+
oriBGE1164	2064185	14.2	18.6	
oriBGE1165	2073831	16.7	20.9	
oriBGE1166	2084565	12.6	22.4	+
oriBGE1167	2095493	7.6	24.3	+
oriBGE1168	2101783	7.0	11.4	
oriBGE1169	2112319	2.7	6.2	
oriBGE1170	2123889	7.9	9.4	
oriBGE1171	2132024	5.6	14.4	+
oriBGE1172	2140329	13.4	36.4	+
oriBGE1173	2157894	9.2	18.0	
oriBGE1174	2173915	14.3	21.5	
oriBGE1175	2188916	25.8	31.5	
oriBGE1176	2194367	37.2	46.6	
oriBGE1177	2208955	28.4	32.8	
oriBGE1178	2215176	24.8	24.8	
oriBGE1179	2228058	34.5	43.7	+
oriBGE1180	2237947	29.2	30.9	
oriBGE1181	2244436	35.4	41.7	
oriBGE1182	2249881	42.8	55.0	+
oriBGE1183	2263318	34.5	43.1	+
oriBGE1184	2273276	33.7	36.2	
oriBGE1185	2280057	38.5	49.7	+
oriBGE1186	2305633	11.2	21.0	+

oriBGE1187	2339782	25.8	38.0	+
oriBGE1188	2349485	25.8	29.0	
oriBGE1189	2357883	18.1	20.1	
oriBGE1190	2363418	8.4	10.0	
oriBGE1191	2378343	6.3	11.4	
oriBGE1192	2385613	7.7	9.5	
oriBGE1193	2398512	11.1	36.7	+
oriBGE1194	2415024	14.0	27.2	+
oriBGE1195	2424923	28.8	39.2	+
oriBGE1196	2441566	36.3	48.9	
oriBGE1197	2451814	33.0	43.3	+
oriBGE1198	2456826	25.0	31.7	
oriBGE1199	2473411	17.3	21.5	
oriBGE1200	2489271	26.9	42.4	+
oriBGE1201	2499282	22.9	29.4	
oriBGE1202	2525733	6.8	27.5	+
oriBGE1203	2538872	3.4	4.5	
oriBGE1204	2557720	5.9	7.2	
oriBGE1205	2578182	36.6	47.2	
oriBGE1206	2600933	28.9	42.3	+
oriBGE1207	2617468	29.6	33.3	
oriBGE1208	2627422	16.0	15.6	
oriBGE1209	2638235	13.2	22.8	+
oriBGE1210	2642609	16.9	35.0	+
oriBGE1211*	2662653	2.4	13.1	+
oriBGE1212	2673297	6.4	16.0	+
oriBGE1213	2685431	4.7	19.6	+
oriBGE1214	2719845	35.3	42.3	
oriBGE1215	2750451	30.8	32.6	
oriBGE1216	2761259	45.8	55.0	
oriBGE1217	2775839	27.4	27.1	
oriBGE1218	2786921	35.2	39.7	
oriBGE1219	2803547	46.0	51.7	
oriBGE1220	2814950	32.2	31.4	
oriBGE1221	2830742	21.3	21.0	
oriBGE1222	2845339	19.7	20.5	
oriBGE1223	2862190	26.5	38.1	+
oriBGE1224	2882448	11.5	28.2	+
oriBGE1225	2912248	32.9	41.6	+
oriBGE1226	2922783	23.9	19.4	
oriBGE1227	2937799	39.9	39.1	
oriBGE1228	2945070	36.4	22.8	
oriBGE1229	2960310	49.8	50.5	
oriBGE1230	2977769	41.1	37.8	
oriBGE1231	2982575	46.0	47.2	
oriBGE1232	3010145	51.0	52.2	
oriBGE1233	3022343	45.4	49.7	
oriBGE1234	3029678	33.6	29.8	

oriBGE1235	3053880	39.5	45.3	
oriBGE1236	3059996	53.2	54.5	
oriBGE1237	3079845	16.7	9.1	
oriBGE1238	3089075	28.8	27.0	
oriBGE1239	3100769	16.6	16.1	
oriBGE1240	3127160	43.1	40.7	
oriBGE1241	3143851	35.9	45.1	+
oriBGE1242	3165033	20.8	22.0	
oriBGE1243	3184050	37.6	51.1	+
oriBGE1244	3207700	32.0	30.3	
oriBGE1245	3218788	25.6	23.4	
oriBGE1246	3226226	30.8	27.8	
oriBGE1247	3232292	26.2	22.3	
oriBGE1248	3245960	45.7	45.5	
oriBGE1249	3269909	42.7	46.1	
oriBGE1250	3275228	36.4	31.4	
oriBGE1251	3279711	34.0	29.2	
oriBGE1252	3285217	28.9	23.7	
oriBGE1253	3300960	36.6	44.8	
oriBGE1254	3320580	50.1	51.7	
oriBGE1255	3333578	21.9	15.6	
oriBGE1256	3346988	2.2	-1.9	
oriBGE1257	3356753	0.5	-0.1	
oriBGE1258	3373054	10.8	6.9	
oriBGE1259	3376238	15.5	11.9	
oriBGE1260	3380582	18.4	13.0	
oriBGE1261	3390707	30.2	27.3	
oriBGE1262	3405185	64.1	57.9	
oriBGE1263	3409375	50.5	48.3	
oriBGE1264	3428909	34.3	24.7	
oriBGE1265	3443698	56.1	46.8	
oriBGE1266	3462486	38.9	33.8	
oriBGE1267	3469574	26.6	23.0	
oriBGE1268	3479669	21.3	19.8	
oriBGE1269	3498066	57.0	32.9	
oriBGE1270	3509397	35.1	34.1	
oriBGE1271	3520721	43.3	41.5	
oriBGE1272	3524818	44.2	41.2	
oriBGE1273	3530831	45.9	37.2	
oriBGE1274	3541842	59.5	43.0	
oriBGE1275	3548856	61.6	58.4	
oriBGE1276	3558981	54.1	54.4	
oriBGE1277	3577816	46.5	39.3	
oriBGE1278	3592599	36.0	35.6	
oriBGE1279	3611682	34.4	36.0	
oriBGE1280	3635828	50.4	48.5	
oriBGE1281	3645401	39.8	34.9	
oriBGE1282	3656622	22.7	18.4	

oriBGE1283	3673580	35.4	30.6	
oriBGE1284	3687641	50.8	48.4	
oriBGE1285	3699905	49.3	54.2	
oriBGE1286	3736206	56.8	55.3	
oriBGE1287	3753367	59.3	53.7	
oriBGE1288	3791186	58.7	57.5	
oriBGE1289	3812022	31.0	26.3	
oriBGE1290	3822187	35.3	27.8	
oriBGE1291	3826029	44.1	33.4	
oriBGE1292	3840194	51.9	48.2	
oriBGE1293	3852409	55.7	54.6	
oriBGE1294	3862792	46.5	43.7	
oriBGE1295	3879635	51.4	47.3	
oriBGE1296	3897669	46.0	45.2	
oriBGE1297	3910014	23.5	16.5	
oriBGE1298	3930617	17.9	16.8	
oriBGE1299	3934943	23.1	17.8	
oriBGE1300	3952743	61.1	54.8	
oriBGE1301	3972851	18.5	17.1	
oriBGE1302	3994435	52.1	45.7	
oriBGE1303	4019232	50.0	50.6	
oriBGE1304	4037608	17.0	12.6	
oriBGE1305	4061323	41.2	36.5	
oriBGE1306	4071675	56.9	56.5	
oriBGE1307	4088139	58.6	54.4	
oriBGE1308	4110046	21.6	-13.8	
oriBGE1309	4120022	25.0	26.7	
oriBGE1310	4137406	38.1	36.8	
oriBGE1311	4153840	36.1	40.4	
oriBGE1312	4162245	32.0	28.4	
oriBGE1313	4184841	39.6	44.5	
oriBGE1314	4197113	36.3	33.2	
oriBGE1315	4205690	25.7	22.6	
oriBGE1316	4226376	33.5	28.0	
oriBGE1317	4231434	33.6	28.4	
oriBGE1318	4239929	39.3	39.8	
oriBGE1319	4254115	42.2	50.3	+
oriBGE1320	4274404	49.3	51.3	
oriBGE1321	4292788	36.5	38.5	
oriBGE1322	4298352	35.9	34.9	
oriBGE1323	4325600	41.6	50.5	+
oriBGE1324	4342829	10.4	7.6	
oriBGE1325	4365255	8.6	30.5	+
oriBGE1326	4386771	12.8	14.1	
oriBGE1327	4393004	14.5	12.9	
oriBGE1328	4414653	21.3	36.6	+
oriBGE1329	4429090	22.3	17.5	
oriBGE1330	4438291	25.1	39.3	+

oriBGE1331	4450582	16.6	36.3	+
oriBGE1332	4467939	15.1	18.5	
oriBGE1333	4483552	43.2	48.1	
oriBGE1334	4490471	33.4	36.0	
oriBGE1335	4512384	26.2	27.8	
oriBGE1336	4517493	32.6	35.5	
oriBGE1337	4533323	48.8	47.4	
oriBGE1338	4540670	38.8	40.9	
oriBGE1339	4549670	25.2	23.2	
oriBGE1340	4558419	20.7	21.1	
oriBGE1341	4562992	16.6	16.2	
oriBGE1342	4577491	29.7	31.5	
oriBGE1343	4588259	16.5	14.9	
oriBGE1344	4603840	12.1	27.3	+
oriBGE1345	4618664	18.5	21.4	
oriBGE1346	4638586	9.9	8.2	
oriBGE1347*	4651967	9.5	21.6	+
oriBGE1348	4662633	9.5	14.3	
oriBGE1349	4686874	-0.2	3.8	
oriBGE1350	4714991	10.5	13.2	
oriBGE1351	4726326	30.2	19.0	
oriBGE1352	4739456	42.0	51.8	+
oriBGE1353	4778441	27.8	40.1	+
oriBGE1354	4797249	22.2	31.2	+
oriBGE1355	4803442	23.2	31.4	+
oriBGE1356	4810839	20.0	18.5	
oriBGE1357	4839034	34.1	31.0	
oriBGE1358	4846037	39.7	43.3	
oriBGE1359	4852547	44.6	49.8	
oriBGE1360	4874223	39.3	40.6	
oriBGE1361	4881851	40.7	48.4	
oriBGE1362	4896041	26.6	28.6	
oriBGE1363	4899649	27.3	26.5	
oriBGE1364	4917065	42.2	46.2	
oriBGE1365	4923833	43.0	40.7	
oriBGE1366	4933722	40.9	40.6	
oriBGE1367	4963629	63.7	56.2	
oriBGE1368	4978290	44.1	42.4	
oriBGE1369	4988130	19.5	18.4	
oriBGE1370	4992762	19.1	18.9	
oriBGE1371	5001902	23.5	23.2	
oriBGE1372	5024232	43.4	50.2	
oriBGE1373	5045030	46.2	55.3	+
oriBGE1374	5065860	22.0	20.7	
oriBGE1375	5077877	14.4	16.3	
oriBGE1376	5096858	17.9	33.9	+
oriBGE1377	5113891	16.2	12.7	
oriBGE1378	5122294	20.7	22.3	

oriBGE1379	5139570	41.4	43.8	
oriBGE1380	5155642	52.1	56.2	
oriBGE1381	5177311	37.4	44.6	
oriBGE1382	5186387	22.8	35.3	+
oriBGE1383	5202668	9.2	8.1	
oriBGE1384	5233342	37.0	44.8	
oriBGE1385	5253088	19.0	29.4	+
oriBGE1386	5272547	-0.6	13.6	+
oriBGE1387	5285047	2.4	5.0	
oriBGE1388	5312172	3.1	5.2	
oriBGE1389*	5321874	7.2	27.0	+
oriBGE1390	5334010	10.5	17.1	
oriBGE1391	5345577	18.9	23.6	
oriBGE1392	5354707	17.4	20.9	
oriBGE1393	5366937	11.8	15.6	
oriBGE1394	5392868	30.7	48.9	+
oriBGE1395	5413534	25.4	31.0	
oriBGE1396	5435002	34.8	42.4	
oriBGE1397	5448209	39.6	55.0	+
oriBGE1398	5470752	25.9	35.9	+
oriBGE1399	5475816	31.5	42.9	+
oriBGE1400	5481743	27.2	42.0	+
oriBGE1401*	5496576	14.9	24.5	+
oriBGE1402	5501610	16.7	33.5	+
oriBGE1403	5516212	7.4	17.7	+
oriBGE1404	5526372	8.4	20.8	+
oriBGE1405*	5537574	-0.3	16.3	+
oriBGE1406*	5541399	-1.4	14.1	+
oriBGE1407*	5544887	0.0	22.1	+
oriBGE1408*	5550942	1.3	21.1	+
oriBGE1409*	5555336	1.1	25.6	+
oriBGE1410*	5557713	3.3	24.4	+

Origin name	Chromosome II coordinates	WT	*rad3*Δ	CIO
oriBGE2001*	53392	12.7	25.9	+
oriBGE2002	61032	14.9	20.9	
oriBGE2003	66785	15.2	26.0	+
oriBGE2004	78105	23.9	38.5	+
oriBGE2005	90664	25.7	41.4	+
oriBGE2006	110067	25.0	39.5	+
oriBGE2007	116973	30.5	43.0	+
oriBGE2008	131049	29.0	44.2	+
oriBGE2009	141198	28.7	49.0	+
oriBGE2010	150965	34.5	43.8	+
oriBGE2011	160344	15.2	21.9	
oriBGE2012	175280	5.6	8.3	
oriBGE2013	193112	3.5	9.3	
oriBGE2014	204150	21.6	19.7	
oriBGE2015	213564	7.0	9.4	
oriBGE2016	219167	5.9	12.4	
oriBGE2017	243572	25.3	31.3	
oriBGE2018	258574	40.3	51.8	+
oriBGE2019	277373	48.4	53.9	
oriBGE2020	288076	41.4	45.9	
oriBGE2021	315349	55.3	58.7	
oriBGE2022	325679	48.1	54.4	
oriBGE2023	332296	46.5	50.5	
oriBGE2024	339809	41.8	43.7	
oriBGE2025	358069	31.0	30.9	
oriBGE2026	360780	28.7	33.5	
oriBGE2027	365327	24.8	23.4	
oriBGE2028	376376	14.8	14.6	
oriBGE2029	389873	25.1	27.1	
oriBGE2030	409100	44.7	46.8	
oriBGE2031	432576	15.7	15.0	
oriBGE2032	448403	29.5	35.0	
oriBGE2033	453565	25.6	37.7	+
oriBGE2034	460344	18.5	26.4	
oriBGE2035	484387	21.4	22.8	
oriBGE2036	487437	22.9	26.9	
oriBGE2037	513432	51.1	55.7	
oriBGE2038	519697	63.0	63.0	
oriBGE2039	536748	35.4	34.1	
oriBGE2040	547141	18.1	18.7	
oriBGE2041	558102	31.9	31.6	
oriBGE2042	570241	53.5	58.3	
oriBGE2043	592961	44.8	50.7	
oriBGE2044	602903	54.3	55.6	
oriBGE2045	636219	49.2	49.8	
oriBGE2046	649394	41.3	39.1	

oriBGE2047	674024	58.4	57.3	
oriBGE2048	683718	58.8	54.3	
oriBGE2049	707532	26.0	21.5	
oriBGE2050	722551	44.0	35.7	
oriBGE2051	745173	48.5	50.2	
oriBGE2052	754745	41.0	37.1	
oriBGE2053	757650	31.4	31.1	
oriBGE2054	784103	29.9	25.8	
oriBGE2055	789347	27.2	25.6	
oriBGE2056	803640	35.1	40.4	
oriBGE2057	823770	53.0	54.4	
oriBGE2058	841709	48.5	45.8	
oriBGE2059	846751	54.2	46.7	
oriBGE2060	883612	5.8	7.9	
oriBGE2061	897781	7.4	12.7	
oriBGE2062	903283	11.6	15.1	
oriBGE2063	914985	22.1	26.8	
oriBGE2064	923379	20.9	16.9	
oriBGE2065	938103	17.7	15.5	
oriBGE2066*	948190	16.7	27.3	+
oriBGE2067	956826	23.2	40.1	+
oriBGE2068	972519	8.9	8.8	
oriBGE2069	991702	9.7	10.5	
oriBGE2070	1001842	11.2	13.3	
oriBGE2071	1007250	21.1	34.6	+
oriBGE2072	1020262	18.8	19.4	
oriBGE2073	1035345	18.5	23.1	
oriBGE2074	1056966	27.6	29.2	
oriBGE2075	1061918	27.6	26.3	
oriBGE2076	1073608	11.4	10.1	
oriBGE2077	1105912	40.3	46.4	
oriBGE2078	1141640	56.1	57.0	
oriBGE2079	1156388	55.6	50.1	
oriBGE2080	1171459	32.2	32.4	
oriBGE2081	1183158	21.7	19.7	
oriBGE2082	1196022	12.1	9.8	
oriBGE2083	1209722	10.5	9.1	
oriBGE2084	1216702	16.2	15.6	
oriBGE2085	1233837	35.0	30.3	
oriBGE2086	1243763	50.1	50.6	
oriBGE2087	1254719	52.2	50.4	
oriBGE2088	1264683	59.6	57.1	
oriBGE2089	1278196	55.7	50.5	
oriBGE2090	1312462	49.6	54.0	
oriBGE2091	1323021	39.7	34.7	
oriBGE2092	1335996	20.4	18.2	
oriBGE2093	1350516	25.1	22.7	
oriBGE2094	1389515	42.2	46.5	

oriBGE2095	1403878	31.9	26.9	
oriBGE2096	1416566	25.7	21.8	
oriBGE2097	1428564	39.6	32.7	
oriBGE2098	1443491	57.9	57.2	
oriBGE2099	1457593	44.1	46.0	
oriBGE2100	1492274	11.4	9.2	
oriBGE2101	1500913	10.6	8.7	
oriBGE2102	1507192	12.0	9.6	
oriBGE2103	1513783	14.9	14.6	
oriBGE2104	1529468	30.1	25.5	
oriBGE2105	1545708	50.0	48.6	
oriBGE2106	1557029	45.1	45.0	
oriBGE2107	1589016	44.6	36.5	
oriBGE2108	1601908	61.1	54.0	
oriBGE2109	1645928	55.7	53.7	
oriBGE2110	1655423	46.4	43.6	
oriBGE2111	1664770	36.3	31.3	
oriBGE2112	1682290	20.3	16.9	
oriBGE2113	1705612	49.9	44.3	
oriBGE2114	1716948	45.5	44.0	
oriBGE2115	1749905	44.6	40.5	
oriBGE2116	1765778	43.6	42.5	
oriBGE2117	1778798	55.1	50.2	
oriBGE2118	1805044	36.0	42.3	
oriBGE2119	1835965	6.2	10.1	
oriBGE2120	1843619	4.1	8.5	
oriBGE2121	1858680	10.6	10.6	
oriBGE2122*	1867764	13.9	26.1	+
oriBGE2123	1878957	20.8	23.9	
oriBGE2124	1892959	30.2	27.0	
oriBGE2125	1914753	35.8	32.7	
oriBGE2126	1926734	37.2	33.2	
oriBGE2127	1941692	48.2	48.0	
oriBGE2128	1951989	42.4	43.6	
oriBGE2129	1963543	49.6	52.4	
oriBGE2130	1980133	23.3	19.1	
oriBGE2131	1983528	19.9	19.9	
oriBGE2132	1988787	17.4	15.3	
oriBGE2133	2008340	18.5	16.9	
oriBGE2134	2022796	52.3	54.1	
oriBGE2135	2031870	53.6	49.5	
oriBGE2136	2051864	45.0	53.7	
oriBGE2137	2070099	26.9	37.8	+
oriBGE2138	2073779	20.5	20.9	
oriBGE2139	2084910	20.8	17.7	
oriBGE2140	2091994	14.0	13.4	
oriBGE2141*	2104495	11.1	29.4	+
oriBGE2142	2117860	24.6	37.7	+

oriBGE2143	2131265	52.0	58.5	
oriBGE2144	2135744	53.5	57.3	
oriBGE2145	2155289	28.7	28.5	
oriBGE2146	2176828	42.4	42.7	
oriBGE2147	2185353	41.1	49.6	+
oriBGE2148	2204788	27.8	29.4	
oriBGE2149	2213894	28.7	33.3	
oriBGE2150	2229425	37.4	33.9	
oriBGE2151	2239300	34.6	30.2	
oriBGE2152	2246174	39.9	46.9	
oriBGE2153	2254266	38.1	40.5	
oriBGE2154	2274292	11.7	18.7	
oriBGE2155	2282645	11.9	13.8	
oriBGE2156	2295239	8.3	10.0	
oriBGE2157	2318971	48.8	51.1	
oriBGE2158*	2338947	10.0	21.2	+
oriBGE2159	2347861	18.5	29.9	+
oriBGE2160	2365840	21.6	22.4	
oriBGE2161	2373003	23.5	20.7	
oriBGE2162	2386458	12.2	13.2	
oriBGE2163	2401817	7.1	11.3	
oriBGE2164	2410748	10.7	29.9	+
oriBGE2165	2434192	33.2	38.5	
oriBGE2166	2443426	49.6	52.4	
oriBGE2167	2451244	37.3	39.0	
oriBGE2168	2468848	15.8	15.7	
oriBGE2169	2484908	25.6	27.7	
oriBGE2170	2498684	21.9	41.3	+
oriBGE2171	2523482	43.6	48.7	
oriBGE2172	2535707	25.7	25.3	
oriBGE2173	2553220	31.8	49.9	+
oriBGE2174	2566699	18.7	23.9	
oriBGE2175*	2581292	17.6	30.8	+
oriBGE2176	2593873	37.6	47.6	+
oriBGE2177	2613250	17.4	21.9	
oriBGE2178	2632210	15.6	28.1	+
oriBGE2179	2640141	14.2	19.3	
oriBGE2180	2661290	15.5	26.1	+
oriBGE2181	2670747	23.4	38.1	+
oriBGE2182	2696047	32.9	29.8	
oriBGE2183	2701825	39.4	48.3	
oriBGE2184	2725749	36.6	32.0	
oriBGE2185	2733340	47.0	46.8	
oriBGE2186	2738266	45.7	54.4	+
oriBGE2187	2750684	15.6	16.9	
oriBGE2188	2768588	24.8	24.3	
oriBGE2189	2778282	37.2	35.7	
oriBGE2190	2791240	49.6	50.1	

oriBGE2191	2798983	46.5	54.1	
oriBGE2192	2809612	23.9	10.8	
oriBGE2193	2814667	12.0	9.1	
oriBGE2194	2824940	13.0	24.5	+
oriBGE2195	2839014	8.7	8.2	
oriBGE2196	2849310	15.1	11.3	
oriBGE2197	2874309	10.2	11.8	
oriBGE2198	2886502	9.9	11.6	
oriBGE2199	2900799	32.6	47.8	+
oriBGE2200	2909239	20.2	25.1	
oriBGE2201	2929636	19.2	15.3	
oriBGE2202	2939452	42.6	51.5	+
oriBGE2203	2951834	19.5	18.3	
oriBGE2204	2967034	18.1	19.1	
oriBGE2205	2976907	28.2	25.9	
oriBGE2206	2985744	36.4	39.0	
oriBGE2207	3022159	5.2	10.5	
oriBGE2208	3035623	15.1	16.1	
oriBGE2209	3051866	29.1	39.7	+
oriBGE2210	3069096	19.9	33.5	+
oriBGE2211	3097859	22.8	40.5	+
oriBGE2212	3118428	17.3	17.7	
oriBGE2213	3126414	14.1	16.4	
oriBGE2214	3137181	20.4	28.6	
oriBGE2215*	3152870	8.0	27.7	+
oriBGE2216	3162762	11.7	24.3	+
oriBGE2217	3176078	39.9	50.9	+
oriBGE2218	3181798	25.2	29.5	
oriBGE2219	3199378	10.7	28.9	+
oriBGE2220	3211266	16.6	22.6	
oriBGE2221	3236787	30.6	41.5	+
oriBGE2222	3251717	23.9	28.1	
oriBGE2223	3260684	11.4	10.9	
oriBGE2224	3268929	13.6	18.1	
oriBGE2225	3287127	38.5	46.4	
oriBGE2226	3302664	23.5	26.4	
oriBGE2227	3323340	17.6	18.4	
oriBGE2228	3333311	35.5	42.3	
oriBGE2229	3338041	36.0	44.3	
oriBGE2230	3347135	23.2	30.4	
oriBGE2231	3360383	27.9	43.3	+
oriBGE2232	3397334	16.6	21.1	
oriBGE2233	3422044	35.8	48.8	+
oriBGE2234	3450295	15.7	17.1	
oriBGE2235	3455496	25.9	23.2	
oriBGE2236	3466883	27.6	26.1	
oriBGE2237	3491037	39.7	45.9	
oriBGE2238	3512792	33.7	38.4	

oriBGE2239	3523499	21.9	19.9	
oriBGE2240	3535744	11.4	10.4	
oriBGE2241	3557026	19.0	36.1	+
oriBGE2242	3585437	13.9	18.4	
oriBGE2243	3591230	24.4	24.9	
oriBGE2244	3597067	34.7	37.9	
oriBGE2245	3605052	37.3	41.6	
oriBGE2246	3615442	30.4	36.5	
oriBGE2247	3634742	46.7	50.4	
oriBGE2248	3659686	38.9	45.4	
oriBGE2249	3670631	32.1	29.2	
oriBGE2250	3680961	24.4	37.1	+
oriBGE2251	3692218	10.4	15.9	
oriBGE2252	3714909	25.1	30.2	
oriBGE2253	3721295	27.6	39.2	+
oriBGE2254	3733250	21.7	21.4	
oriBGE2255	3753374	30.9	34.3	
oriBGE2256	3762927	41.3	47.3	
oriBGE2257	3777228	16.3	17.5	
oriBGE2258	3785539	24.0	24.6	
oriBGE2259	3801240	38.2	38.8	
oriBGE2260	3815500	43.5	49.8	
oriBGE2261	3826728	42.3	48.0	
oriBGE2262	3839190	40.2	49.3	+
oriBGE2263	3869263	15.5	19.4	
oriBGE2264	3898107	21.5	21.2	
oriBGE2265	3915944	40.6	45.7	
oriBGE2266	3926179	41.3	48.0	
oriBGE2267	3937859	41.5	51.4	+
oriBGE2268	3944513	38.4	42.1	
oriBGE2269	3956593	23.5	26.9	
oriBGE2270	3970088	12.5	15.9	
oriBGE2271	3989755	16.7	27.5	+
oriBGE2272	3999936	23.5	32.6	+
oriBGE2273	4019504	44.4	51.9	
oriBGE2274	4029239	36.2	50.9	+
oriBGE2275	4048685	25.3	37.0	+
oriBGE2276	4066677	16.6	21.3	
oriBGE2277	4082217	8.2	8.9	
oriBGE2278	4094098	13.9	16.1	
oriBGE2279	4108009	10.6	23.5	+
oriBGE2280	4127855	17.7	19.5	
oriBGE2281	4140082	37.4	52.9	+
oriBGE2282	4143673	34.7	41.3	
oriBGE2283	4172101	19.8	23.4	
oriBGE2284	4177432	15.3	20.2	
oriBGE2285	4195333	26.7	33.3	
oriBGE2286	4202802	31.6	51.7	+

oriBGE2287	4218231	16.8	24.4	
oriBGE2288	4226107	22.5	42.1	+
oriBGE2289	4237196	22.4	38.1	+
oriBGE2290	4241327	17.6	26.9	+
oriBGE2291*	4252171	8.5	24.8	+
oriBGE2292	4268700	9.1	17.3	+
oriBGE2293	4292228	6.4	26.3	+
oriBGE2294	4298210	5.0	5.4	
oriBGE2295	4302543	6.3	11.3	
oriBGE2296	4314944	8.0	11.6	
oriBGE2297	4321474	11.9	16.1	
oriBGE2298	4335121	11.8	16.3	
oriBGE2299*	4343709	8.5	25.2	+
oriBGE2300	4350577	12.4	21.8	+
oriBGE2301	4360173	28.3	44.1	+
oriBGE2302	4375402	20.8	37.1	+
oriBGE2303	4403130	14.0	24.0	+
oriBGE2304	4413030	19.0	36.7	+
oriBGE2305	4419904	20.6	35.1	+
oriBGE2306*	4426261	14.7	27.4	+
oriBGE2307	4439913	19.4	40.0	+
oriBGE2308	4452478	21.1	36.9	+
oriBGE2309	4468111	17.9	34.7	+
oriBGE2310	4477969	16.0	33.2	+
oriBGE2311	4491129	12.6	27.9	+

Origin name	Chromosome III coordinates	WT	*rad3*Δ	CIO
oriBGE3001	35352	46.9	48.0	
oriBGE3002	51806	34.0	27.6	
oriBGE3003	61450	38.8	37.7	
oriBGE3004	69571	38.4	33.6	
oriBGE3005	76370	50.6	50.1	
oriBGE3006	91924	28.1	29.1	
oriBGE3007	100580	29.2	24.9	
oriBGE3008	109386	44.6	40.7	
oriBGE3009	122985	58.2	53.4	
oriBGE3010	148049	26.3	24.4	
oriBGE3011	163568	14.7	12.1	
oriBGE3012	188494	38.8	34.0	
oriBGE3013	205826	46.1	44.0	
oriBGE3014	212804	45.8	34.7	
oriBGE3015	217421	47.0	42.1	
oriBGE3016	232110	53.8	51.8	
oriBGE3017	253688	43.1	35.5	
oriBGE3018	278484	45.0	40.2	
oriBGE3019	287447	53.2	52.4	
oriBGE3020	300114	40.5	39.9	
oriBGE3021	309654	43.8	42.4	
oriBGE3022	319296	40.5	38.1	
oriBGE3023	332086	46.7	42.2	
oriBGE3024	339004	32.4	25.2	
oriBGE3025	348452	22.8	18.2	
oriBGE3026	369752	60.4	61.8	
oriBGE3027	382485	40.2	33.6	
oriBGE3028	398000	54.8	57.6	
oriBGE3029	414852	31.6	27.2	
oriBGE3030	421198	31.5	27.5	
oriBGE3031	435177	25.9	25.7	
oriBGE3032	454640	38.2	29.8	
oriBGE3033	473056	50.3	43.1	
oriBGE3034	483688	38.3	36.0	
oriBGE3035	505412	55.8	53.3	
oriBGE3036	519157	59.4	57.1	
oriBGE3037	528729	45.0	37.8	
oriBGE3038	554055	37.8	28.0	
oriBGE3039	568068	57.6	55.0	
oriBGE3040	574524	53.9	51.8	
oriBGE3041	605443	46.0	52.5	
oriBGE3042	616169	38.2	32.4	
oriBGE3043	643228	58.6	59.4	
oriBGE3044	666596	34.5	45.0	
oriBGE3045	682051	14.7	6.2	
oriBGE3046	690007	21.9	17.9	

oriBGE3047	707983	41.9	39.6	
oriBGE3048	720070	55.9	51.7	
oriBGE3049	729007	45.5	37.0	
oriBGE3050	736453	28.8	26.2	
oriBGE3051	751743	43.6	39.4	
oriBGE3052	765474	51.6	48.5	
oriBGE3053	791098	25.2	20.0	
oriBGE3054	800830	25.2	20.1	
oriBGE3055	821292	57.7	51.1	
oriBGE3056	828741	46.3	40.7	
oriBGE3057	837502	46.7	43.7	
oriBGE3058	844580	45.9	43.1	
oriBGE3059	854087	54.8	54.7	
oriBGE3060	873747	20.9	18.4	
oriBGE3061	883315	23.8	20.1	
oriBGE3062	899748	40.1	34.8	
oriBGE3063	905710	42.6	36.9	
oriBGE3064	936120	59.4	58.1	
oriBGE3065	955441	27.2	21.5	
oriBGE3066	962226	41.8	25.8	
oriBGE3067	971929	61.0	58.6	
oriBGE3068	976212	45.9	38.3	
oriBGE3069	985891	47.7	50.8	
oriBGE3070	1002295	27.9	27.7	
oriBGE3071	1010895	26.3	21.7	
oriBGE3072	1023611	22.8	21.2	
oriBGE3073	1039325	16.7	29.7	+
oriBGE3074	1065780	61.3	56.7	
oriBGE3075	1141383	57.0	51.9	
oriBGE3076	1151271	40.9	33.8	
oriBGE3077	1168640	28.8	28.6	
oriBGE3078	1193774	53.3	52.9	
oriBGE3079	1216692	19.5	17.1	
oriBGE3080	1229261	13.8	10.0	
oriBGE3081	1252967	54.5	54.1	
oriBGE3082	1267433	41.4	32.9	
oriBGE3083	1282724	28.9	28.8	
oriBGE3084	1297025	27.4	23.4	
oriBGE3085	1323220	64.4	57.7	
oriBGE3086	1342861	38.8	41.6	
oriBGE3087	1370975	59.0	52.9	
oriBGE3088	1395731	57.6	51.1	
oriBGE3089	1410390	65.4	63.1	
oriBGE3090	1415473	54.9	50.9	
oriBGE3091	1423298	44.2	42.3	
oriBGE3092	1448627	63.0	61.2	
oriBGE3093	1459178	42.7	39.2	
oriBGE3094	1468689	31.9	24.5	

oriBGE3095	1472802	32.4	25.8
oriBGE3096	1482115	26.5	21.1
oriBGE3097	1496967	37.9	32.4
oriBGE3098	1510066	53.1	50.4
oriBGE3099	1531239	51.5	47.0
oriBGE3100	1555354	48.5	44.4
oriBGE3101	1576300	51.9	52.3
oriBGE3102	1594687	58.0	52.2
oriBGE3103	1608489	67.1	62.5
oriBGE3104	1633993	17.4	13.9
oriBGE3105	1654204	26.5	24.4
oriBGE3106	1674301	47.9	46.5
oriBGE3107	1683568	58.5	57.5
oriBGE3108	1687750	54.9	43.7
oriBGE3109	1706435	40.3	29.2
oriBGE3110	1721883	57.3	53.2
oriBGE3111	1745489	52.8	50.7
oriBGE3112	1754185	53.1	51.5
oriBGE3113	1782973	27.2	22.2
oriBGE3114	1796997	32.1	27.8
oriBGE3115	1813978	54.8	52.2
oriBGE3116	1821881	59.3	57.8
oriBGE3117	1844115	59.1	58.7
oriBGE3118	1867147	55.5	53.8
oriBGE3119	1895660	18.7	15.0
oriBGE3120	1929217	56.9	53.4
oriBGE3121	1937726	36.4	30.5
oriBGE3122	1968719	66.0	56.8
oriBGE3123	1994371	35.0	31.4
oriBGE3124	2000161	32.1	29.7
oriBGE3125	2010157	28.3	25.0
oriBGE3126	2022689	44.7	36.2
oriBGE3127	2035249	53.4	57.1
oriBGE3128	2044423	39.8	36.3
oriBGE3129	2063186	51.7	48.1
oriBGE3130	2066338	50.5	50.5
oriBGE3131	2078654	34.2	25.1
oriBGE3132	2106962	52.2	53.8
oriBGE3133	2115176	34.9	32.1
oriBGE3134	2139009	38.7	34.6
oriBGE3135	2151753	29.9	26.8
oriBGE3136	2158836	29.2	25.4
oriBGE3137	2170670	24.5	21.4
oriBGE3138	2187036	24.2	23.5
oriBGE3139	2200798	46.5	52.7
oriBGE3140	2209628	36.7	36.1
oriBGE3141	2220190	27.6	34.4
oriBGE3142	2230371	29.1	26.3

oriBGE3143	2242543	19.5	16.8	
oriBGE3144	2257678	24.2	25.6	
oriBGE3145	2276299	47.2	50.2	
oriBGE3146	2291012	23.2	25.2	
oriBGE3147	2299583	26.9	35.4	+
oriBGE3148	2336182	33.4	41.8	
oriBGE3149	2349605	22.2	22.7	
oriBGE3150	2364110	37.5	40.8	
oriBGE3151	2382163	51.9	55.1	
oriBGE3152	2392027	38.2	35.1	
oriBGE3153	2406731	24.7	22.5	
oriBGE3154	2419309	32.8	34.4	
oriBGE3155	2428929	35.1	41.1	

Supplemental Table S2: List of *C*heckpoint-*I*nhibited *O*rigins (CIOs). Values indicate differences in origin efficiencies (*rad3Δ* - WT).

Origin name	Chromosome I coordinates	Difference in efficiency
oriBGE1001	6212	17.6
oriBGE1002	14096	20.5
oriBGE1003	19570	14.7
oriBGE1004	51004	9.1
oriBGE1006	71137	9.5
oriBGE1007	79544	10.3
oriBGE1008	84480	8.8
oriBGE1009	86730	10.2
oriBGE1010	94607	12.9
oriBGE1012	112286	10.4
oriBGE1013	124602	10.4
oriBGE1017	164454	10.3
oriBGE1020	189672	9.7
oriBGE1021	199362	13.6
oriBGE1023	240008	15.7
oriBGE1027	293566	21.9
oriBGE1028	311940	10.3
oriBGE1029	319141	8.1
oriBGE1030	325923	20.7
oriBGE1031	364660	21.1
oriBGE1034	410626	14
oriBGE1035	434067	13.6
oriBGE1036	439953	19.5
oriBGE1037	463593	9.9
oriBGE1038	473721	18.5
oriBGE1039	490088	14.9
oriBGE1046	562906	18.7
oriBGE1049	608104	21.3
oriBGE1051	650229	20.2
oriBGE1061	765612	17.3
oriBGE1062	794338	14.3
oriBGE1083	1027338	17.3
oriBGE1099	1276292	10.4
oriBGE1106	1359944	11.6
oriBGE1121	1574006	15.8
oriBGE1125	1603801	12.9
oriBGE1156	1954759	8
oriBGE1157	1974622	9.6
oriBGE1162	2025258	18.3
oriBGE1163	2041847	13.4
oriBGE1166	2084565	9.8
oriBGE1167	2095493	16.7

oriBGE1171	2132024	8.8
oriBGE1172	2140329	23
oriBGE1179	2228058	9.2
oriBGE1182	2249881	12.2
oriBGE1183	2263318	8.6
oriBGE1185	2280057	11.2
oriBGE1186	2305633	9.8
oriBGE1187	2339782	12.2
oriBGE1193	2398512	25.6
oriBGE1194	2415024	13.2
oriBGE1195	2424923	10.4
oriBGE1197	2451814	10.3
oriBGE1200	2489271	15.5
oriBGE1202	2525733	20.7
oriBGE1206	2600933	13.4
oriBGE1209	2638235	9.6
oriBGE1210	2642609	18.1
oriBGE1211	2662653	10.7
oriBGE1212	2673297	9.6
oriBGE1213	2685431	14.9
oriBGE1223	2862190	11.6
oriBGE1224	2882448	16.7
oriBGE1225	2912248	8.7
oriBGE1241	3143851	9.2
oriBGE1243	3184050	13.5
oriBGE1319	4254115	8.1
oriBGE1323	4325600	8.9
oriBGE1325	4365255	21.9
oriBGE1328	4414653	15.3
oriBGE1330	4438291	14.2
oriBGE1331	4450582	19.7
oriBGE1344	4603840	15.2
oriBGE1347	4651967	12.1
oriBGE1352	4739456	9.8
oriBGE1353	4778441	12.3
oriBGE1354	4797249	9
oriBGE1355	4803442	8.2
oriBGE1373	5045030	9.1
oriBGE1376	5096858	16
oriBGE1382	5186387	12.5
oriBGE1385	5253088	10.4
oriBGE1386	5272547	14.2
oriBGE1389	5321874	19.8
oriBGE1394	5392868	18.2
oriBGE1397	5448209	15.4
oriBGE1398	5470752	10
oriBGE1399	5475816	11.4
oriBGE1400	5481743	14.8

oriBGE1401	5496576	9.6
oriBGE1402	5501610	16.8
oriBGE1403	5516212	10.3
oriBGE1404	5526372	12.4
oriBGE1405	5537574	16.6
oriBGE1406	5541399	15.5
oriBGE1407	5544887	22.1
oriBGE1408	5550942	19.8
oriBGE1409	5555336	24.5
oriBGE1410	5557713	21.1

Origin name	**Chromosome II coordinates**	**Difference in efficiency**
oriBGE2001	53392	13.2
oriBGE2003	66785	10.8
oriBGE2004	78105	14.6
oriBGE2005	90664	15.7
oriBGE2006	110067	14.5
oriBGE2007	116973	12.5
oriBGE2008	131049	15.2
oriBGE2009	141198	20.3
oriBGE2010	150965	9.3
oriBGE2018	258574	11.5
oriBGE2033	453565	12.1
oriBGE2066	948190	10.6
oriBGE2067	956826	16.9
oriBGE2071	1007250	13.5
oriBGE2122	1867764	12.2
oriBGE2137	2070099	10.9
oriBGE2141	2104495	18.3
oriBGE2142	2117860	13.1
oriBGE2147	2185353	8.5
oriBGE2158	2338947	11.2
oriBGE2159	2347861	11.4
oriBGE2164	2410748	19.2
oriBGE2170	2498684	19.4
oriBGE2173	2553220	18.1
oriBGE2175	2581292	13.2
oriBGE2176	2593873	10
oriBGE2178	2632210	12.5
oriBGE2180	2661290	10.6
oriBGE2181	2670747	14.7
oriBGE2186	2738266	8.7
oriBGE2194	2824940	11.5
oriBGE2199	2900799	15.2
oriBGE2202	2939452	8.9
oriBGE2209	3051866	10.6
oriBGE2210	3069096	13.6

oriBGE2211	3097859	17.7
oriBGE2215	3152870	19.7
oriBGE2216	3162762	12.6
oriBGE2217	3176078	11
oriBGE2219	3199378	18.2
oriBGE2221	3236787	10.9
oriBGE2231	3360383	15.4
oriBGE2233	3422044	13
oriBGE2241	3557026	17.1
oriBGE2250	3680961	12.7
oriBGE2253	3721295	11.6
oriBGE2262	3839190	9.1
oriBGE2267	3937859	9.9
oriBGE2271	3989755	10.8
oriBGE2272	3999936	9.1
oriBGE2274	4029239	14.7
oriBGE2275	4048685	11.7
oriBGE2279	4108009	12.9
oriBGE2281	4140082	15.5
oriBGE2286	4202802	20.1
oriBGE2288	4226107	19.6
oriBGE2289	4237196	15.7
oriBGE2290	4241327	9.3
oriBGE2291	4252171	16.3
oriBGE2292	4268700	8.2
oriBGE2293	4292228	19.9
oriBGE2299	4343709	16.7
oriBGE2300	4350577	9.4
oriBGE2301	4360173	15.8
oriBGE2302	4375402	16.3
oriBGE2303	4403130	10
oriBGE2304	4413030	17.7
oriBGE2305	4419904	14.5
oriBGE2306	4426261	12.7
oriBGE2307	4439913	20.6
oriBGE2308	4452478	15.8
oriBGE2309	4468111	16.8
oriBGE2310	4477969	17.2
oriBGE2311	4491129	15.3

Origin name	**Chromosome III coordinates**	**Difference in efficiency**
oriBGE3073	1039325	13
oriBGE3147	2299583	8.5

Supplemental Table S3: Replication origins that show decreased efficiencies in *rad3Δ* vs. wild-type cells. Values indicate differences in origin efficiencies (*rad3Δ* - WT).

Origin name	Chromosome coordinates	Difference in efficiency
oriBGE1264	chrI:3428909	-9.6
oriBGE1291	chrI:3826029	-10.7
oriBGE2107	chrII:1589016	-8.1
oriBGE3066	chrIII:962226	-16
oriBGE3122	chrIII:1968719	-9.2
oriBGE3126	chrIII:2022689	-8.5

Supplemental Table S4: Replication origins mapped in the *rif1*Δ background. Values indicate origin efficiencies.

Origin name	***rif1*Δ**	***rif1*Δ*rad3*Δ**	***rif1*Δ-CIO**
oriBGE1001	53.5	54.5	
oriBGE1002	60.7	66.6	
oriBGE1003	55.7	59.5	
oriBGE1004	55.6	51.4	
oriBGE1005	56.5	61.6	
oriBGE1006	63.4	57.9	
oriBGE1007	60.3	61.7	
oriBGE1008	57.8	55.4	
oriBGE1009	58.9	55.8	
oriBGE1010	53.0	55.4	
oriBGE1011	44.8	42.7	
oriBGE1012	44.9	44.0	
oriBGE1013	45.2	54.6	+
oriBGE1014	42.8	38.1	
oriBGE1015	29.7	26.7	
oriBGE1016	25.4	30.8	
oriBGE1017	20.1	29.3	
oriBGE1018	24.5	23.5	
oriBGE1019	28.9	22.7	
oriBGE1020	43.0	39.6	
oriBGE1021	46.5	50.7	
oriBGE1022	12.5	12.7	
oriBGE1023	44.5	50.3	
oriBGE1024	11.3	7.0	
oriBGE1025	15.6	16.3	
oriBGE1026	25.8	19.9	
oriBGE1027	45.5	54.6	+
oriBGE1028	37.2	39.9	
oriBGE1029	40.6	42.3	
oriBGE1030	42.9	52.2	
oriBGE1031	44.7	58.6	+
oriBGE1032	23.1	18.5	
oriBGE1033	14.9	21.8	
oriBGE1034	33.8	48.1	+
oriBGE1035	40.2	42.1	
oriBGE1036	46.6	50.1	
oriBGE1037	36.4	41.8	
oriBGE1038	38.1	39.1	
oriBGE1039	43.7	53.1	
oriBGE1040	13.8	15.5	
oriBGE1041	17.1	16.7	
oriBGE1042	19.9	19.3	

oriBGE1043	14.5	10.7	
oriBGE1044	25.7	22.8	
oriBGE1045	31.9	38.0	
oriBGE1046	41.9	49.4	
oriBGE1047	21.3	30.6	+
oriBGE1048	22.9	27.4	
oriBGE1049	45.6	51.7	
oriBGE1050	16.8	21.9	
oriBGE1051	34.2	40.8	
oriBGE1052	20.5	28.9	
oriBGE1053	11.8	16.8	
oriBGE1054	15.8	22.4	
oriBGE1055	17.3	21.9	
oriBGE1056	37.6	35.4	
oriBGE1057	47.8	49.5	
oriBGE1058	16.9	15.5	
oriBGE1059	12.6	16.3	
oriBGE1060	18.6	23.6	
oriBGE1061	48.0	47.7	
oriBGE1062	37.3	49.9	+
oriBGE1063	16.9	19.9	
oriBGE1064	11.6	14.1	
oriBGE1065	9.1	8.5	
oriBGE1066	16.2	17.6	
oriBGE1067	37.0	51.8	+
oriBGE1068	35.0	49.7	+
oriBGE1069	33.6	43.6	+
oriBGE1070	41.7	48.0	
oriBGE1071	28.6	29.3	
oriBGE1072	18.2	21.9	
oriBGE1073	22.4	23.2	
oriBGE1074	23.4	29.5	
oriBGE1075	36.5	38.1	
oriBGE1076	46.7	55.2	+
oriBGE1077	26.5	33.0	
oriBGE1078	18.3	18.5	
oriBGE1079	15.1	23.3	
oriBGE1080	21.9	27.6	
oriBGE1081	31.7	32.6	
oriBGE1082	43.5	38.6	
oriBGE1083	58.2	54.2	
oriBGE1084	18.4	31.1	+
oriBGE1085	52.6	49.8	
oriBGE1086	51.1	54.9	
oriBGE1087	49.3	50.5	
oriBGE1088	21.8	26.1	
oriBGE1089	14.8	10.5	
oriBGE1090	31.8	39.9	+

oriBGE1091	28.2	33.3	
oriBGE1092	28.8	37.8	+
oriBGE1093	31.5	37.7	
oriBGE1094	45.6	46.6	
oriBGE1095	47.5	50.9	
oriBGE1096	12.3	10.9	
oriBGE1097	16.9	26.7	
oriBGE1098	39.4	55.2	+
oriBGE1099	43.6	51.5	
oriBGE1100	44.8	46.5	
oriBGE1101	24.0	26.4	
oriBGE1102	30.4	31.6	
oriBGE1103	25.1	24.3	
oriBGE1104	23.0	22.5	
oriBGE1105	42.4	37.8	
oriBGE1106	50.0	47.6	
oriBGE1107	35.4	32.2	
oriBGE1108	28.2	29.7	
oriBGE1109	33.3	40.1	
oriBGE1110	18.8	20.4	
oriBGE1111	32.2	38.5	
oriBGE1112	40.5	37.8	
oriBGE1113	49.9	62.0	+
oriBGE1114	37.8	40.5	
oriBGE1115	29.9	38.0	
oriBGE1116	45.2	54.6	
oriBGE1117	21.2	21.5	
oriBGE1118	16.3	26.5	+
oriBGE1119	16.5	21.2	
oriBGE1120	15.3	16.1	
oriBGE1121	40.1	53.4	
oriBGE1122	28.7	21.0	
oriBGE1123	33.8	30.8	
oriBGE1124	40.4	43.4	
oriBGE1125	44.2	45.0	
oriBGE1126	25.5	27.1	
oriBGE1127	20.8	26.7	
oriBGE1128	16.3	21.8	
oriBGE1129	13.3	14.4	
oriBGE1130	48.0	53.9	
oriBGE1131	15.8	20.5	
oriBGE1132	19.9	23.6	
oriBGE1133	36.8	53.6	+
oriBGE1134	37.7	48.7	+
oriBGE1135	44.6	49.5	
oriBGE1136	35.8	36.7	
oriBGE1137	20.1	23.2	
oriBGE1138	21.2	26.8	

oriBGE1139	18.3	21.0	
oriBGE1140	20.2	19.5	
oriBGE1141	21.3	30.9	+
oriBGE1142	20.4	23.9	
oriBGE1143	20.5	27.5	
oriBGE1144	24.8	21.9	
oriBGE1145	47.0	54.9	
oriBGE1146	48.4	59.9	+
oriBGE1147	20.1	24.5	
oriBGE1148	33.6	41.0	
oriBGE1149	36.2	31.4	
oriBGE1150	41.6	49.4	
oriBGE1151	40.3	30.3	
oriBGE1152	22.2	20.4	
oriBGE1153	21.2	24.7	
oriBGE1154	20.5	27.3	
oriBGE1155	28.2	26.2	
oriBGE1156	53.8	56.4	
oriBGE1157	45.3	48.4	
oriBGE1158	38.8	37.1	
oriBGE1159	25.2	29.6	
oriBGE1160	15.3	17.4	
oriBGE1161	33.2	34.7	
oriBGE1162	42.6	43.1	
oriBGE1163	42.8	47.9	
oriBGE1164	14.1	21.1	
oriBGE1165	22.5	30.2	
oriBGE1166	34.1	37.7	
oriBGE1167	41.7	49.2	
oriBGE1168	31.5	28.7	
oriBGE1169	17.4	20.4	
oriBGE1170	18.8	21.4	
oriBGE1171	31.7	30.7	
oriBGE1172	43.0	52.9	
oriBGE1173	26.4	30.7	
oriBGE1174	26.3	26.1	
oriBGE1175	36.9	39.5	
oriBGE1176	44.0	54.4	+
oriBGE1177	28.3	38.4	+
oriBGE1178	26.2	20.9	
oriBGE1179	36.3	42.4	
oriBGE1180	36.6	34.5	
oriBGE1181	38.8	48.9	+
oriBGE1182	43.6	50.2	
oriBGE1183	39.1	46.3	
oriBGE1184	38.1	42.0	
oriBGE1185	39.9	53.4	+
oriBGE1186	39.6	42.3	

oriBGE1187	46.1	49.2	
oriBGE1188	36.0	36.3	
oriBGE1189	31.0	25.3	
oriBGE1190	15.6	14.6	
oriBGE1191	16.4	18.2	
oriBGE1192	20.1	22.0	
oriBGE1193	46.0	53.2	
oriBGE1194	46.3	50.0	
oriBGE1195	40.7	43.8	
oriBGE1196	46.1	54.8	
oriBGE1197	40.1	41.3	
oriBGE1198	33.3	38.8	
oriBGE1199	28.6	33.2	
oriBGE1200	36.0	43.5	
oriBGE1201	32.5	43.6	+
oriBGE1202	44.6	45.5	
oriBGE1203	21.3	17.8	
oriBGE1204	16.4	17.8	
oriBGE1205	38.5	46.0	
oriBGE1206	36.0	43.1	
oriBGE1207	33.8	43.9	+
oriBGE1208	27.9	27.2	
oriBGE1209	44.4	41.8	
oriBGE1210	41.7	51.2	+
oriBGE1211	45.6	44.1	
oriBGE1212	38.8	35.9	
oriBGE1213	32.4	37.8	
oriBGE1214	42.0	53.8	+
oriBGE1215	30.2	35.8	
oriBGE1216	49.0	52.1	
oriBGE1217	30.6	27.6	
oriBGE1218	27.5	38.2	+
oriBGE1219	47.1	43.3	
oriBGE1220	36.4	31.3	
oriBGE1221	19.2	26.5	
oriBGE1222	27.2	24.7	
oriBGE1223	39.6	52.4	+
oriBGE1224	44.7	46.3	
oriBGE1225	35.0	48.1	+
oriBGE1226	26.0	25.8	
oriBGE1227	30.9	40.4	+
oriBGE1228	29.9	28.6	
oriBGE1229	42.6	51.5	
oriBGE1230	41.4	47.6	
oriBGE1231	45.1	52.9	
oriBGE1232	39.5	47.5	
oriBGE1233	38.4	52.1	+
oriBGE1234	35.8	33.8	

oriBGE1235	40.4	45.8	
oriBGE1236	44.5	55.2	
oriBGE1237	12.5	14.2	
oriBGE1238	21.8	28.7	
oriBGE1239	12.0	12.7	
oriBGE1240	28.6	48.3	+
oriBGE1241	39.9	52.4	+
oriBGE1242	37.1	37.7	
oriBGE1243	44.1	50.1	
oriBGE1244	23.5	33.5	+
oriBGE1245	19.7	23.4	
oriBGE1246	20.9	27.7	
oriBGE1247	21.1	19.6	
oriBGE1248	32.4	43.6	+
oriBGE1249	38.2	51.3	
oriBGE1250	30.5	30.9	
oriBGE1251	30.1	31.0	
oriBGE1252	24.0	25.0	
oriBGE1253	33.1	44.1	+
oriBGE1254	41.8	48.8	
oriBGE1255	21.1	17.6	
oriBGE1256	5.5	3.1	
oriBGE1257	0.5	4.9	
oriBGE1258	9.4	12.0	
oriBGE1259	13.0	14.0	
oriBGE1260	16.2	14.8	
oriBGE1261	22.8	22.6	
oriBGE1262	52.8	56.3	
oriBGE1263	47.0	51.5	
oriBGE1264	17.8	19.4	
oriBGE1265	40.1	49.3	
oriBGE1266	24.5	34.6	+
oriBGE1267	18.5	17.5	
oriBGE1268	15.3	16.6	
oriBGE1269	43.2	52.0	+
oriBGE1270	30.6	26.5	
oriBGE1271	30.9	28.2	
oriBGE1272	29.4	35.0	
oriBGE1273	28.9	25.6	
oriBGE1274	40.4	39.4	
oriBGE1275	43.2	48.0	
oriBGE1276	35.0	46.8	+
oriBGE1277	44.6	45.0	
oriBGE1278	24.5	29.0	
oriBGE1279	23.2	28.9	
oriBGE1280	37.4	46.2	
oriBGE1281	23.5	24.4	
oriBGE1282	8.6	14.5	

oriBGE1283	17.5	25.8	+
oriBGE1284	29.3	34.3	
oriBGE1285	42.0	45.4	
oriBGE1286	36.1	40.5	
oriBGE1287	46.7	44.2	
oriBGE1288	41.4	47.1	
oriBGE1289	19.3	24.0	
oriBGE1290	17.7	21.5	
oriBGE1291	22.9	24.1	
oriBGE1292	42.3	48.3	
oriBGE1293	38.8	55.3	+
oriBGE1294	28.9	24.5	
oriBGE1295	47.8	49.3	
oriBGE1296	23.1	34.6	+
oriBGE1297	17.1	18.1	
oriBGE1298	10.0	14.5	
oriBGE1299	9.2	14.3	
oriBGE1300	40.7	53.6	+
oriBGE1301	12.0	15.3	
oriBGE1302	43.8	52.6	
oriBGE1303	43.3	53.7	
oriBGE1304	11.5	9.4	
oriBGE1305	29.7	26.6	
oriBGE1306	41.1	45.5	
oriBGE1307	46.7	53.6	
oriBGE1308	7.2	5.3	
oriBGE1309	21.4	27.3	
oriBGE1310	42.8	46.7	
oriBGE1311	32.6	46.7	+
oriBGE1312	27.0	31.3	
oriBGE1313	47.7	51.8	
oriBGE1314	31.4	40.0	+
oriBGE1315	24.2	20.3	
oriBGE1316	24.5	28.2	
oriBGE1317	32.3	30.7	
oriBGE1318	42.3	44.7	
oriBGE1319	41.2	50.3	+
oriBGE1320	35.9	52.9	+
oriBGE1321	33.6	33.8	
oriBGE1322	31.3	41.7	+
oriBGE1323	38.5	44.9	
oriBGE1324	13.0	12.9	
oriBGE1325	22.7	46.2	+
oriBGE1326	10.4	15.6	
oriBGE1327	14.5	15.4	
oriBGE1328	39.6	47.9	+
oriBGE1329	30.0	26.7	
oriBGE1330	36.0	50.9	+

oriBGE1331	43.8	53.3	+
oriBGE1332	25.2	29.9	
oriBGE1333	38.2	50.6	+
oriBGE1334	30.0	30.9	
oriBGE1335	28.8	33.9	
oriBGE1336	34.9	38.9	
oriBGE1337	46.3	48.2	
oriBGE1338	33.5	39.3	
oriBGE1339	21.6	21.3	
oriBGE1340	17.8	13.8	
oriBGE1341	14.8	13.4	
oriBGE1342	25.5	41.4	+
oriBGE1343	24.8	20.9	
oriBGE1344	45.9	49.2	
oriBGE1345	26.8	25.8	
oriBGE1346	23.0	16.3	
oriBGE1347	41.1	47.4	
oriBGE1348	35.1	32.7	
oriBGE1349	17.0	15.3	
oriBGE1350	31.2	31.9	
oriBGE1351	34.2	24.1	
oriBGE1352	46.6	52.3	
oriBGE1353	44.2	52.1	
oriBGE1354	36.1	39.8	
oriBGE1355	33.6	37.4	
oriBGE1356	24.1	21.5	
oriBGE1357	29.8	33.9	
oriBGE1358	40.2	42.4	
oriBGE1359	36.3	49.0	+
oriBGE1360	44.3	52.0	
oriBGE1361	44.5	51.5	
oriBGE1362	30.1	30.7	
oriBGE1363	28.8	33.2	
oriBGE1364	40.2	45.3	
oriBGE1365	37.6	43.6	
oriBGE1366	30.8	40.0	+
oriBGE1367	47.8	63.6	+
oriBGE1368	30.4	38.2	
oriBGE1369	14.5	12.8	
oriBGE1370	9.9	17.3	
oriBGE1371	17.3	28.0	
oriBGE1372	35.4	49.2	+
oriBGE1373	36.3	45.9	+
oriBGE1374	11.2	22.9	+
oriBGE1375	16.8	21.5	
oriBGE1376	46.2	56.3	+
oriBGE1377	17.6	13.1	
oriBGE1378	16.6	20.5	

oriBGE1379	30.2	40.7	
oriBGE1380	45.1	47.3	
oriBGE1381	45.9	48.5	
oriBGE1382	45.1	41.9	
oriBGE1383	16.4	12.0	
oriBGE1384	38.6	44.7	
oriBGE1385	31.1	37.1	
oriBGE1386	53.6	48.2	
oriBGE1387	28.4	19.7	
oriBGE1388	31.8	27.4	
oriBGE1389	46.9	47.9	
oriBGE1390	28.6	30.3	
oriBGE1391	21.4	25.6	
oriBGE1392	17.2	27.6	+
oriBGE1393	13.5	21.7	+
oriBGE1394	42.1	52.0	
oriBGE1395	25.7	27.4	
oriBGE1396	38.9	48.7	
oriBGE1397	48.2	56.2	
oriBGE1398	44.2	52.0	
oriBGE1399	47.8	49.1	
oriBGE1400	51.0	48.9	
oriBGE1401	51.4	54.8	
oriBGE1402	59.3	56.4	
oriBGE1403	54.6	52.2	
oriBGE1404	64.1	60.7	
oriBGE1405	56.6	55.8	
oriBGE1406	57.8	58.1	
oriBGE1407	58.3	61.2	
oriBGE1408	61.3	61.7	
oriBGE1409	54.4	64.6	+
oriBGE1410	55.4	46.7	

Origin name	***rif1*Δ**	***rif1*Δ*rad3*Δ**	***rif1*Δ CIO**
oriBGE2001	57.2	59.9	
oriBGE2002	55.2	57.6	
oriBGE2003	57.3	59.6	
oriBGE2004	62.5	55.6	
oriBGE2005	61.5	55.8	
oriBGE2006	63.4	61.7	
oriBGE2007	58.2	63.9	
oriBGE2008	54.2	57.6	
oriBGE2009	53.1	53.1	
oriBGE2010	46.0	52.4	
oriBGE2011	24.3	30.1	
oriBGE2012	11.3	12.2	
oriBGE2013	35.8	34.7	
oriBGE2014	64.3	64.3	
oriBGE2015	29.0	26.9	
oriBGE2016	24.3	25.0	
oriBGE2017	20.0	27.9	
oriBGE2018	39.1	53.3	+
oriBGE2019	37.8	46.9	
oriBGE2020	34.9	39.2	
oriBGE2021	48.4	58.8	+
oriBGE2022	55.3	54.1	
oriBGE2023	49.3	49.8	
oriBGE2024	38.2	39.4	
oriBGE2025	22.1	24.7	
oriBGE2026	22.3	27.8	
oriBGE2027	20.0	19.3	
oriBGE2028	8.2	11.1	
oriBGE2029	25.6	33.6	+
oriBGE2030	37.4	52.9	+
oriBGE2031	14.5	22.3	
oriBGE2032	40.1	50.2	
oriBGE2033	43.5	52.9	+
oriBGE2034	40.0	40.1	
oriBGE2035	15.7	19.9	
oriBGE2036	17.6	23.4	
oriBGE2037	47.3	45.5	
oriBGE2038	48.7	53.6	
oriBGE2039	21.6	21.1	
oriBGE2040	18.4	11.4	
oriBGE2041	22.0	16.6	
oriBGE2042	40.2	49.8	+
oriBGE2043	40.4	48.6	+
oriBGE2044	41.9	55.9	+
oriBGE2045	38.5	56.3	+
oriBGE2046	28.4	36.0	

oriBGE2047	42.6	60.5	+
oriBGE2048	38.0	45.3	
oriBGE2049	14.5	15.2	
oriBGE2050	27.7	34.8	
oriBGE2051	42.0	51.7	
oriBGE2052	30.5	29.9	
oriBGE2053	25.2	29.3	
oriBGE2054	24.6	26.3	
oriBGE2055	17.9	20.4	
oriBGE2056	28.9	41.4	+
oriBGE2057	38.1	48.6	+
oriBGE2058	48.7	46.0	
oriBGE2059	45.7	47.3	
oriBGE2060	42.6	34.6	
oriBGE2061	33.7	37.1	
oriBGE2062	26.3	27.3	
oriBGE2063	19.1	35.2	+
oriBGE2064	16.5	15.7	
oriBGE2065	32.0	32.0	
oriBGE2066	52.0	50.2	
oriBGE2067	45.2	49.9	
oriBGE2068	23.6	15.8	
oriBGE2069	16.9	15.7	
oriBGE2070	30.2	31.1	
oriBGE2071	40.5	47.9	
oriBGE2072	24.4	27.8	
oriBGE2073	20.3	32.6	+
oriBGE2074	25.4	35.1	
oriBGE2075	23.8	33.4	+
oriBGE2076	33.0	35.7	
oriBGE2077	43.2	54.7	+
oriBGE2078	41.0	48.6	
oriBGE2079	47.0	53.7	
oriBGE2080	24.3	26.3	
oriBGE2081	13.0	16.2	
oriBGE2082	6.2	10.0	
oriBGE2083	6.4	7.3	
oriBGE2084	14.0	21.4	
oriBGE2085	28.8	27.1	
oriBGE2086	39.6	44.4	
oriBGE2087	38.2	42.8	
oriBGE2088	54.6	52.8	
oriBGE2089	45.5	49.3	
oriBGE2090	42.4	50.8	+
oriBGE2091	27.9	32.6	
oriBGE2092	12.9	13.9	
oriBGE2093	16.4	28.1	+
oriBGE2094	31.9	46.3	+

oriBGE2095	18.0	25.6	
oriBGE2096	15.1	14.1	
oriBGE2097	26.7	32.1	
oriBGE2098	44.6	55.8	+
oriBGE2099	42.1	46.1	
oriBGE2100	17.0	18.5	
oriBGE2101	25.8	27.6	
oriBGE2102	15.9	13.7	
oriBGE2103	18.3	19.8	
oriBGE2104	26.3	26.2	
oriBGE2105	38.0	48.8	
oriBGE2106	34.0	35.4	
oriBGE2107	30.0	36.2	
oriBGE2108	49.8	45.6	
oriBGE2109	43.1	48.5	
oriBGE2110	37.4	41.9	
oriBGE2111	22.4	28.8	
oriBGE2112	11.7	14.2	
oriBGE2113	38.2	40.0	
oriBGE2114	35.6	43.9	+
oriBGE2115	37.8	44.0	
oriBGE2116	34.3	31.8	
oriBGE2117	35.2	47.7	+
oriBGE2118	38.2	48.3	+
oriBGE2119	8.2	14.5	
oriBGE2120	5.9	10.5	
oriBGE2121	29.4	28.0	
oriBGE2122	44.3	50.6	
oriBGE2123	25.7	39.2	+
oriBGE2124	20.8	28.9	
oriBGE2125	27.2	31.3	
oriBGE2126	21.3	30.0	
oriBGE2127	37.6	43.5	
oriBGE2128	71.3	64.1	
oriBGE2129	44.0	50.7	
oriBGE2130	16.2	18.0	
oriBGE2131	14.4	14.9	
oriBGE2132	13.1	13.9	
oriBGE2133	16.2	16.7	
oriBGE2134	44.2	57.2	+
oriBGE2135	39.9	48.5	+
oriBGE2136	43.3	52.2	+
oriBGE2137	37.9	42.8	
oriBGE2138	38.2	36.1	
oriBGE2139	23.7	18.4	
oriBGE2140	28.1	30.1	
oriBGE2141	47.7	56.0	
oriBGE2142	39.3	46.3	

oriBGE2143	48.0	59.4	
oriBGE2144	47.1	56.3	
oriBGE2145	26.0	33.2	
oriBGE2146	44.7	44.2	
oriBGE2147	48.4	57.5	+
oriBGE2148	28.4	32.7	
oriBGE2149	30.3	38.0	
oriBGE2150	27.4	33.6	
oriBGE2151	32.1	34.9	
oriBGE2152	37.0	39.8	
oriBGE2153	35.5	47.7	+
oriBGE2154	30.2	36.5	
oriBGE2155	18.6	21.7	
oriBGE2156	11.0	13.1	
oriBGE2157	42.9	52.8	
oriBGE2158	40.0	61.3	+
oriBGE2159	33.2	39.9	
oriBGE2160	19.9	30.3	+
oriBGE2161	24.2	25.7	
oriBGE2162	15.0	15.1	
oriBGE2163	31.5	30.0	
oriBGE2164	37.9	48.7	+
oriBGE2165	34.7	34.4	
oriBGE2166	50.0	47.4	
oriBGE2167	37.3	45.6	+
oriBGE2168	12.6	16.8	
oriBGE2169	20.5	33.2	+
oriBGE2170	37.9	43.6	
oriBGE2171	37.2	40.8	
oriBGE2172	28.2	25.5	
oriBGE2173	41.8	46.6	
oriBGE2174	30.9	40.0	
oriBGE2175	42.3	55.3	+
oriBGE2176	44.5	52.0	
oriBGE2177	19.2	25.1	
oriBGE2178	32.0	36.7	
oriBGE2179	38.0	42.4	
oriBGE2180	38.1	43.8	
oriBGE2181	40.6	53.5	+
oriBGE2182	39.9	35.7	
oriBGE2183	45.3	53.7	+
oriBGE2184	30.3	32.4	
oriBGE2185	48.9	44.3	
oriBGE2186	46.0	52.6	
oriBGE2187	13.8	18.1	
oriBGE2188	19.2	22.7	
oriBGE2189	24.3	30.7	
oriBGE2190	51.3	58.9	

oriBGE2191	46.4	60.1	+
oriBGE2192	24.8	18.2	
oriBGE2193	25.6	14.3	
oriBGE2194	45.7	47.1	
oriBGE2195	30.6	30.5	
oriBGE2196	21.0	20.5	
oriBGE2197	11.8	22.3	+
oriBGE2198	20.0	18.9	
oriBGE2199	41.7	56.7	
oriBGE2200	33.9	38.8	
oriBGE2201	28.5	30.5	
oriBGE2202	42.2	58.1	+
oriBGE2203	28.7	21.7	
oriBGE2204	17.8	25.7	
oriBGE2205	24.8	21.1	
oriBGE2206	43.1	52.3	
oriBGE2207	21.6	19.2	
oriBGE2208	23.3	24.9	
oriBGE2209	35.2	43.3	
oriBGE2210	38.5	45.6	
oriBGE2211	47.6	52.1	
oriBGE2212	24.9	23.9	
oriBGE2213	20.7	18.4	
oriBGE2214	29.0	39.7	+
oriBGE2215	39.9	48.1	+
oriBGE2216	37.5	38.4	
oriBGE2217	40.6	53.8	+
oriBGE2218	35.5	35.5	
oriBGE2219	36.4	48.0	+
oriBGE2220	30.1	26.6	
oriBGE2221	43.3	55.1	+
oriBGE2222	27.2	35.6	+
oriBGE2223	10.7	7.1	
oriBGE2224	15.8	13.7	
oriBGE2225	43.1	52.7	+
oriBGE2226	26.8	32.1	
oriBGE2227	21.7	29.2	
oriBGE2228	46.0	45.8	
oriBGE2229	42.1	51.5	
oriBGE2230	36.2	38.3	
oriBGE2231	43.1	53.8	+
oriBGE2232	22.8	31.6	+
oriBGE2233	38.3	51.0	+
oriBGE2234	18.2	26.0	
oriBGE2235	23.7	27.9	
oriBGE2236	29.6	26.4	
oriBGE2237	44.1	50.4	
oriBGE2238	43.4	48.2	

oriBGE2239	27.3	24.0	
oriBGE2240	14.0	17.8	
oriBGE2241	35.4	51.7	+
oriBGE2242	27.7	32.4	
oriBGE2243	28.2	28.0	
oriBGE2244	28.3	44.1	+
oriBGE2245	36.1	42.1	
oriBGE2246	30.3	36.8	
oriBGE2247	41.4	51.6	+
oriBGE2248	34.4	46.7	+
oriBGE2249	28.2	35.3	
oriBGE2250	35.6	47.6	
oriBGE2251	36.2	32.6	
oriBGE2252	38.7	45.8	
oriBGE2253	41.3	49.8	+
oriBGE2254	27.9	28.7	
oriBGE2255	36.8	42.9	
oriBGE2256	45.7	50.5	
oriBGE2257	22.5	21.7	
oriBGE2258	21.1	31.6	+
oriBGE2259	36.8	43.3	
oriBGE2260	43.0	45.2	
oriBGE2261	38.8	43.9	
oriBGE2262	41.9	51.4	
oriBGE2263	19.7	27.3	
oriBGE2264	21.5	25.0	
oriBGE2265	39.1	44.4	
oriBGE2266	44.2	44.3	
oriBGE2267	46.0	55.4	
oriBGE2268	40.8	49.7	
oriBGE2269	31.3	28.3	
oriBGE2270	31.5	34.0	
oriBGE2271	37.5	41.8	
oriBGE2272	36.5	39.5	
oriBGE2273	42.6	58.6	+
oriBGE2274	55.7	51.2	
oriBGE2275	30.7	42.6	+
oriBGE2276	17.6	22.7	
oriBGE2277	10.0	18.0	+
oriBGE2278	20.3	17.4	
oriBGE2279	44.7	48.2	
oriBGE2280	32.5	33.6	
oriBGE2281	43.0	54.6	+
oriBGE2282	43.4	50.3	
oriBGE2283	18.0	25.8	
oriBGE2284	16.1	22.7	
oriBGE2285	40.5	40.6	
oriBGE2286	43.4	50.2	

oriBGE2287	32.9	33.4	
oriBGE2288	39.7	46.7	
oriBGE2289	44.2	45.5	
oriBGE2290	39.6	36.7	
oriBGE2291	39.2	45.8	
oriBGE2292	25.6	27.5	
oriBGE2293	38.3	50.1	+
oriBGE2294	30.9	37.5	
oriBGE2295	23.5	25.0	
oriBGE2296	18.3	17.7	
oriBGE2297	14.1	24.1	
oriBGE2298	26.2	28.8	
oriBGE2299	39.6	43.7	
oriBGE2300	34.1	36.2	
oriBGE2301	39.0	48.5	+
oriBGE2302	38.2	43.9	
oriBGE2303	28.8	37.0	+
oriBGE2304	42.7	47.8	
oriBGE2305	47.3	48.7	
oriBGE2306	43.2	39.7	
oriBGE2307	51.6	58.3	
oriBGE2308	54.2	57.3	
oriBGE2309	54.2	51.8	
oriBGE2310	55.7	52.0	
oriBGE2311	53.2	66.3	

Origin name	***rif1*Δ**	***rif1*Δ*rad3*Δ**	***rif1*Δ CIO**
oriBGE3001	57.8	59.2	
oriBGE3002	32.1	31.4	
oriBGE3003	32.7	37.1	
oriBGE3004	30.9	23.8	
oriBGE3005	33.9	42.2	+
oriBGE3006	20.8	20.1	
oriBGE3007	19.5	17.3	
oriBGE3008	26.5	34.7	
oriBGE3009	49.6	59.5	+
oriBGE3010	21.0	22.0	
oriBGE3011	11.7	17.4	
oriBGE3012	25.7	34.9	
oriBGE3013	40.5	53.2	
oriBGE3014	34.6	32.6	
oriBGE3015	30.7	34.1	
oriBGE3016	36.6	45.2	
oriBGE3017	31.6	36.1	
oriBGE3018	33.6	31.6	
oriBGE3019	33.6	42.0	+
oriBGE3020	27.5	38.5	+
oriBGE3021	33.8	41.3	
oriBGE3022	24.6	25.0	
oriBGE3023	32.1	45.2	+
oriBGE3024	22.0	24.3	
oriBGE3025	10.7	11.8	
oriBGE3026	45.7	58.8	+
oriBGE3027	25.4	21.1	
oriBGE3028	40.4	57.1	+
oriBGE3029	18.1	18.2	
oriBGE3030	16.1	24.6	+
oriBGE3031	14.2	14.2	
oriBGE3032	18.2	26.6	
oriBGE3033	30.1	46.8	+
oriBGE3034	25.1	26.2	
oriBGE3035	40.8	45.9	
oriBGE3036	39.6	53.1	+
oriBGE3037	29.2	35.3	
oriBGE3038	16.8	20.2	
oriBGE3039	42.0	42.0	
oriBGE3040	37.5	44.0	
oriBGE3041	32.6	44.0	+
oriBGE3042	22.7	22.3	
oriBGE3043	37.7	49.6	+
oriBGE3044	37.9	49.5	+
oriBGE3045	11.9	8.4	
oriBGE3046	13.1	16.1	

oriBGE3047	25.5	36.4	+
oriBGE3048	38.7	40.6	
oriBGE3049	26.8	31.7	
oriBGE3050	17.4	15.2	
oriBGE3051	23.9	27.0	
oriBGE3052	43.4	49.3	
oriBGE3053	15.3	24.8	+
oriBGE3054	16.3	21.0	
oriBGE3055	39.4	47.0	
oriBGE3056	31.2	36.5	
oriBGE3057	24.8	30.4	
oriBGE3058	30.3	34.2	
oriBGE3059	39.0	46.6	
oriBGE3060	9.6	8.6	
oriBGE3061	12.5	18.1	
oriBGE3062	23.0	26.0	
oriBGE3063	25.1	36.8	+
oriBGE3064	41.3	50.4	+
oriBGE3065	16.2	13.8	
oriBGE3066	24.1	21.5	
oriBGE3067	47.5	54.7	
oriBGE3068	34.8	34.0	
oriBGE3069	27.4	40.4	+
oriBGE3070	17.4	19.3	
oriBGE3071	18.5	20.9	
oriBGE3072	19.1	22.2	
oriBGE3073	38.6	50.6	+
oriBGE3074	44.0	50.7	
oriBGE3075	45.1	40.6	
oriBGE3076	17.9	15.9	
oriBGE3077	18.8	30.6	+
oriBGE3078	34.2	48.7	+
oriBGE3079	11.7	13.6	
oriBGE3080	7.6	9.9	
oriBGE3081	40.8	48.0	
oriBGE3082	23.6	21.5	
oriBGE3083	21.7	26.2	
oriBGE3084	14.6	22.0	
oriBGE3085	37.9	50.6	+
oriBGE3086	38.4	42.8	
oriBGE3087	45.0	47.7	
oriBGE3088	42.1	45.1	
oriBGE3089	48.1	57.9	+
oriBGE3090	45.6	46.7	
oriBGE3091	33.5	25.3	
oriBGE3092	43.0	47.5	
oriBGE3093	26.6	26.2	
oriBGE3094	18.9	26.5	

oriBGE3095	22.1	23.7	
oriBGE3096	13.1	15.8	
oriBGE3097	22.1	23.7	
oriBGE3098	36.7	41.5	
oriBGE3099	32.8	48.8	+
oriBGE3100	26.8	35.5	+
oriBGE3101	33.8	45.1	+
oriBGE3102	47.9	52.4	
oriBGE3103	41.1	56.1	+
oriBGE3104	8.5	15.6	
oriBGE3105	15.2	25.8	+
oriBGE3106	32.8	31.6	
oriBGE3107	45.0	52.3	
oriBGE3108	39.0	47.3	+
oriBGE3109	27.1	18.6	
oriBGE3110	53.0	62.4	
oriBGE3111	27.6	29.1	
oriBGE3112	37.5	44.5	
oriBGE3113	17.4	27.1	+
oriBGE3114	16.6	20.8	
oriBGE3115	38.0	38.2	
oriBGE3116	43.5	51.4	
oriBGE3117	38.4	44.3	
oriBGE3118	38.5	48.1	+
oriBGE3119	13.3	17.8	
oriBGE3120	39.8	50.7	+
oriBGE3121	34.5	35.1	
oriBGE3122	47.0	48.4	
oriBGE3123	20.0	24.1	
oriBGE3124	18.0	26.6	
oriBGE3125	15.2	22.5	
oriBGE3126	28.6	37.9	
oriBGE3127	41.6	50.5	+
oriBGE3128	33.8	34.3	
oriBGE3129	39.5	47.9	+
oriBGE3130	48.2	50.2	
oriBGE3131	23.6	21.7	
oriBGE3132	38.4	53.5	+
oriBGE3133	27.1	25.7	
oriBGE3134	33.8	39.2	
oriBGE3135	21.0	26.0	
oriBGE3136	17.3	22.9	
oriBGE3137	21.5	25.8	
oriBGE3138	20.7	30.8	+
oriBGE3139	41.1	55.5	+
oriBGE3140	35.5	30.6	
oriBGE3141	20.8	31.1	+
oriBGE3142	16.1	25.1	

oriBGE3143	18.8	23.0	
oriBGE3144	28.4	32.3	
oriBGE3145	46.0	59.9	+
oriBGE3146	28.0	28.1	
oriBGE3147	40.7	46.2	
oriBGE3148	40.4	46.1	
oriBGE3149	17.3	15.7	
oriBGE3150	30.9	47.2	+
oriBGE3151	47.9	54.9	
oriBGE3152	28.1	31.0	
oriBGE3153	18.6	23.9	
oriBGE3154	40.8	44.4	
oriBGE3155	46.0	56.7	+

Supplemental Table S5: List of *rif1Δ-CIOs*. Values indicate differences in origin efficiencies (*rif1Δ rad3Δ* - *rif1Δ*).

Origin name	Difference in efficiency
oriBGE1013	9.4
oriBGE1027	9.1
oriBGE1031	13.9
oriBGE1034	14.3
oriBGE1047	9.3
oriBGE1062	12.6
oriBGE1067	14.8
oriBGE1068	14.7
oriBGE1069	10
oriBGE1076	8.5
oriBGE1084	12.7
oriBGE1090	8.1
oriBGE1092	9
oriBGE1098	15.8
oriBGE1113	12.1
oriBGE1118	10.2
oriBGE1133	16.8
oriBGE1134	11
oriBGE1141	9.6
oriBGE1146	11.5
oriBGE1176	10.4
oriBGE1177	10.1
oriBGE1181	10.1
oriBGE1185	13.5
oriBGE1201	11.1
oriBGE1207	10.1
oriBGE1210	9.5
oriBGE1214	11.8
oriBGE1218	10.7
oriBGE1223	12.8
oriBGE1225	13.1
oriBGE1227	9.5
oriBGE1233	13.7
oriBGE1240	19.7
oriBGE1241	12.5
oriBGE1244	10
oriBGE1248	11.2
oriBGE1253	11
oriBGE1266	10.1
oriBGE1269	8.8
oriBGE1276	11.8
oriBGE1283	8.3

oriBGE1293	16.5
oriBGE1296	11.5
oriBGE1300	12.9
oriBGE1311	14.1
oriBGE1314	8.6
oriBGE1319	9.1
oriBGE1320	17
oriBGE1322	10.4
oriBGE1325	23.5
oriBGE1328	8.3
oriBGE1330	14.9
oriBGE1331	9.5
oriBGE1333	12.4
oriBGE1342	15.9
oriBGE1359	12.7
oriBGE1366	9.2
oriBGE1367	15.8
oriBGE1372	13.8
oriBGE1373	9.6
oriBGE1374	11.7
oriBGE1376	10.1
oriBGE1392	10.4
oriBGE1393	8.2
oriBGE1409	10.2
oriBGE2018	14.2
oriBGE2021	10.4
oriBGE2029	8
oriBGE2030	15.5
oriBGE2033	9.4
oriBGE2042	9.6
oriBGE2043	8.2
oriBGE2044	14
oriBGE2045	17.8
oriBGE2047	17.9
oriBGE2056	12.5
oriBGE2057	10.5
oriBGE2063	16.1
oriBGE2073	12.3
oriBGE2075	9.6
oriBGE2077	11.5
oriBGE2090	8.4
oriBGE2093	11.7
oriBGE2094	14.4
oriBGE2098	11.2
oriBGE2114	8.3
oriBGE2117	12.5
oriBGE2118	10.1
oriBGE2123	13.5

oriBGE2134	13
oriBGE2135	8.6
oriBGE2136	8.9
oriBGE2147	9.1
oriBGE2153	12.2
oriBGE2158	21.3
oriBGE2160	10.4
oriBGE2164	10.8
oriBGE2167	8.3
oriBGE2169	12.7
oriBGE2175	13
oriBGE2181	12.9
oriBGE2183	8.4
oriBGE2191	13.7
oriBGE2197	10.5
oriBGE2202	15.9
oriBGE2214	10.7
oriBGE2215	8.2
oriBGE2217	13.2
oriBGE2219	11.6
oriBGE2221	11.8
oriBGE2222	8.4
oriBGE2225	9.6
oriBGE2231	10.7
oriBGE2232	8.8
oriBGE2233	12.7
oriBGE2241	16.3
oriBGE2244	15.8
oriBGE2247	10.2
oriBGE2248	12.3
oriBGE2253	8.5
oriBGE2258	10.5
oriBGE2273	16
oriBGE2275	11.9
oriBGE2277	8
oriBGE2281	11.6
oriBGE2293	11.8
oriBGE2301	9.5
oriBGE2303	8.2
oriBGE3005	8.3
oriBGE3009	9.9
oriBGE3019	8.4
oriBGE3020	11
oriBGE3023	13.1
oriBGE3026	13.1
oriBGE3028	16.7
oriBGE3030	8.5
oriBGE3033	16.7

oriBGE3036	13.5
oriBGE3041	11.4
oriBGE3043	11.9
oriBGE3044	11.6
oriBGE3047	10.9
oriBGE3053	9.5
oriBGE3063	11.7
oriBGE3064	9.1
oriBGE3069	13
oriBGE3073	12
oriBGE3077	11.8
oriBGE3078	14.5
oriBGE3085	12.7
oriBGE3089	9.8
oriBGE3099	16
oriBGE3100	8.7
oriBGE3101	11.3
oriBGE3103	15
oriBGE3105	10.6
oriBGE3108	8.3
oriBGE3113	9.7
oriBGE3118	9.6
oriBGE3120	10.9
oriBGE3127	8.9
oriBGE3129	8.4
oriBGE3132	15.1
oriBGE3138	10.1
oriBGE3139	14.4
oriBGE3141	10.3
oriBGE3145	13.9
oriBGE3150	16.3
oriBGE3155	10.7

Supplemental Table S6. *Schizosaccharomyces pombe* strains used in this study.

Strain	Genotype	Source
PN292	*h+ cdc25-22*	P. Nurse
JW154	*h- cdc25-22 rad3Δ::ura4*$^{+}$	This study
JW129	*h- cdc25-22 polα-HA:kanMX6 cdc45-YFP:ura4*$^{+}$ *polδ-Flag:his3*$^{+}$ *ura4-D18*	This study
JW131	*h- cdc25-22 rad3Δ::ura4*$^{+}$ *polα-HA:kanMX6 cdc45-YFP:ura4*$^{+}$ *polδ-Flag:his3*$^{+}$ *ura4-D18*	This study
JW133	*h- cdc25-22 ssb1-HA:kanMX6 cdc45-YFP:ura4*$^{+}$ *polδ-Flag:his3*$^{+}$ *ura4-D18*	This study
JW135	*h- cdc25-22 rad3Δ::ura4*$^{+}$ *ssb1-HA:kanMX6 cdc45-YFP:ura4*$^{+}$ *polδ-Flag:his3*$^{+}$ *ura4-D18*	This study
JW1183	*h- cdc25-22 rif1Δ::natMX6 ssb1-HA:kanMX6 cdc45-YFP:ura4*$^{+}$ *polδ-Flag:his3*$^{+}$ *ura4-D18*	This study
JW1184	*h- cdc25-22 rif1Δ::natMX6 rad3Δ::ura4*$^{+}$ *ssb1-HA:kanMX6 cdc45-YFP:ura4*$^{+}$ *polδ-Flag:his3*$^{+}$ *ura4-D18*	This study
PN2483	*h- nda3-km311*	P. Nurse
JW1135	*h- nda3-km311 rad3Δ ::kanMX6*	This study
PN1	*h- 972*	P. Nurse
PN1400	*h- cig1Δ::ura4 cig2Δ::ura4 ura4-D18*	P. Nurse

Supplemental Table S7. Primers used in this study for ChIP-qPCR assays.

Primers	Sequence (5' – 3')	Location
OJW63	TTGCTTATCTTTTGGGTAGTTTTCG	*ori2004 (oriBGE2105)* Chr II:1545708
OJW64	CTTACATTTTCGGGAACTTATTAGTCAA	
OJW129	TTCAGGGCTCAAAGTTAGAAAAATCAAGT	*ori2060 (oriBGE2122)* Chr II:1867764
OJW130	CCCGAAATTGCACGGATAGTATAATT	
OJW812	GACTTTGACGATGCTCCACC	Chr III: 1644050
OJW813	CACCTTCTCCATCACCGTCT	
OJW814	ATGGATATGGCTTCGACGCT	Chr III:1652167
OJW815	TGTTTGCAGCGGACATAGTG	
OJW816	GTCGACGTTCTCTGGCTAAA	Chr III:1647131 (within duplicated region)
OJW817	GCTCCCATGGATGCTACTGA	
OJW822	CACCTTGGACTCGCTCAAAC	Chr III: 1646529 (within duplicated region)
OJW823	TGTAGACGACTTGAAACCCGA	
OJW1060	TGCGATAAAAAGAAATGTACCAA	*oriBGE3101* Chr III: 1575500
OJW1061	GCCTGCAAACACCGAATTTA	